ERDC TR-11-5

Engineer Research and Development Center

US Army Corps of Engineers®
Engineer Research and Development Center

Navigation Systems Research Program

Deformable Bullnose Energy Absorbing System (BEAS)

Report 2: Head-On Impact with a Deformable BEAS and Introducing a Collapsible Arch

Robert M. Ebeling, Barry C. White, Ralph W. Strom,
John E. Hite, Jr., Bruce C. Barker, and Richard W. Haskins

July 2011

Bullnose Type	Barge Train Size	Barge Train Integrity Limit Velocity (fps)
Rigid	3x5	3.3
Deformable BEAS	3x5	4.5
Rigid	3x4	3.0
Deformable BEAS	3x4	4.7

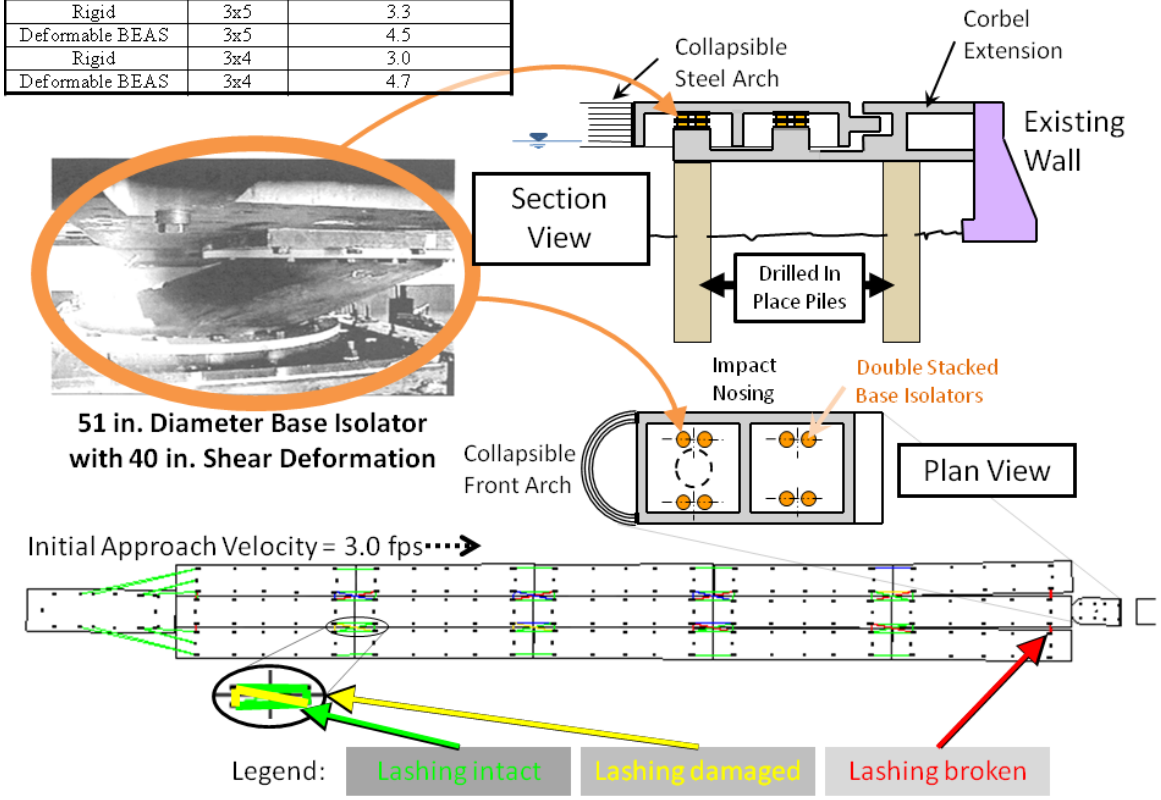

Deformable Bullnose Energy Absorbing System (BEAS)

Report 2: Head-On Impact with a Deformable BEAS and Introducing a Collapsible Arch

Robert M. Ebeling, Barry C. White, Bruce C. Barker, and Richard W. Haskins

Information Technology Laboratory
U.S. Army Engineer Research and Development Center
3909 Halls Ferry Road
Vicksburg, MS 39180-6199

John E. Hite, Jr.

Coastal and Hydraulics Laboratory
U.S. Army Engineer Research and Development Center
3909 Halls Ferry Road
Vicksburg, MS 39180-6199

Ralph W. Strom

9474 SE Carnaby Way
Happy Valley, OR 97986

Report 2 of a series

Prepared for Headquarters, U.S. Army Engineer District
441 G. Street, NW
Washington, DC 20314-1000

Abstract: An impact between a tow and the bullnose of a lock approach wall can result in the tow breaking up with loose barges moving out of control toward the lock or navigation dam with serious consequences. Project operations can be severely affected or even shut down. The loose barges can cause a high safety risk to personnel involved and if the navigation pool is lost or the lock is damaged, significant economic impacts may result. This Technical Report discusses the second stage of research into the development of a Deformable Bullnose Energy Absorbing System (BEAS) impact structure that would help reduce or prevent lashing failures and loose barges due to an impact between a tow and a lock approach wall bullnose.

In simulations, the first improvement for limiting approach velocity to maintain barge integrity was achieved by the proper selection of lashing layout. The second improvement was achieved by the introduction of the Deformable BEAS. For a head-on collision between a three by five barge train at 3.3 feet per second and a rigid bullnose, barge train integrity is lost. For the same barge train, this report shows that the addition of an impact nosing with double stacked, soft base isolators for a Deformable BEAS extends the maintenance of barge train integrity to 4.5 feet per second. For a head-on collision between a three by four barge train at 3.0 feet per second and a rigid bullnose, barge train integrity is lost. For the same barge train, this report shows that the addition of the collapsible front arch to an impact nosing with double stacked, soft base isolators for a Deformable BEAS extends the maintenance of barge train integrity to 4.7 feet per second. These results imply that the addition of other innovative energy absorbing features could allow for even higher approach velocities.

Contents

Figures and Tables

Figures

Tables

Preface

The investigation reported herein was authorized by the Headquarters, U.S. Army Corps of Engineers and was performed during the period January 2010 to September 2011 under the Navigation Systems Research Program. The research was performed under Work Unit 33D89G, entitled "Navigation Safety Initiative". The HQUSACE Technical Monitor on this work unit's research was Tom Hood, LRN-OP-ETR-A. Jim Walker is the HQUSACE Navigation Business Line Manager.

The Program Manager for the Navigation Systems Research Program is Charles Wiggins in the Coastal and Hydraulics Laboratory (CHL), U.S. Army Engineer Research and Development Center (ERDC). Jeff Lillycrop is the Technical Director for Navigation in CHL. The research is being led by Dr. Robert M. Ebeling of the Information Technology Laboratory under the general supervision of Dr. Reed L. Mosher, Director ITL: Dr. Deborah F. Dent, Deputy Director ITL; Dr. Robert M. Wallace, Chief of the Engineering and Informatic Systems Division, ITL. Dr. Ebeling is the Principal Investigator of the Navigation Systems "Navigation Safety Initiative" work unit under which this research was performed.

This report was authored by Dr. Ebeling and Barry C. White of ITL, Ralph W. Strom, consultant, and Dr. John E. Hite, Jr. of the Navigation Branch, CHL. White is in the Computational Analysis Branch, ITL. Dr. Hite operates under the general supervision of Dr. William D. Martin, Director, CHL; Jose E. Sanchez, Deputy Director, CHL; Dr. Rose M. Kress, Chief of the Navigation Division, CHL. Deformable BEAS designs, dBEAS software development and simulations were made by Dr. Ebeling, White and Strom. Deformable BEAS designs/developments were made by Dr. Ebeling, White and Strom. Dr. Hite and Bruce C. Barker and Richard E. Haskins, both of the Sensor Measurement and Instrumentation Branch, ITL, collected and processed the six months of traffic studies at Markland lock that is discussed in this report. Barge train approach information for both Markland Lock and the Newt Graham Lock and Dam 18 was assembled and interpreted by Dr. Hite.

Robert Willis (retired), Chad Linna, and Kareem EL-Naggar of the Great Lakes and Ohio River Division (LRD), John Clarkson and Jeff Maynard of

the Huntington District, Corps of Engineers, and Kent Hokens of the St. Paul District, Corps of Engineers are team members providing oversight and guidance for this research effort.

Richard Femrite and Kent Hokens of the St. Paul District developed a costing (for material, construction and engineering) for a Deformable BEAS using a "rudimentary" sketch developed by the authors of this report. Using his knowledge on cost effective structural system features, Kent Hokens, Structural Engineer, was able to suggest clever, cost effective changes to the non-moving foundation substructure portion of the Deformable BEAS structural system. This more cost effective foundation substructure is shown in Chapter 5 (Figure 5.13).

To provide a basis for judging the construction cost of a Deformable BEAS, costs were also acquired for representative "rigid" bullnoses of the type that are found at the Corps projects and using costing data based on recent projects. David Sullivan, Bryan Bledsole and Derek Maxey, all of the Huntington District, kindly developed a costing for three rigid bullnoses based on recent material and construction costing for the upstream and downstream rounded bullnoses used at the center wall at Robert C. Byrd Lock and Dam and a concrete filled cellular bullnose using data based on recent construction at Marmet Lock and Dam. Byron McClellan, retired Chief of Structures for the Louisville District, Larry Dalton II, Louisville District's Chief of Navigation Design Section, and Kathy Feger, Senior Structural Engineer, provided costing information on the rigid bullnose used at the McAlpine Lock and Dam replacement.

Bob Willis, retired Chief of operations for the Great Lakes and Ohio River Division, observes that material, construction and engineering costs may not be the only basis for evaluating the usefulness of a Deformable BEAS as compared to a rigid bullnose. In support of this assertion, David Sullivan supplied the Corps Navigation Economics PDT tabulation of costs over time for full closure at the Corps lock and dam structures. Bob Willis also supplied the costing data gathered by the Corps of Engineers after the 2005 Belleville incident (involving barges in the dam gates) which accounted for costs to shippers and end users for the products not delivered.

COL Kevin J. Wilson was Commander and Executive Director of ERDC. Dr. Jeffery P. Holland was Director.

Unit Conversion Factors

Multiply	By	To Obtain
cubic feet	0.02831685	cubic meters
feet	0.3048	meters
inches	0.0254	meters
miles per hour	0.44704	meters per second
pounds (force) per square inch	6.894757	kilopascals
pounds (mass)	0.45359237	kilograms
pounds (mass) per cubic foot	16.01846	kilograms per cubic meter
square inches	6.4516 E-04	square meters
tons (2,000 pounds, mass)	907.1847	kilograms

1 Introduction

1.1 Problem to be solved and research efforts

In recent years the Corps has been experiencing an increase in the number of navigation accidents on inland waterways. Examples of these allisions[1] from tows (i.e., barges) striking Corps navigation structures, locks, and dams are discussed in Ebeling et al. (2010). This research report discusses the continued investigation of new engineering methodologies and new structural design concepts for bullnoses to mitigate/eliminate the potential for rupture of the lashings that then allow "break-away" barges to occur. Impact simulations with rigid and with deformable bullnoses show that the primary threat to the failure of lashings that result in "break-away," out of control barges, is due to head-on impacts. This report discusses the results of impact simulations with a Deformable Bullnose Energy Absorbing System (Deformable BEAS) that were made using the PC-based software dBEAS. Due to District interests, potential Deformable BEAS designs for the Markland Lock and Dam (Louisville District) and for the Newt Graham Lock and Dam 18 (Tulsa District) sites are investigated through impact simulations using dBEAS software. The results from the research conducted to-date are discussed in this report as well as the design modifications to be made to the Deformable BEAS structural features that will be investigated during the next stage of research.

The efforts included in the research investigation discussed in this Technical Report include:

- Field data collection of barge train approach angles and approach velocities at two operating Corps projects.
- Use of a probabilistic based procedure for processing the field velocity data captured in a limited time window at the Corps Navigation project.
- Numerical model development to determine the interaction of a Deformable BEAS with a barge train during impacts and the forces developing with the lashings of the barge train.

[1] Allision is defined as the act of dashing against or striking upon; it is often used to describe the action of one boat hitting against a stationary boat, or of a sea dashing against a boat. The word is commonly used in place of "collision" to distinguish that one of the objects was fixed. For this report, the words will be used interchangeably.

- Numerical modeling to determine lashing forces for varying project conditions and tow/lashing configurations.
- Development of a structural design to absorb energy and reduce the potential for lashing failure.
- Addition to the design of a collapsible arch to absorb additional energy at the Deformable BEAS.

1.2 History of Deformable BEAS designs to date

Ebeling et al. (2010) summarizes the initial development of the Deformable BEAS structural concepts through 2010. This subsection discusses some of the key structural design concepts that have been proposed and then investigated. It concludes with a description of the latest design configuration to be investigated with the dBEAS simulation results summarized in this report. The impact nosing for the Deformable BEAS evolved over time, in much the same way that the barge train model evolved. The initial designs were for a single impact nosing section with a fixed or floating-pier corbel extension on the wall for the impact nosing to rest on (Figures 1.1 and 1.2). In a piece of far-sightedness, a two-part impact nosing using a tongue-and-groove sliding connection was designed with the goal being to handle barge trains of different masses (Figures 1.3 and 1.4).

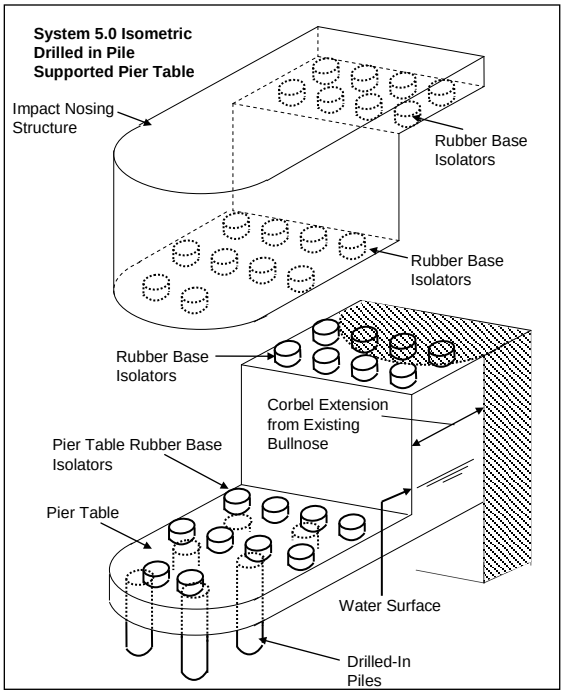

Figure 1.1 Fixed Corbel extension single impact nosing.

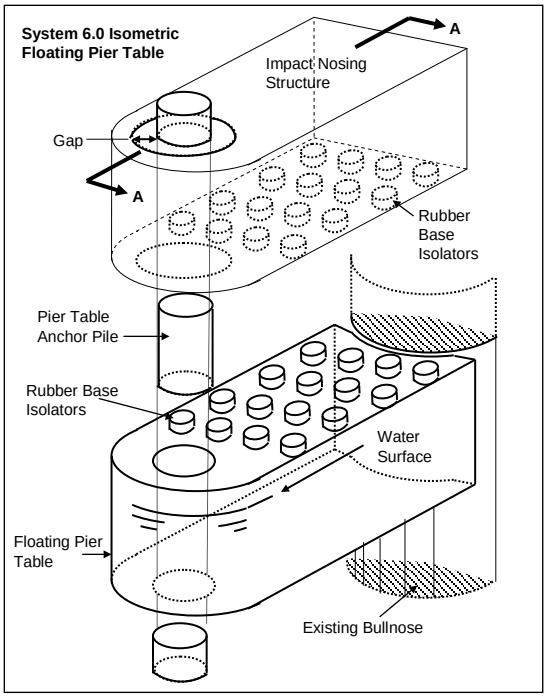

Figure 1.2 Floating-pier impact nosing.

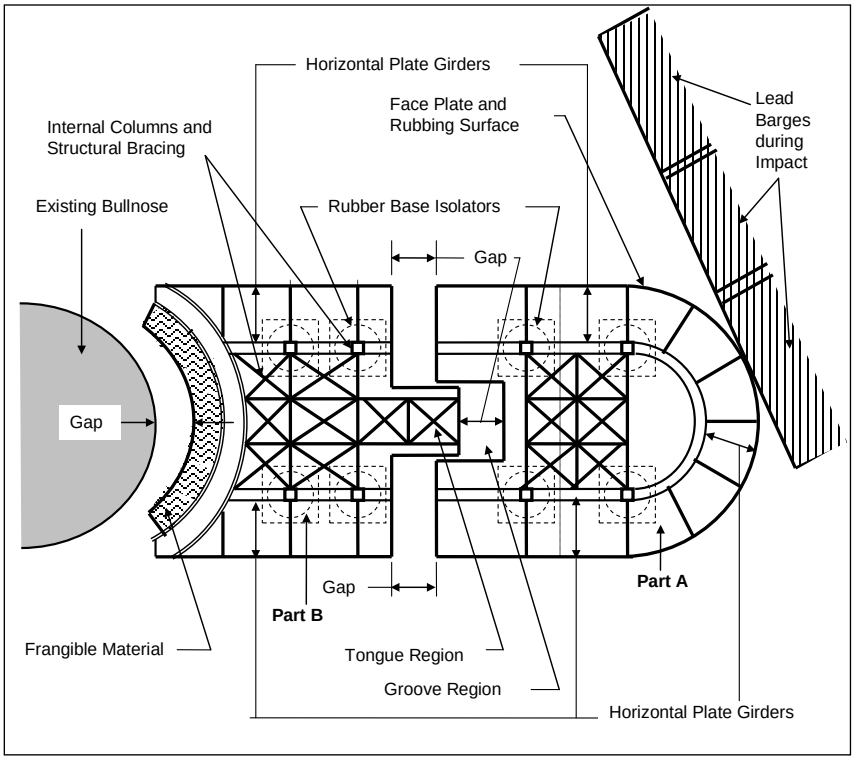

Figure 1.3 A multi-part tongue-and-groove impact nosing.

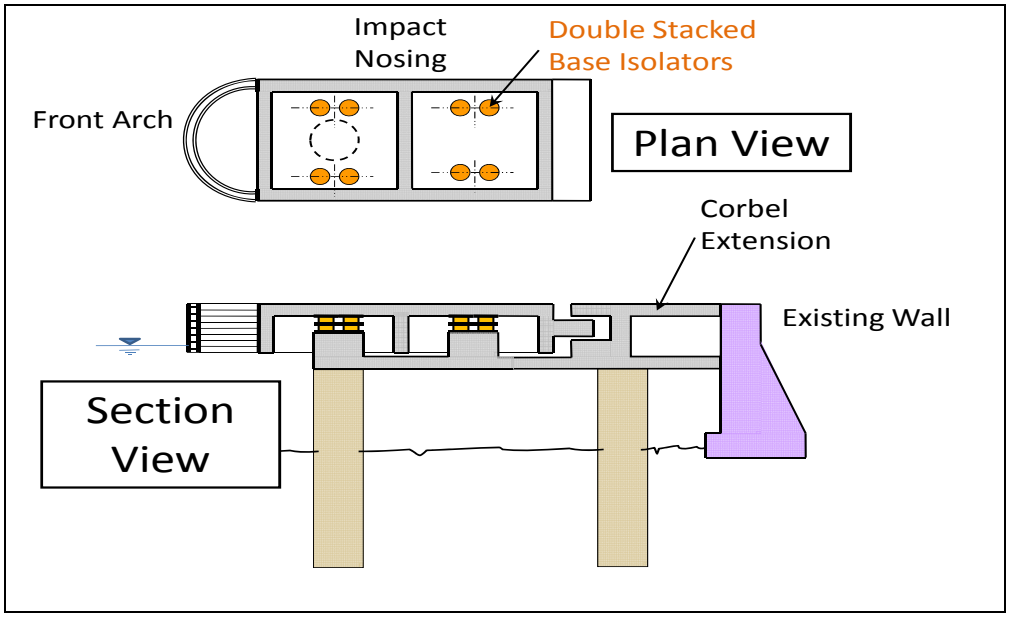

Figure 1.4 A single-part impact nosing with stacked base isolators and collapsible front arch.

The complicated two-part tongue-and-groove impact nosing model became superfluous with the discovery in 2010 that base isolators could be built that would not engage until the impact nosing had travelled a certain distance. The “delayed engagement” base isolators numerical model was formulated and incorporated into the dBEAS software model. Further design/development resumed on a one-part impact nosing for the Deformable BEAS.

It was also determined that base isolator stiffness could be reduced by “stacking” base isolators. The resulting base isolator stack would exhibit the same forces but over a longer deformation period.

The dimensions of a designed impact nosing that could withstand the impacts required are presented in Figure 1.5. The total weight of the impact nosing section would be 762 tons.

The Figures 1.4 and 1.5 section and plan views of Deformable BEAS reflect the essential features of the structural system that is investigated and results are summarized in this research report. Note the impact arch structural feature mounted at the front of the impact nosing in Figure 1.5. Both an impact arch as well as a newly developed collapsible front arch, replacing the Figure 1.5 impact arch, used to absorb energy during high approach velocity events, was investigated during the course of the current research effort.

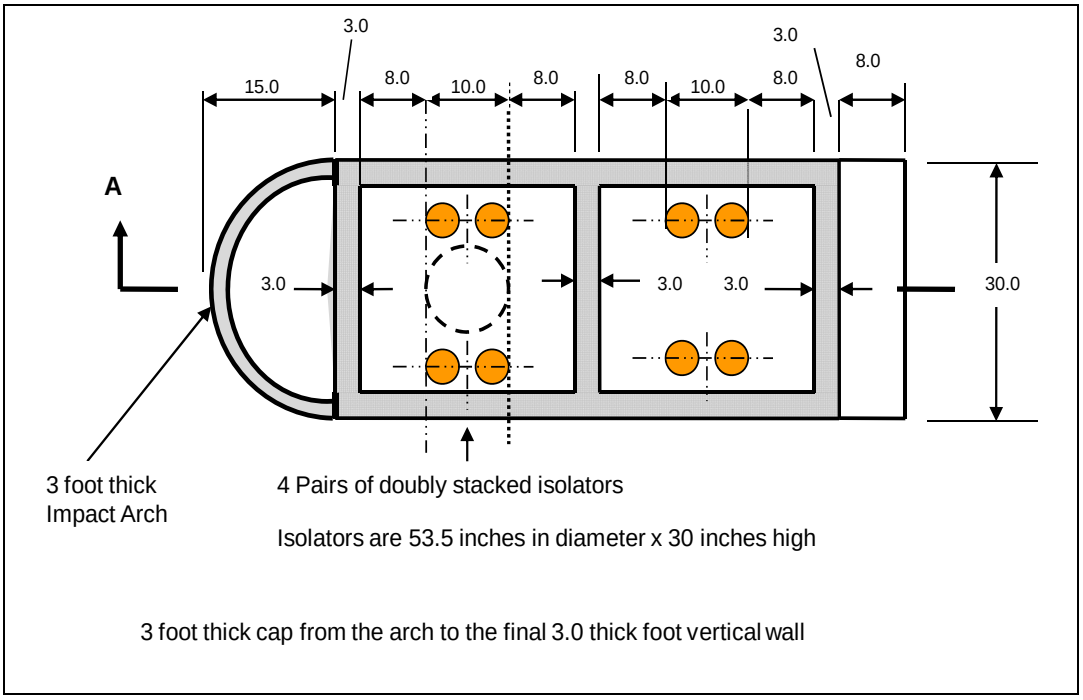

Figure 1.5 Dimensions (in feet) of a designed impact nosing for a Deformable BEAS.

1.3 Load conditions

ETL 1110-2-563 establishes the three impact event load cases that the Deformable BEAS is to be designed for. They are designated as the Usual, Unusual and Extreme load conditions and each possesses unique performance criteria, given in Table 1.1. This guidance document also provides non-site specific approach velocity criteria that may be used when site specific data is not available.

Table 1.1. Three load condition categories, frequency of loadings, and performance criteria (ETL 1110-2-563).

Load Condition Category	Annual Probability of Exceedence	Return Period (years)	Performance Criteria	Forward Velocity (fps)	Lateral Velocity (fps)	Approach Angle (degrees)
Usual	Greater than or equal to 0.1	1-10	No damage	0.5 - 2	0.01 - 0.1	5-10
Unusual	Less than 0.1 but greater than 0.00333	10-300	Repairable damage	2 - 4	0.4 - 0.5	10-20
Extreme	Less than 0.00333	>300	Non-collapse	4 - 6	<1.0	20-35

Corps design criteria stipulates that hydraulic structural features must be designed for three levels of loading and three corresponding levels of performance. Load condition probabilities and associated performance objectives similar to those described in Chapter 3 of EM 1110-2-2100 have been used to develop loading, loading frequency, and performance criteria for barge impact. This information is contained in Table 1.1 and is an adaptation of information previously provided in ETL1110-2-563.

Observe in Table 1.1 that of the three load condition categories, the Usual load condition category is the most frequent of the three design events, as reflected in the higher value for annual probability of exceedence or a lower value for return period (in years). Return period is equal to the inverse of the annual probability of exceedence. The associated performance criterion is for no damage during the Usual design event. Prior to the availability of results from a site-specific barge traffic data study for a project, the non-site specific forward velocity data listed in Table 1.1 may be used for preliminary design calculations for each of the three load condition categories. For the Usual load condition category, the non-site specific forward velocity typically ranges in value from 0.5 to 2 fps.

The Unusual load condition category is less frequent than the Usual design load case. Consequently, its associated performance criterion is for limited, easily repairable damage. For the Unusual load condition category, the non-site specific forward velocity typically ranges in value from 2 to 4 fps.

The extreme load condition category is even less frequent than the Unusual design load case. Consequently, its associated performance criterion is to allow for damage but to avoid collapse. For the extreme load condition category, the non-site specific forward velocity typically ranges in value from 4 to 6 fps.

This design criterion was developed in 2004 for design of rigid approach walls. These non-site specific approach velocities were adapted for use in this research study. Because this study focuses primarily on head-on impacts with bullnoses, the approach angles and the transverse approach velocities are disregarded; only the longitudinal velocities are being used. When approach angles are used, site-specific geometric data acquired at the site will be used. This is the case for the Markland Locks and Dam and Newt Graham Lock and Dam 18 that are discussed in this report.

1.4 Report contents

Chapter 2 summarizes a field study involving the collection and processing of site-specific approach velocity data and barge train traffic gathered at Markland Locks and Dam on the Ohio River. The data collected also includes the flow conditions. An assessment of the approach conditions on the Ohio River and Newt Graham Lock and Dam 18 on the Verdigris River near Tulsa, Oklahoma, is also included in this chapter. Discussion of Usual, Unusual, and Extreme Load Condition Categories according to ETL 1110-2-563 at these sites is discussed.

Chapter 3 discusses the dBEAS program simulation variables for a Deformable BEAS being impacted by a three-by-five barge train typical for the Markland site. It also discusses parametric simulation results for head-on, off-center, and glancing blow impacts.

Chapter 4 discusses changes that were made to the Deformable BEAS impact nosing structure as a result of simulation performed in Chapter 3. The discussion covers the addition of a collapsible front arch to lower the stiffness of the Deformable BEAS in an effort to provide more protection for barge train integrity. Parametric simulation results for a three-by-four barge train that typical for the Newt Graham site were gathered and the results are presented.

Chapter 5 summarizes insights from the studies discussed in previous chapters and suggests possible future research efforts.

2 Approach Angle and Velocity Investigation

2.1 Background

The investigation into the use of a deformable Bullnose Energy Absorbing System (BEAS) at a project should include an investigation of the flow conditions in the upper lock approach and the characteristics of the barge tows that use the lock. Good estimates of the barge tow size, weight, and maneuverability need to be known so that the expected impact loads on the Deformable BEAS can be determined. Information regarding the upper pool elevation, river currents, tow approach angles and velocities is necessary to help develop the design.

2.2 Markland Locks and Dam, Ohio River

The guard wall in the upper approach at Markland Locks and Dam was selected tentatively as the first site to install the Deformable BEAS. A U.S. Army Engineer Waterways Experiment Station (1957) model study provided the best information available for the flow conditions in the upper approach at the Markland Project. The ERDC Information Technology Laboratory developed a prototype testing plan to obtain information concerning the barge tow size and approach angles and velocities. Instrumentation to determine approach angles and approach velocities for a tow entering the main chamber was scheduled to be installed in early FY 2010, but the main lock chamber was out of operation due to a miter gate failure. The lock went back into operation in March 2010 and the instrumentation was installed and data were collected between 1 April and 10 October 2010.

2.2.1 Navigation conditions in the upper approach

Markland Project personnel have indicated that outdraft occurs at the project for higher flows. Outdraft is the crosscurrent in the upper approach due to discharge through the dam. The normal upper pool elevation is 455 and the locks go out of service at el 463. Project personnel describe the outdraft as a “hot” condition. Once the gate opening on the dam reaches 150 to 200 ft[1], the hot condition exists. Downbound tows approach on the

[1] The gate opening is the sum of the gate opening heights for all of the gates.

Kentucky bank side and drive toward the locks staying close to this bank. Once the head of the tow is fairly deep into the approach, sometimes almost to the nose of the landside guide wall for the auxiliary lock (see Figure 2.1), the tow slides across to the guard wall for entrance into the main lock. For low flow conditions, the tows come in closer to the guard wall, as shown in Figure 2.2. The head of this tow landed on the guard wall about 650 ft upstream from main lock. Project personnel described another approach where the outdraft catches the tow causing it to be more riverward than desired. In this case, the pilot steers the head toward the bank and has even grounded the barges on the bank. An item to note for the Deformable BEAS design is that the Markland project receives the most drift and debris of the navigation projects in Louisville District.

2.2.2 Approach flow velocities

A U.S. Army Engineer Waterways Experiment Station (1957) model study, mentioned previously, was performed to investigate the navigation conditions at Markland Locks and Dam. Current patterns and velocity information were determined with all gates open for upper pool elevations of 455, 460, and 464 and corresponding discharges of 420,000, 500,000, and 560,000 cfs. Figure 2.3 shows the current direction and flow velocities

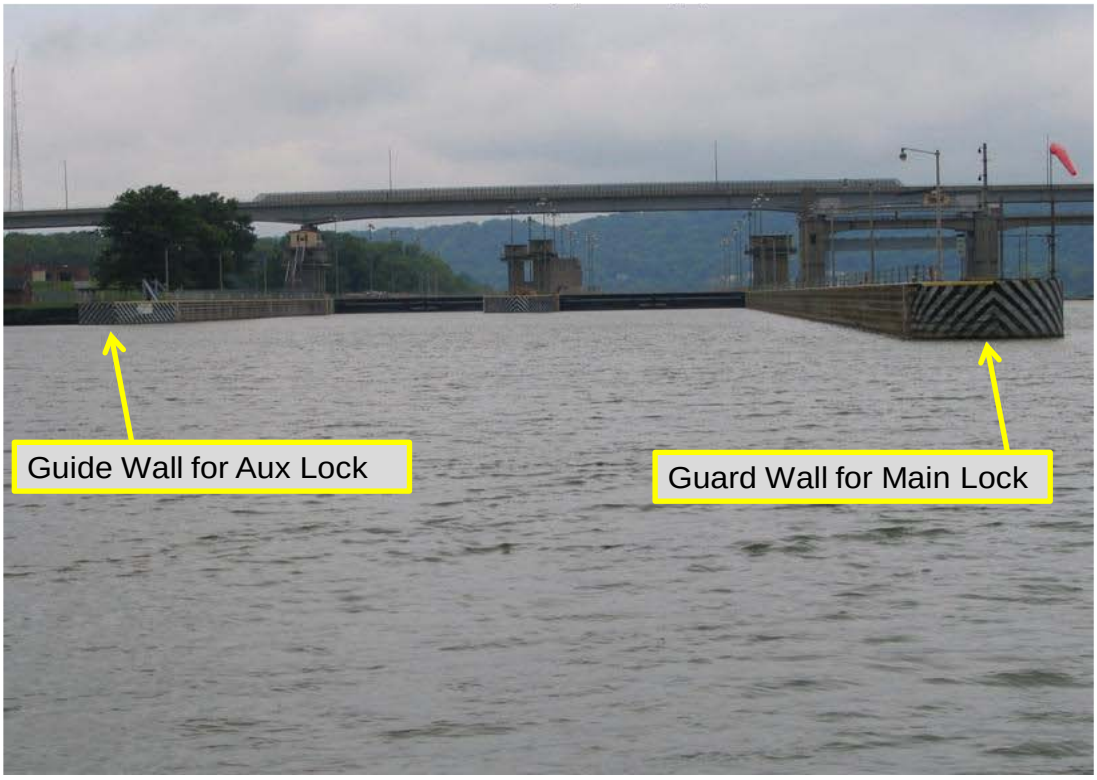

Figure 2.1. Markland Locks.

Figure 2.2. Low flow downbound tow approaching guard wall at Markland main lock.

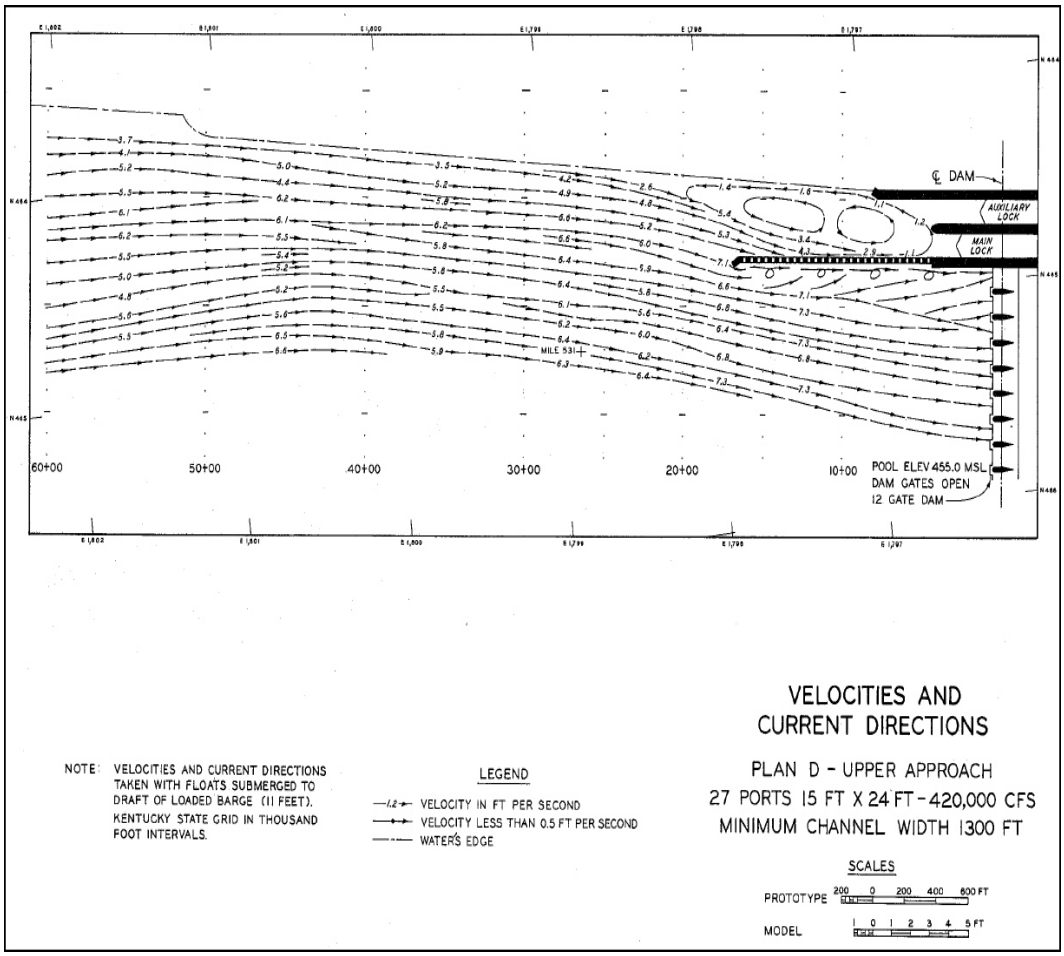

Figure 2.3. Flow conditions with discharge of 420,000 cfs from model study.

with a discharge of 420,000 cfs and an upper pool el of 455. Velocities in the upper approach approximately 600 ft upstream from the guard wall bullnose ranged from 2.6 to 6.0 ft/sec and cross stream velocities at the guard wall bullnose ranged from 5.4 to 7.1 ft/sec. An eddy forms in the upper lock approach as shown in Figure 2.3. Figure 2.4 shows the current direction and flow velocities with a discharge of 500,000 cfs and an upper pool el of 460. Velocities in the upper approach approximately 600 ft upstream from the guard wall bullnose ranged from 3.5 to 6.0 ft/sec and cross stream velocities at the guard wall bullnose ranged from 4.2 to 7.2 ft/sec. The velocities were not much higher with the increased discharge. Figure 2.5 shows the current direction and flow velocities with a discharge of 560,000 cfs and an upper pool el of 464. Velocities in the upper approach approximately 600 ft upstream from the guard wall bullnose ranged from 1.3 to 6.4 ft/sec and cross stream velocities at the guard wall bullnose ranged from 3.5 to 7.4 ft/sec. The velocities were slightly higher close to the bullnose.

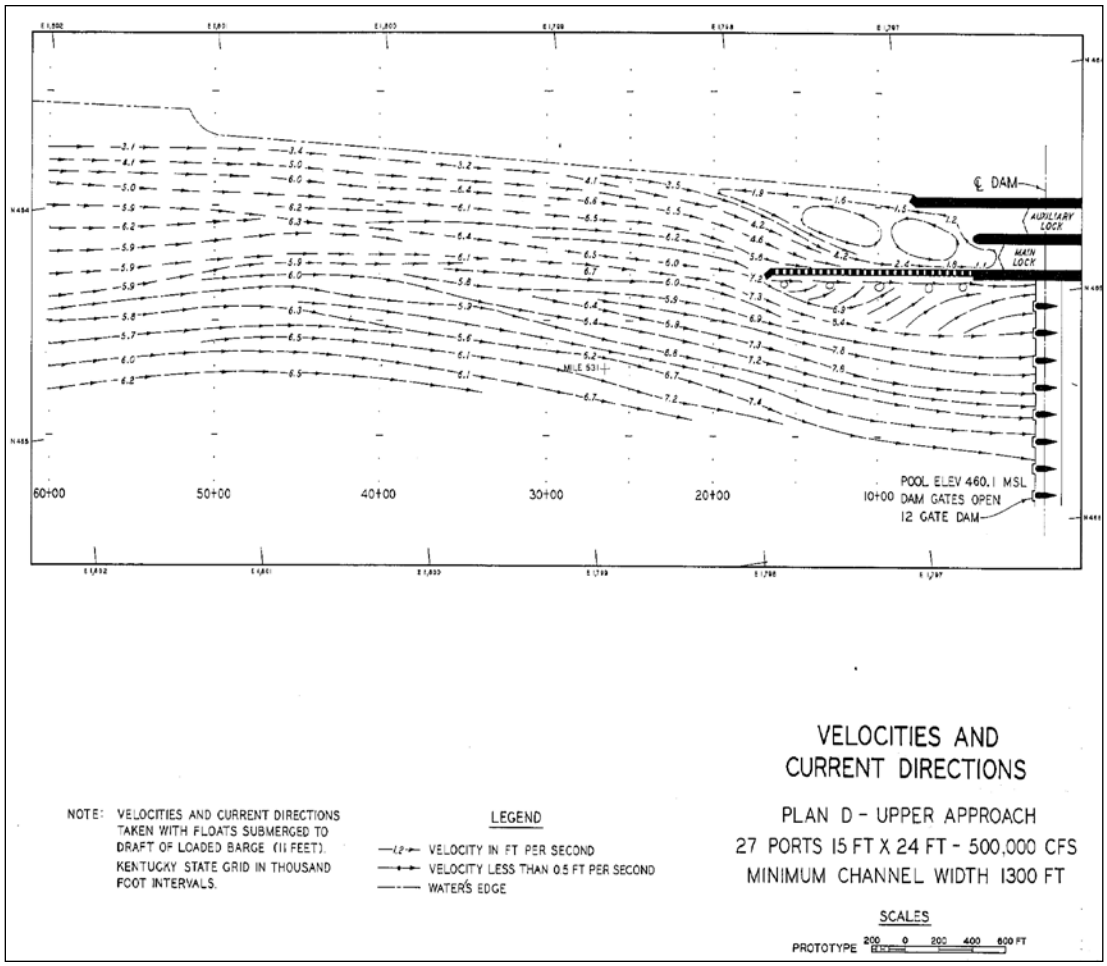

Figure 2.4. Flow conditions with a discharge of 500,000 cfs from model study.

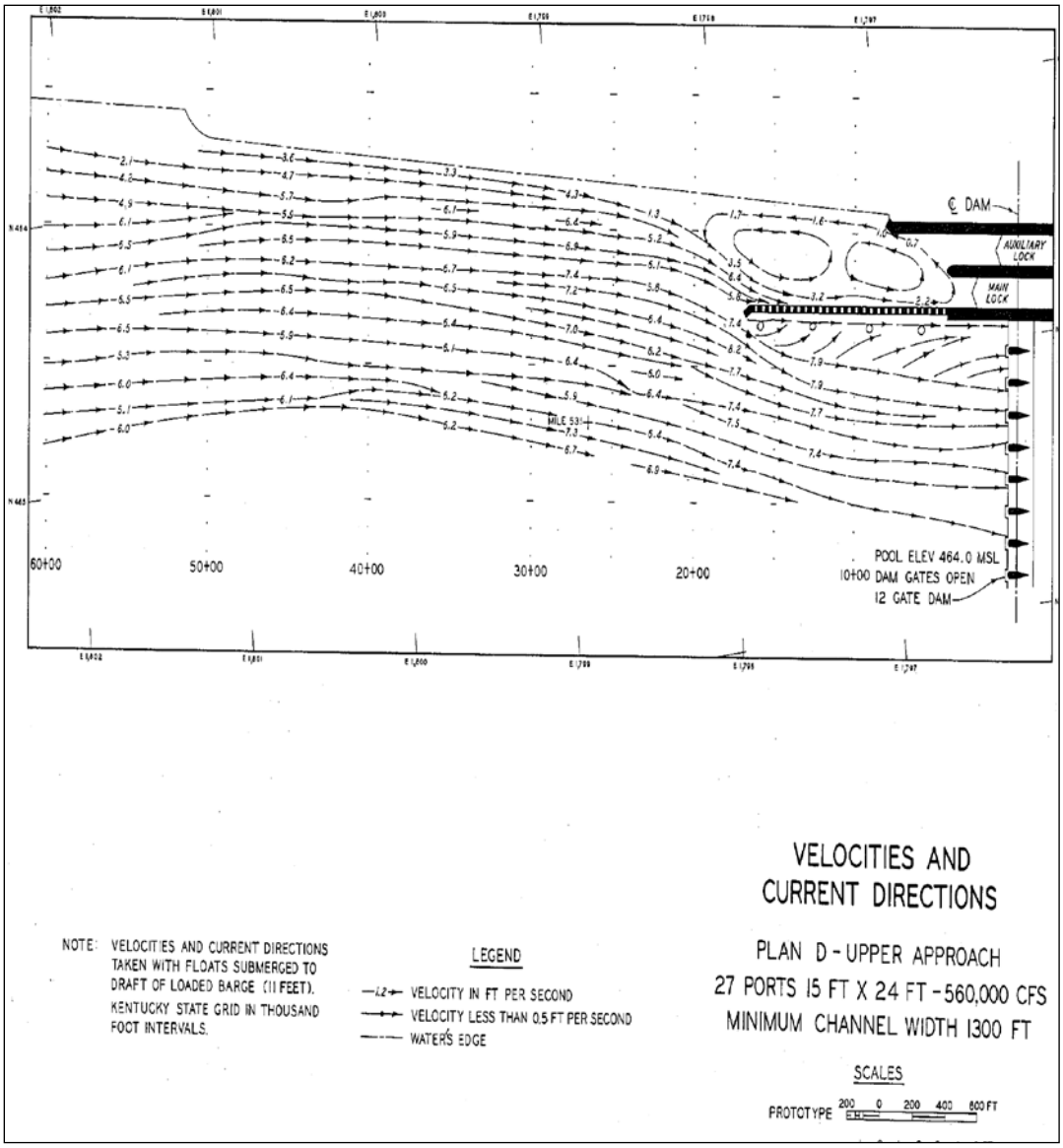

Figure 2.5. Flow conditions with a discharge of 560,000 cfs from model study.

The estimated flow velocity near the bullnose when the tows were approaching the lock was considered important to understand how tows approach the lock under varying flow conditions. The flow data from the model report were interpreted to develop a relationship between the discharge and an estimation of the velocity near the upstream end of the bullnose, as shown in Figure 2.6. A 3rd order polynomial curve was fit to the data to estimate velocities for the varying discharge. This curve was used for later efforts to observe trends between flow velocity and tow velocity.

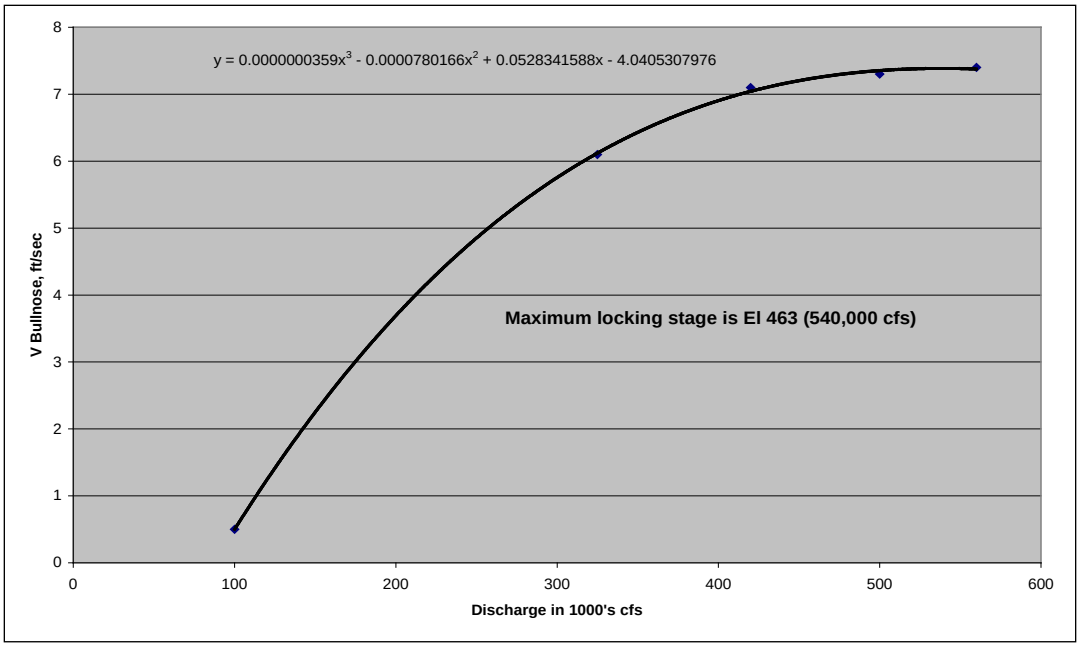

Figure 2.6. Estimated velocity at bullnose based on model report data.

The next effort was to determine the project discharge based on the information provided in the OMNI data base. The upper and lower pool elevations and the total feet of gate opening are available in the Corps' OMNI database along with other information concerning the vessel and barge train. A sample of this information with the hydraulic data extracted is shown in Table 2.1. The lower gage reading could be used to determine discharge from the tailwater rating curve shown in Figure 2.7 (obtained from the model report). The model report curve was compared to one provided by the Louisville District Office and showed a good comparison; therefore, it was used in the following analyses. Using the data from the OMNI report and the tailwater curve from the model report, a plot of the lower gage reading versus total gate opening in ft between 1 April and 10 October 2010 was made and is shown in Figure 2.8. There was generally an upper and lower bound to the data. The lower gage reading was converted to tailwater and a plot of tailwater elevation versus total gate opening was developed. Curves were fitted through the upper and lower bounds as shown in Figure 2.9.

The computed values for the upper and lower bounds of tailwater and total gate opening could then be converted to upper and lower bounds of discharge based on the tailwater rating curve in Figure 2.7. These discharge bounds could then be converted to an estimated upper and lower value of velocity at the bullnose based on the curve in Figure 2.6. Table 2.2 lists the values of velocity at the bullnose using this procedure.

Table 2.1. Sample of Hydraulic Data from OMNI Database.

WinOMNI/HYDR > HRE22 Readings/Gate Opening Report (v1.3a)7/21/2010 at 21:21:53:86				
Ohio	Markland Lock	// 2010/04/01 at 0000	thru 2010/07/21	at 2359
Total	Gate Opening is	Computed for Reading	Types:	
GA(Gate), RO(Roller),		TA(Tainter)		
Total	Gate Opening	EXCLUDES Readings	of 900 or Greater (Out of Operation)	
*Report is not accurate for stations with more than 6 Reading Types				
Date	**Time**	**Upper**	**Lower**	**Total Gate Opening, ft**
4/1/2010	0:00	12.2	29.5	79.00
4/1/2010	1:00	12.2	29.5	79.00
4/1/2010	2:00	12.2	29.5	79.00
4/1/2010	3:00	12.2	29.5	79.00
4/1/2010	4:00	12.2	29.5	79.00
4/1/2010	5:00	12.2	29.5	79.00
4/1/2010	6:00	12.2	29.5	79.00
4/1/2010	7:00	12.2	29.5	79.00
4/1/2010	8:00	12.2	29.5	79.00
4/1/2010	9:00	12.2	29.4	79.00
4/1/2010	10:00	12.2	29.4	79.00
4/1/2010	11:00	12.1	29.4	79.00
4/1/2010	12:00	12.1	29.4	76.00
4/1/2010	13:00	12.2	29.3	76.00
4/1/2010	14:00	12.2	29.2	76.00

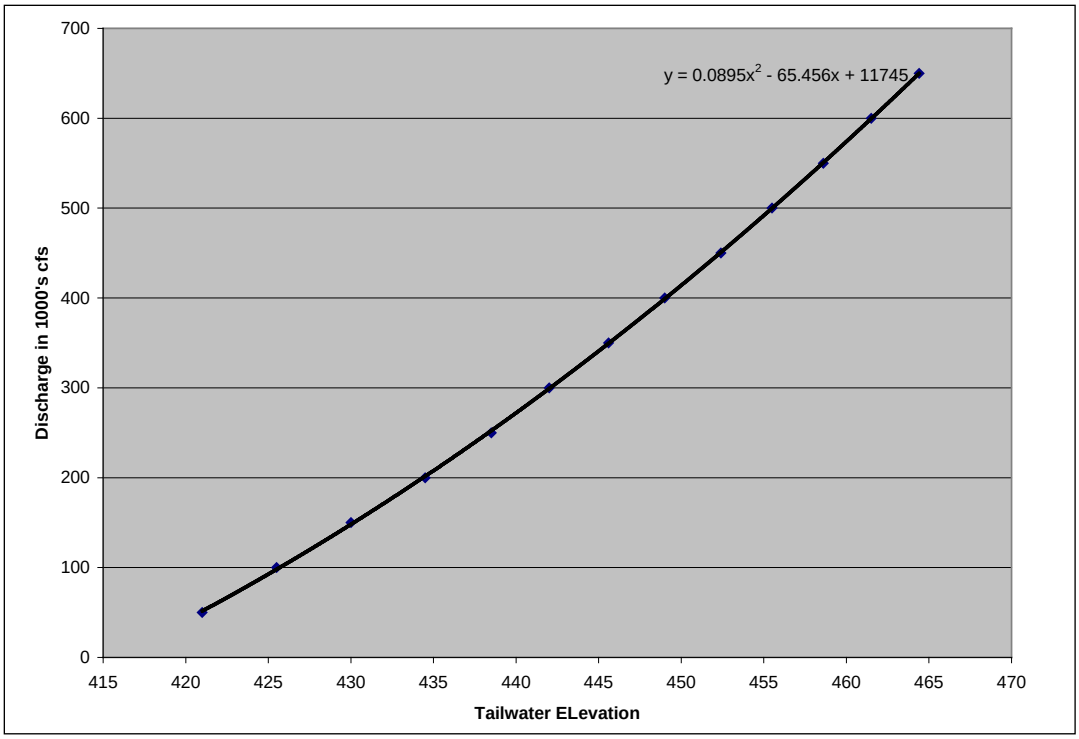

Figure 2.7. Markland Dam tailwater rating curve from model report.

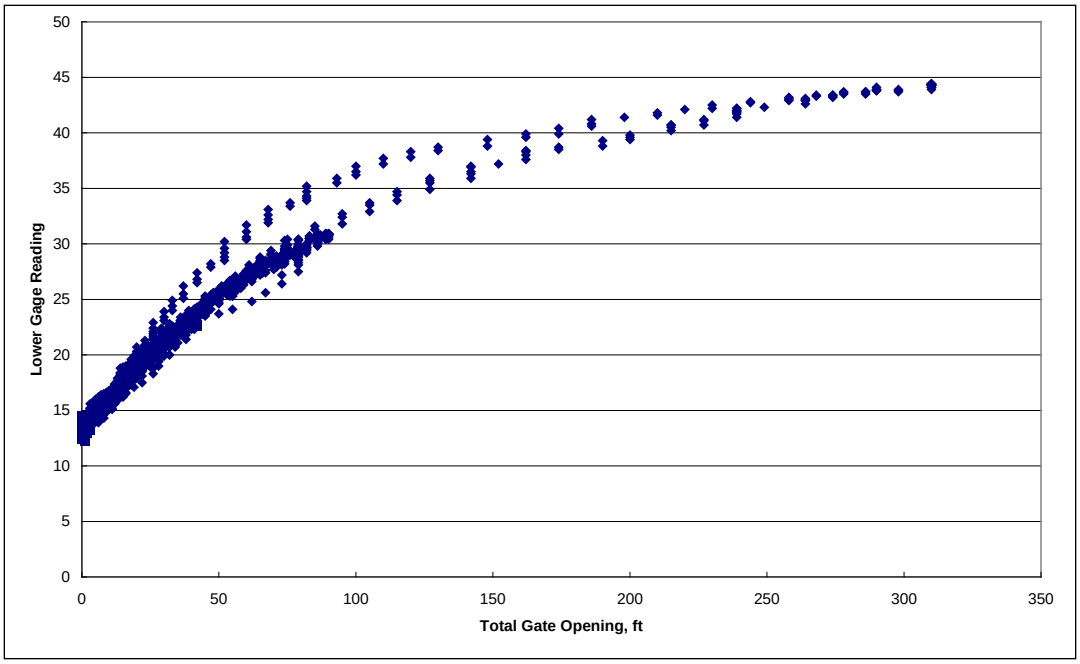

Figure 2.8. Lower gage reading versus total gate opening for OMNI data at Markland Lock between 1 April and 10 October 2010.

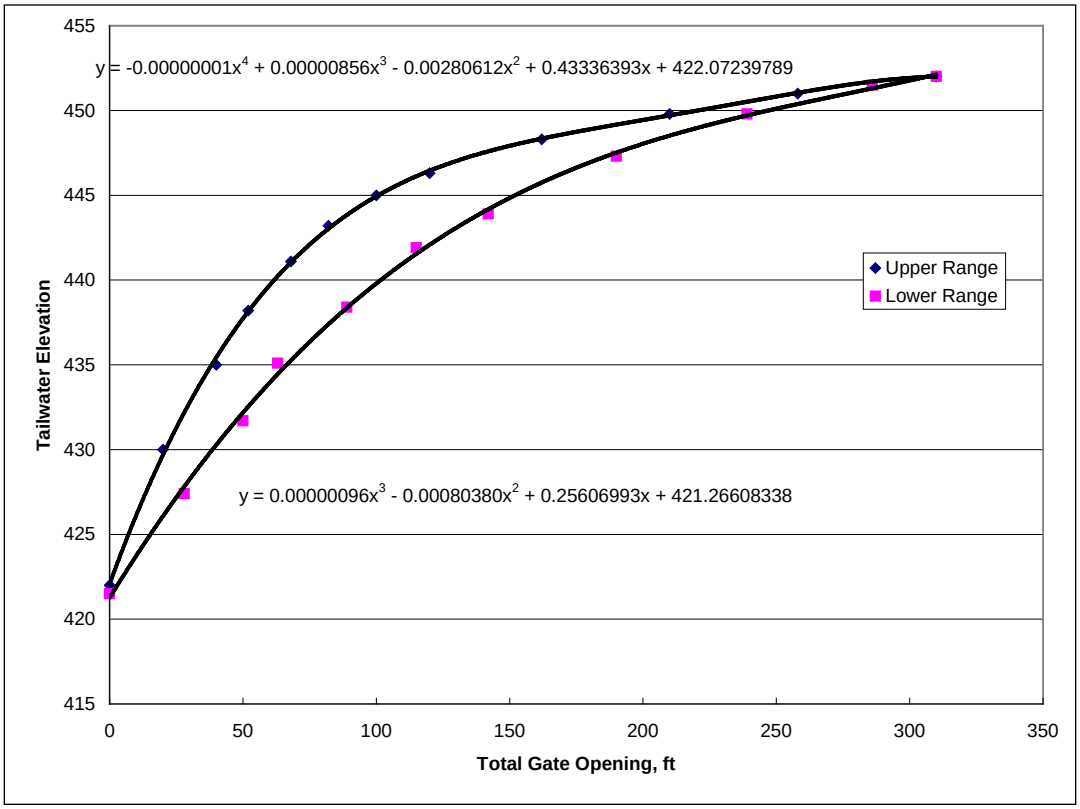

Figure 2.9. Computed upper and lower bounds for tailwater el versus total gate opening for Markland OMNI data.

Table 2.2. Velocities at bullnose from developed from OMNI data and model report.

Actual TW EL	Upper Range Computed TW EL	Lower Range Computed TW EL	Upper Range Discharge 1000's cfs	Lower Range Discharge 1000's cfs	Upper Range Velocity at Bullnose ft/sec	Lower Range Velocity at Bullnose ft/sec
437.5	442.6	437.0	307	232	5.9	4.5
437.5	442.6	437.0	307	232	5.9	4.5
437.5	442.6	437.0	307	232	5.9	4.5
437.5	442.6	437.0	307	232	5.9	4.5
437.5	442.6	437.0	307	232	5.9	4.5
437.5	442.6	437.0	307	232	5.9	4.5
437.4	442.6	437.0	307	232	5.9	4.5
437.2	442.2	436.5	302	226	5.8	4.3
437.2	442.2	436.5	302	226	5.8	4.3
437.2	442.2	436.5	302	226	5.8	4.3
437.2	442.2	436.5	302	226	5.8	4.3
437.1	442.2	436.5	302	226	5.8	4.3
437.1	442.2	436.5	302	226	5.8	4.3
437	441.8	436.1	296	220	5.7	4.2
436.8	441.8	436.1	296	220	5.7	4.2
436.7	441.8	436.1	296	220	5.7	4.2
435.7	440.2	434.5	274	201	5.3	3.7
435.6	440.2	434.5	274	201	5.3	3.7
435.1	439.7	433.9	267	194	5.2	3.5
434.5	438.9	433.3	258	186	5.0	3.3
434.4	438.9	433.3	258	186	5.0	3.3

If one compares the actual tailwater elevation reported in the OMNI database to the computed values for the upper and lower bounds of tailwater, the best estimate of discharge and subsequently velocity, would be the value of the upper or lower bound of computed tailwater that was closest to the actual tailwater. For example, in Table 2.2 for the first entry, the actual tailwater el is 437.5 which is closer to the lower bound of 437. Consequently, the project discharge is closer to 232,000 cfs and the velocity at the bullnose is closer to 4.5 ft/sec.

2.2.3 Tow approach angle and velocity

Personnel from ITL installed an Automatic Identification System (AIS) receiver at Markland to record the AIS transmissions from vessels in the vicinity of the project. The AIS is a shipboard broadcast system that acts like a transponder, operating in the VHF maritime band that is capable of handling well over 4,500 reports per minute and updates as often as every two seconds. Information concerning tow location and speed can be determined from these AIS reports. The information desired from the AIS reports was the tow approach angle when entering the upper lock approach and the tow approach velocity. ITL personnel developed programs to extract this information from the reports. The approach velocity for the tow was considered to be the speed of the tow when it crossed a plane perpendicular to the end of the bullnose. The approach angle was defined as the angle between the true heading of the tow and the guard wall when the tow crossed the plane perpendicular to the end of the guard wall.

During the period from March 31 to October 10, 2010, close to 900 tows with AIS capability used the locks at Markland. The tows of major interest for this investigation were 15 barge tows headed downstream. Approximately 320 tows fell into this category. Figure 2.10 shows the tow approach velocities for the downbound 3 x 5 barge tows. The notation 3 x 5 represents a tow that is 3 barges wide by 5 barges long. Approach velocities over 7 ft/sec were observed with most of the approach speeds between 2.2 and 5.0 ft/sec.

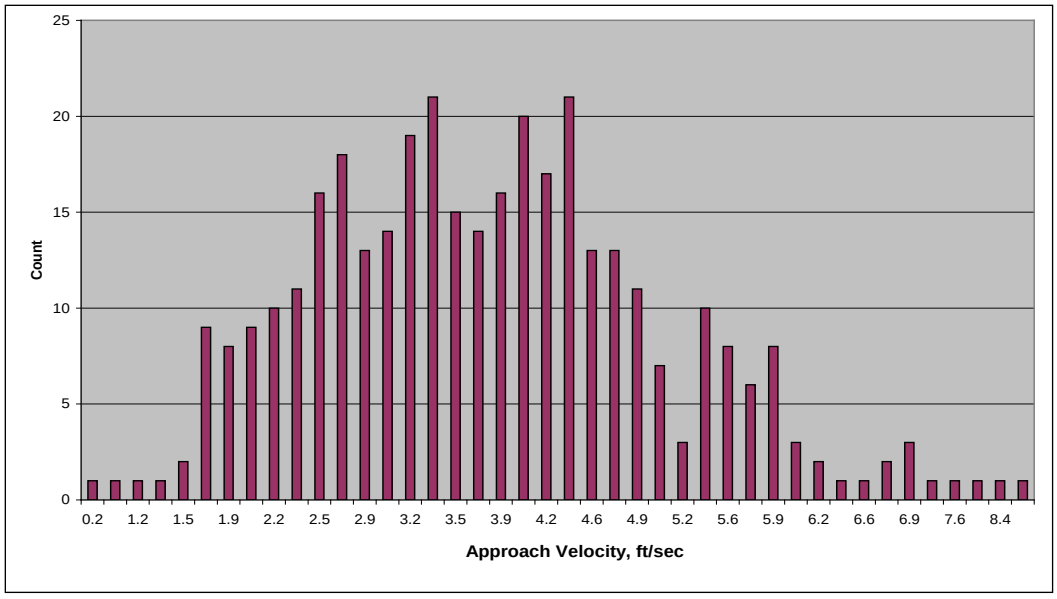

Figure 2.10. Approach velocities determined for downbound 3 x 5 tows at Markland Locks between 1 April and 10 October 2010.

The tow velocity at the bullnose versus the flow velocity at the bullnose was plotted in Figure 2.11 to see if any tends were present. The data indicate that most downbound lockages during this period occurred when the tow approach velocity and flow velocity were less than 5 ft/sec. A plot of tow approach velocity versus the reported tonnage of the cargo is shown in Figure 2.12. The plot shows that most of the tows with tonnage greater than 10,000 approach the lock at less than 6 ft/sec and most of the tows greater than 22,500 approach the lock at less than 5 ft/sec.

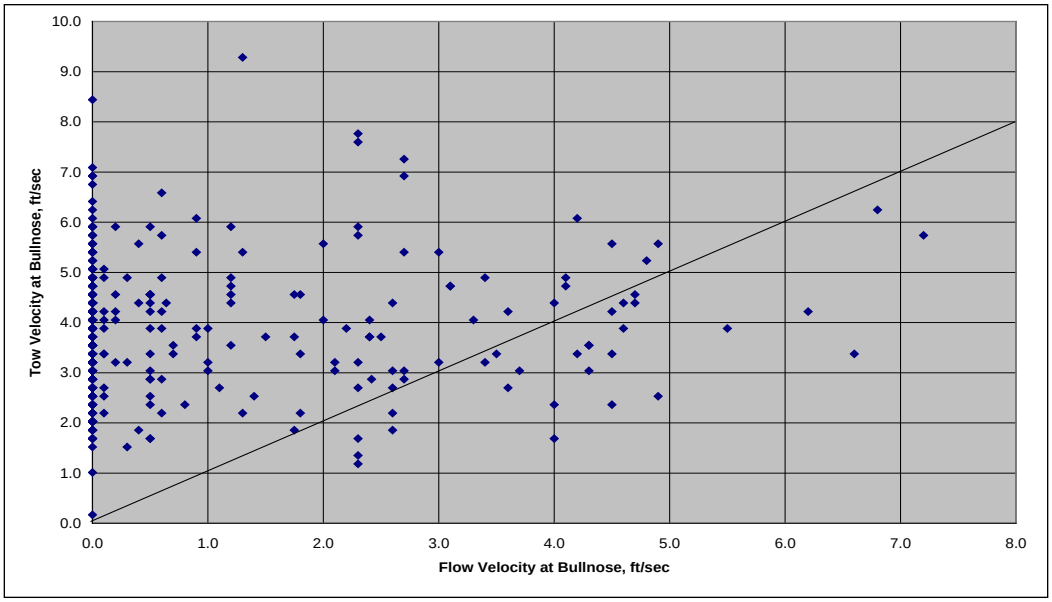

Figure 2.11. Tow velocity versus flow velocity for 3 x 5 downbound barge tows at Markland during 1 April to 10 October 2010.

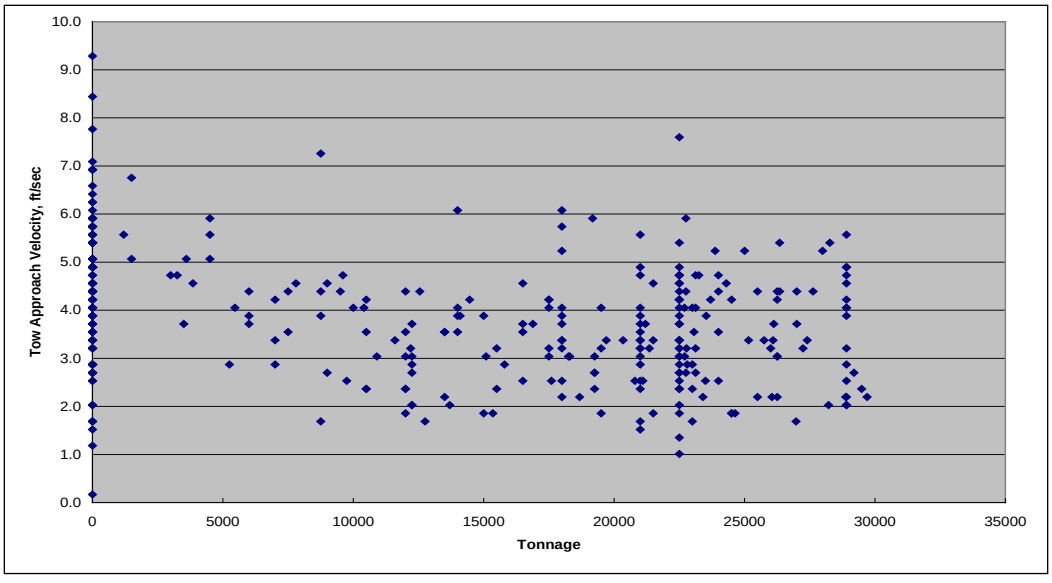

Figure 2.12. Tow approach velocity versus cargo tonnage for 3 x 5 downbound barge tows at Markland during 1 April to 10 October 2010.

2.2.4 Approach angle

The approach angles for the 3 x 5 downbound tows entering the lock approach during 1 April to 10 October 2010 are shown in Figure 2.13. Approach angles between 0 and 5 degrees were the most common during this period. A positive approach angle represents a tow with the stern closer to the left descending bank than the bow and likewise a negative approach angle would be a tow with the bow closer to the left descending bank than the stern. Most landside impacts between the bow of the barges and the bullnose are expected to occur with a positive approach angle.

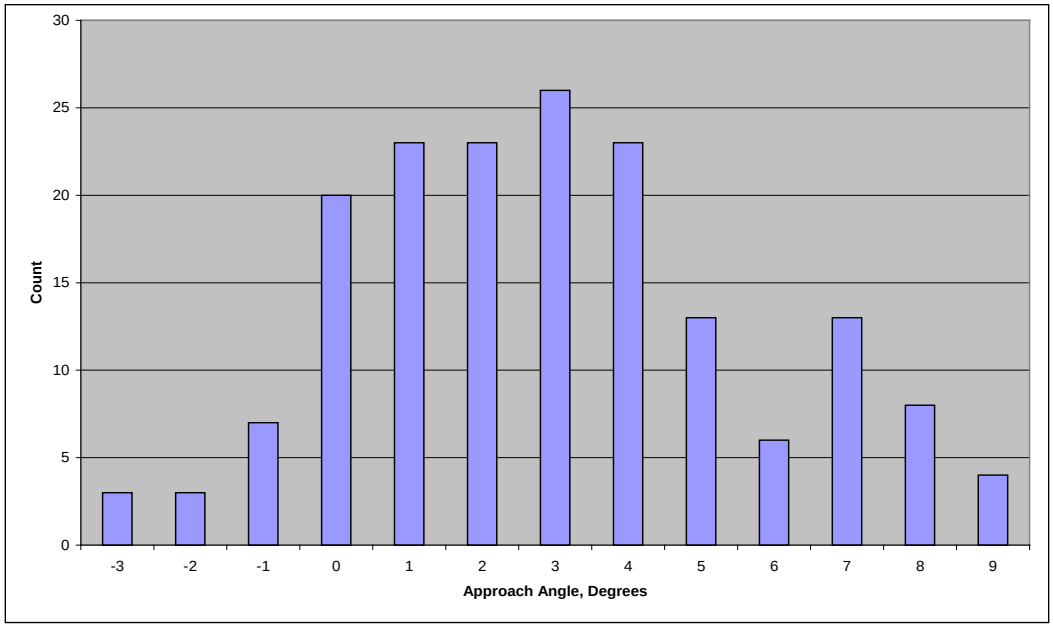

Figure 2.13. Approach angles determined for downbound 3 x 5 barge tows at Markland Locks between 1 April and 10 October 2010.

2.2.4.1 Approach angle limitations based on project geometry

The geometry of the guard wall, the left descending bank, and the tow size can restrict the maximum approach angle. Figure 2.14 depicts an impact between the center of a 3 x 5 barge tow and the center of the bullnose. Further movement of the stern of the tow is limited by the left descending bank when the center of the bow is impacting the bullnose. This approach angle was determined to be 17 degrees. Table 2.3 lists the geometry limited approach angles for a 3 x 5 barge tow impacting the bullnose on the land-side of the guard wall. Approach angles for impacts on the riverside of the bullnose would be small and probably less than 5 degrees, since a tow on this side of the guard wall would be swept quickly toward the dam by the river currents.

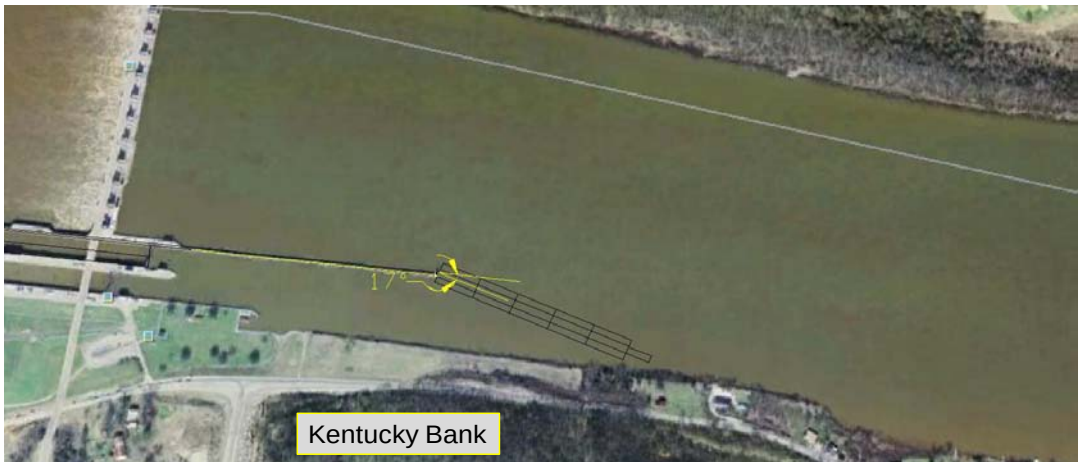

Figure 2.14. Depiction of geometry limited approach angle for 3 x 5 barge tow impacting the bullnose.

Table 2.3. Markland Locks and Dam geometry limited approach angle estimations for a 3 x 5 barge tow based on geometry of left bank.

Barge Impact Point	Wall Impact Point	Impact Angle, Degrees
Front Starboard Corner	Middle of Bullnose	16
Front Port Corner	Middle of Bullnose	20
Middle of Front Barges	Middle of Bullnose	17
Front Starboard Corner	Left Side of Bullnose	14

Tables 2.4-2.7 list the approach angles limited by the left bank for tow sizes of 3 x 4, 3 x 3, 3 x 2, and 3 x 1. Some of the impact angles with the 3 x 1 size tow are not limited by the left bank and are noted as not restricted.

2.2.5 Probability of flow events at Markland Locks and Dam

The Deformable BEAS will be designed for Usual, Unusual and Extreme load conditions, as described in Chapter 1. The Usual, Unusual, and Extreme load condition categories for non site-specific project conditions are defined in Headquarters (2004), ETL 1110-2-563. The discharges associated with the annual probability of exceedence from the ETL were determined for Markland from the plot of discharge versus annual exceedance shown in Figure 2.15. The annual probabilities of exceedence for the Usual, Unusual, and Extreme load conditions recommended in ETL are also shown on the plot.

Table 2.4. Markland Locks and Dam geometry limited approach angle estimations for a 3 x 4 barge tow based on geometry of left bank.

Barge Impact Point	Wall Impact Point	Impact Angle, Degrees
Front Starboard Corner	Middle of Bullnose	17
Front Port Corner	Middle of Bullnose	24
Middle of Front Barges	Middle of Bullnose	21
Front Starboard Corner	Left Side of Bullnose	16

Table 2.5. Markland Locks and Dam geometry limited approach angle estimations for a 3 x 3 barge tow based on geometry of left bank.

Barge Impact Point	Wall Impact Point	Impact Angle, Degrees
Front Starboard Corner	Middle of Bullnose	23
Front Port Corner	Middle of Bullnose	31
Middle of Front Barges	Middle of Bullnose	27
Front Starboard Corner	Left Side of Bullnose	22

Table 2.6. Markland Locks and Dam geometry limited approach angle estimations for a 3 x 2 barge tow based on geometry of left bank.

Barge Impact Point	Wall Impact Point	Impact Angle, Degrees
Front Starboard Corner	Middle of Bullnose	33
Front Port Corner	Middle of Bullnose	45
Middle of Front Barges	Middle of Bullnose	39
Front Starboard Corner	Left Side of Bullnose	31

Table 2.7. Markland Locks and Dam geometry limited approach angle estimations for a 3 x 1 barge tow based on geometry of left bank.

Barge Impact Point	Wall Impact Point	Impact Angle, Degrees
Front Starboard Corner	Middle of Bullnose	Not Restricted
Front Port Corner	Middle of Bullnose	Not Restricted
Middle of Front Barges	Middle of Bullnose	Not Restricted
Front Starboard Corner	Left Side of Bullnose	64

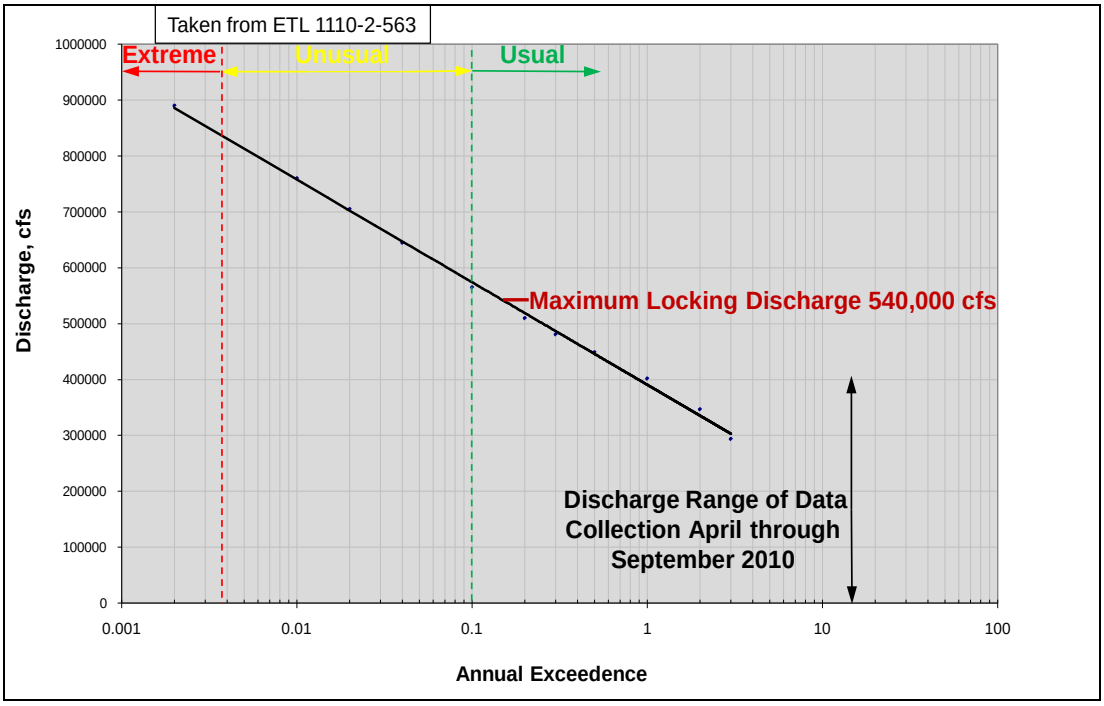

Figure 2.15. Annual exceedence discharge frequencies from ORLED-TH 1998 for Markland Locks and Dam.

Table 2.8 lists these discharges for the Usual, Unusual, and Extreme load condition categories. The site-specific velocities at Markland were estimated for these discharges and were considerably higher than the non site-specific values recommended in the ETL.

The discharge for the Usual load condition ranges from 0 to 565,000 cfs. The current operating practice at Markland is to cease locking for a discharge greater than 540,000 cfs. Based on the recommendations in the

Table 2.8. Usual, unusual, and extreme load condition categories from ETL 1110-2-563 and associated flow conditions at Markland Locks and Dam. *

Load Condition	Annual Probability of Exceedence (Return Period)	Range of Non Site-Specific Approach Velocity, fps	Associated Markland Discharge, 1000's cfs	Markland Site-Specific Flow Velocity at Bullnose, fps (based on ETL Probabilistic Criteria)
Usual	Greater than 0.1	0.5 - 2.0	0 - 565	0 - 7.4
Unusual	0.0033 - 0.1	2.0 - 4.0	565 - 850	7.4 - 8
Extreme	Less than 0.0033	4.0 - 6.0	> 850	> 8

* Cease locking at 540,000 cfs with estimated flow velocity at bullnose of 7.4 ft/sec

ETL and shown in Figure 2.15, all Markland load conditions would therefore fall in the Usual range. This indicates the need for the load conditions to be developed based on site-specific project conditions. The estimated velocity at the bullnose for a discharge of 540,000 cfs is 7.4 ft/sec. The tow velocity with a flow velocity of 7.4 ft/sec would be about 6 ft/sec and would be near the upper limit for the design of the Deformable BEAS. Between 1988 and 2008 there have been 27 documented impacts with the bullnose at the Markland project. Ebeling, et al. (2010) provides additional information on the impacts at this project. The discharges during these 27 impacts were estimated using the technique discussed in section 2.2.2 and then the annual probability of exceedance associated with these discharges were determined from Figure 2.15. The annual probability of exceedance for these 27 impacts were plotted in Figure 2.16. As shown in Figure 2.16, 6 of the 27 impacts occurred with an annual probability of exceedance of 40 which indicates that these impacts occurred under what would be considered normal or non extreme flow conditions. The estimated discharge from Figure 2.15 for an annual probability of exceedance of 40 is approximately 90,000 cfs. Also, all the impacts occurred at annual probabilities of exceedance greater than 0.1. Again, this points out that the flow conditions present when these impacts occurred were not extreme. This is a limited amount of data but it does demonstrate that these impacts occurred at the usual load conditions shown in Figure 2.15.

2.2.6 Estimated load conditions for Markland Locks and Dam

Estimates of velocity and approach angle for Markland need to be determined for the Usual, Unusual, and Extreme load conditions. Ideally, several years' worth of information on flow velocities, approach velocities, and approach angles would provide the best estimates of the load conditions. An example procedure is described here based on the data

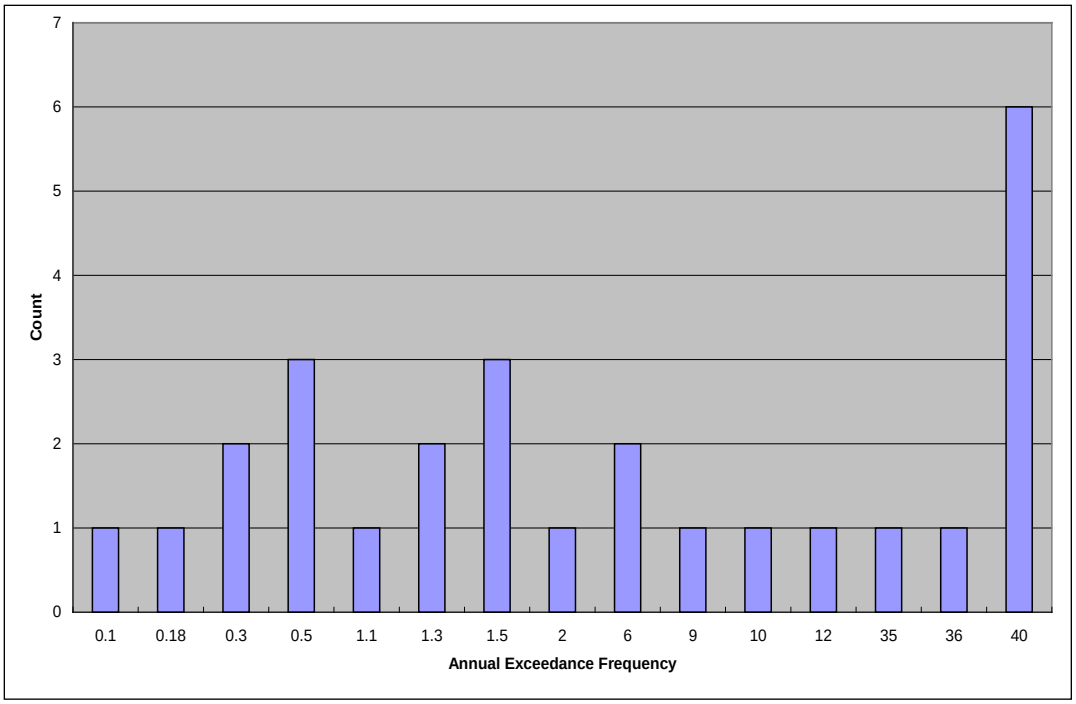

Figure 2.16. Relation between bullnose impacts and flow frequencies between August 1988 and May 2008.

collected between April and October 2010 for the 3 x 5 barge tows. The approach velocities shown in Figures 2.10 and 2.11 indicate that most of the 3 x 5 barge tows enter the upper approach at speeds less than 6 ft/sec. This would be considered the Usual load condition for approach velocity during the period of April to October 2010 based on the data presented in Figures 2.10 and 2.11. The upper range of Usual flow velocity from Figures 2.3 and 2.4 would be around 7 ft/sec. Extreme approach velocities and angles are much more difficult to estimate based on a limited amount of data, and those shown in Table 2.9 are based on the highest recorded during the collection period, regardless of barge tow weight and size.

Table 2.9. Usual, unusual, and extreme estimates for approach velocity and approach angle for Markland Locks and Dam based on data collected for fully loaded 3 x 5 barge tows between April and October 2010. *

Load Condition	Approach Velocity, Fps	Approach Angle, Degrees
Usual	0 to 6	-3 to 6
Unusual	6 to 7.6	6 to 9
Extreme	> 7.6	> 9

* Cease locking at 540,000 cfs with estimated flow velocity at bullnose of 7.4 ft/sec

The approach velocities associated with the extreme approach angles shown in Tables 2.3-2.7 would be in the lower end of the Usual range, especially for fully loaded tows. The tow would be out of shape for the approach and would most likely be in reverse trying to straighten out. If not in reverse, the limited room between the left bank and the guard wall would cause the approach velocity to be low.

2.3 Newt Graham Lock and Dam 18, Verdigris River, Oklahoma

2.3.1 Guide wall condition

The upper guide wall at Newt Graham Lock and Dam 18 on the Verdigris River was severely damaged by an impact with a loaded 10-barge tow in August 2008. The vessel was making an approach and apparently lost control. The rear of the tow moved out to the right (looking downstream) causing the bow to move toward the landside of the approach. The tow hit hard on the curved section of the short guide wall. The tow broke apart and some barges went into the lock chamber. The river flow was between 12,000-14,000 cfs and the speed of the tow was estimated to be between 5-7 mph (7.3 and 10.3 ft/sec).

An aerial view of the project is shown in Figure 2.17 and the upper approach to the lock chamber is shown in Figures 2.18 and 2.19. Figure 2.19 shows some of the damage to the guide wall. A view of the damage to the barges that hit the wall is shown in Figure 2.20. The Tulsa District was considering a Deformable BEAS as a possible replacement for the damaged guide wall.

The lock chamber is nominally 600 ft long and 110 ft wide, and a typical barge tow is 3 wide by 4 long. Two lockages are required for a 3 x 4 barge tow. The normal upper pool elevation ranges from 532.0 to 532.5 and project personnel indicated that a strong outdraft occurs when the discharge reaches 15,000 cfs. The flow information provided to the project users is shown below.

- 0 cfs to 18,000 cfs, normal operations
- 18,000 to 30,000 cfs, modified operations, some impacts
- 30,000 cfs and above, limited to no operations, major impacts

Some of the towing companies do not try to approach the lock when the discharge is greater than 15,000 cfs.

Figure 2.17. Aerial view of Newt Graham Lock and Dam 18.

Figure 2.18. Looking upstream at lock approach to Newt Graham Lock and Dam 18 with floating debris in the channel.

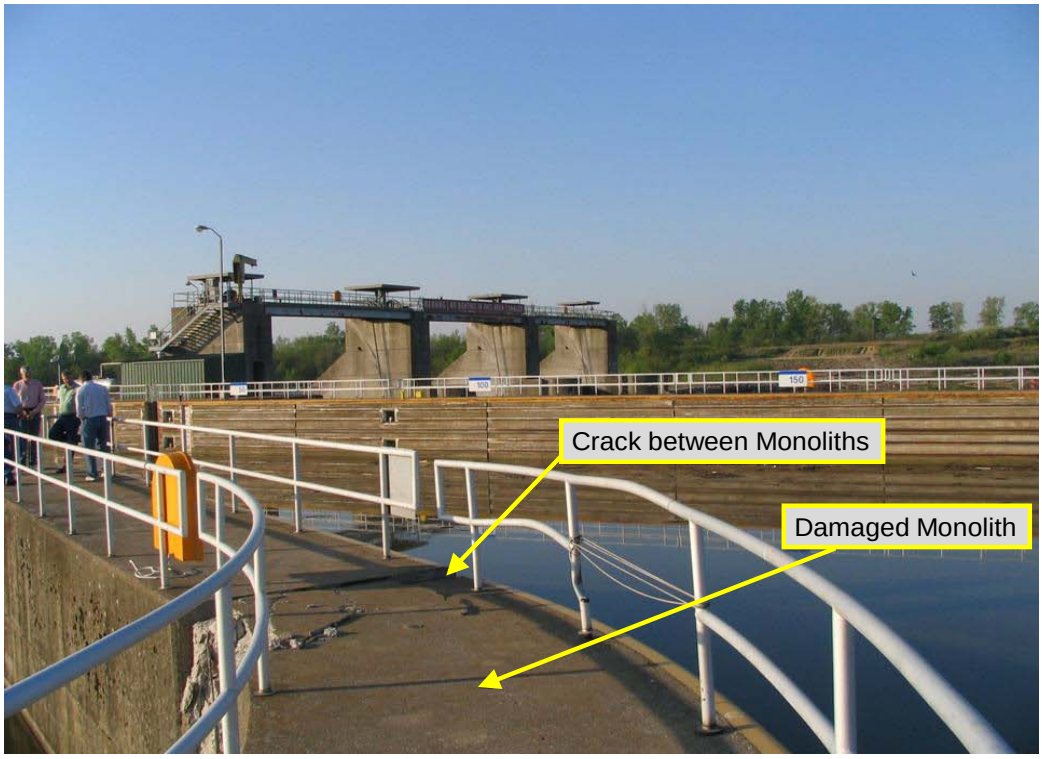

Figure 2.19. Downstream at lock approach to Newt Graham Lock and Dam 18.

Figure 2.20. View of damage to barges that hit the guide wall at Newt Graham Lock and Dam 18.

2.3.2 Approach velocities and approach angles at Newt Graham Lock and Dam 18

Very limited information was available concerning the flow conditions in the upper approach at the lock. The estimated approach velocity of the tow that hit the guide wall was 5 to 7 mph or 7.3 to 10.3 ft/sec, and the discharge was between 12,000 and 14,000 cfs. An approach velocity of 10.3 ft/sec would be considered extreme. Although the project is smaller than Markland, the flow directions and magnitudes in the vicinity of the bullnose would be similar since both have outdraft. Until site-specific velocity data are collected, the velocities shown in Table 2.9 for the Markland project could also be used for estimates of Usual, Unusual, and Extreme approach velocity for the guard wall at Newt Graham Lock and Dam 18.

The flow conditions near the end of the guide wall are quite different than those at the end of the guard wall. The outdraft condition at the end of the guard wall causes a low velocity circulating flow (eddy) in the upper lock approach. The flow direction near the end of the guide wall is generally upstream and the velocity magnitude is low. Current directions and velocities shown in Franco and Shows (1968), Franco and McKellar (1968), and Franco and Shows (1971) for lock and dams on the Arkansas River show upstream velocities ranging from less than 0.5 to 1.4 ft/sec near the end of the guide wall. The tow velocities would also be low in this area since the tow would be slowing down to prepare for entrance into the lock.

Table 2.10 shows estimates of the Usual, Unusual, and Extreme approach flow velocities based on a review of similar upper approach conditions for Arkansas River locks. The tow approach velocities were estimated at one half of those determined from the Markland lock approach velocity study. The Usual, Unusual and Extreme approach angle estimates were determined using the geometry limited approach angles for a 3 x 4 barge tow.

Table 2.10. Usual, unusual, and extreme estimates of approach velocity and approach angle for impacts with Newt Graham Lock and Dam 18 guide wall based on generalized approach conditions for similar projects with outdraft on the Arkansas River.

Load Condition	Flow Velocity, Fps **	Approach Velocity, Fps	Approach Angle, Degrees
Usual	0 to -0.5	0 to 3	-3 to 3
Unusual	-0.5 to -1.5	3 to 4.5	4.5 to -4.5
Extreme	> -1.5	> 4.5	-6 to 6

** Negative flow velocities denote upstream velocity and is due to eddy condition between guard wall and guide wall

The approach angles limited by project geometry for the different size barge tows are listed in Tables 2.11-2.14 for impacts with the guide wall and guard wall. Figure 2.21 shows the front center of a 3 x 4 barge tow impacting the end of the guide wall.

2.4 Summary of approach angle and velocity investigation

The information provided in this chapter for the Markland Project is based on data received from the Louisville District and data collected during April to October 2010. It is intended to serve as a guide for the process of determining approach angles and velocities at a project. A project considering the use of a Deformable BEAS should try to collect at least one year of traffic data in the upper approach to determine better estimates for approach angles and approach velocities to capture seasonal differences in flow and traffic. The estimates for the Newt Graham Lock and Dam 18 are based on very limited information and it is recommended that an approach angle and velocity investigation should be conducted at this site if the Deformable BEAS is chosen as the guide wall replacement.

Table 2.11. Newt Graham Lock and Dam 18 geometry limited approach angle estimations for a 3 x 4 barge tow.

Approach Angle Estimations for Guide Wall and Left Bank		
Barge Impact Point	**Wall Impact Point**	**Impact Angle, Degrees**
Front Starboard Corner	U/S End of Guide Wall	Not Possible
Front Port Corner	U/S End of Guide Wall	6
Middle of Front Barges	U/S End of Guide Wall	1
Approach Angle Estimations for Guide Wall and Guard Wall		
Front Starboard Corner	U/S End of Guide Wall	-17
Front Port Corner	U/S End of Guide Wall	-6
Middle of Front Barges	U/S End of Guide Wall	-11
Approach Angle Estimations for Guard Wall Bullnose and Left Bank		
Front Starboard Corner	Middle of Bullnose	10
Front Port Corner	Middle of Bullnose	18
Middle of Front Barges	Middle of Bullnose	14

Table 2.12. Newt Graham Lock and Dam 18 geometry limited approach angle estimations for a 3 x 3 barge tow.

Approach Angle Estimations for Guide Wall and Left Bank		
Barge Impact Point	**Wall Impact Point**	**Impact Angle, Degrees**
Front Starboard Corner	U/S End of Guide Wall	Not Possible
Front Port Corner	U/S End of Guide Wall	7
Middle of Front Barges	U/S End of Guide Wall	2
Approach Angle Estimations for Guide Wall and Guard Wall		
Front Starboard Corner	U/S End of Guide Wall	-17
Front Port Corner	U/S End of Guide Wall	-6
Middle of Front Barges	U/S End of Guide Wall	-11
Approach Angle Estimations for Guard Wall Bullnose and Left Bank		
Front Starboard Corner	Middle of Bullnose	14
Front Port Corner	Middle of Bullnose	23
Middle of Front Barges	Middle of Bullnose	19

Comparison of Tables 2.8 and 2.9 show the differences between the load conditions based on the information in the ETL and the limited amount of velocity and approach angle data obtained at Markland. In Figure 2.12, the data shown for tonnage equal to or greater than 22,500 represent loaded 3 x 5 barge tows with drafts of at least 9 ft. Most of these barge tows approach the lock at velocities less than 6 ft/sec. There is one that approaches at 7.6 ft/sec. As mentioned in section 2.2.1, approaching tows usually stay close to the Kentucky side and start slowing down once the head of the tow is inside the guard wall. Looking at the range of velocities shown in Figure 2.12, the higher approach velocities are probably barge tows closer to the bank and the slower velocities are those closer to the guard wall.

Table 2.13. Newt Graham Lock and Dam 18 geometry limited approach angle estimations for a 3 x 2 barge tow.

Approach Angle Estimations for Guide Wall and Left Bank		
Barge Impact Point	**Wall Impact Point**	**Impact Angle, Degrees**
Front Starboard Corner	U/S End of Guide Wall	Not Possible
Front Port Corner	U/S End of Guide Wall	9
Middle of Front Barges	U/S End of Guide Wall	2
Approach Angle Estimations for Guide Wall and Guard Wall		
Front Starboard Corner	U/S End of Guide Wall	-21
Front Port Corner	U/S End of Guide Wall	-7
Middle of Front Barges	U/S End of Guide Wall	-15
Approach Angle Estimations for Guard Wall Bullnose and Left Bank		
Front Starboard Corner	Middle of Bullnose	21
Front Port Corner	Middle of Bullnose	32
Middle of Front Barges	Middle of Bullnose	26

If one were to assign Usual, Unusual, and Extreme load conditions for this data in Figure 2.12, the approach velocity of 6 ft/sec would be the maximum value of the Usual range (Table 2.9). This value is much higher than the 2.0 ft/sec maximum, non-site specific velocity shown in Table 2.8 for the Usual load condition based on ETL 1110-2-563 guidance. This discrepancy points out the need to obtain extended periods of site-specific velocity information for projects considering installation of a Deformable BEAS. Tow tracks would also be useful to help decide appropriate approach velocity information. Barge tows at the Markland project approaching near the bank would be much less likely to impact the bullnose, especially for a head-on collision.

Table 2.14. Newt Graham Lock and Dam 18 geometry limited approach angle estimations for a 3 x 1 barge tow.

Approach Angle Estimations for Guide Wall and Left Bank		
Barge Impact Point	**Wall Impact Point**	**Impact Angle, Degrees**
Front Starboard Corner	U/S End of Guide Wall	Not Possible
Front Port Corner	U/S End of Guide Wall	18
Middle of Front Barges	U/S End of Guide Wall	3
Approach Angle Estimations for Guide Wall and Guard Wall		
Front Starboard Corner	U/S End of Guide Wall	-35
Front Port Corner	U/S End of Guide Wall	-15
Middle of Front Barges	U/S End of Guide Wall	-26
Approach Angle Estimations for Guard Wall Bullnose and Left Bank		
Front Starboard Corner	Middle of Bullnose	36
Front Port Corner	Middle of Bullnose	56
Middle of Front Barges	Middle of Bullnose	47

Figure 2.21. Depiction of geometry limited approach angle for 3 x 4 barge tow impacting the guide wall.

3 Three-by-Five Barge Train Impacts With Deformable BEAS

3.1 Introduction

This chapter summarizes the verification made of the dBEAS program which simulates barge train impact with a Deformable BEAS structure. It also discusses the parametric studies made of impact events between a three-by-five fully ballasted barge train and Deformable BEAS of various structural characteristics. The Chapter 2 studies that showed the physical conditions and statistical studies of barge traffic for Markland Lock and Dams helped to establish the approach angles and velocities used in these simulations. Both head-on and glancing blow impacts with Deformable BEAS of different characteristics were studied so that essential structural requirements and demand characteristics can be established for a Deformable BEAS subjected to impacts with a three-by-five barge train. Conclusions are reached, based on these results that will influence the design of the Deformable BEAS for the three-by-five design barge train.

3.2 Load Conditions

ETL 1110-2-563 establishes the three impact event load cases that the Deformable BEAS is to be designed for. They are designated as the Usual, Unusual and Extreme load conditions and their respective performance criteria are discussed in Chapter 1. Recall that the non-site specific approach velocities listed in Table 3.1 were developed originally for the design of approach walls for glancing blow events. After careful consideration and until additional data becomes available, these values for non-site specific approach velocities have been adopted for the majority of the extreme impact simulations made in this chapter. The April through September 2010 approach velocity information collected at Markland Lock & Dams is being used to supplement the Table 3.1 values; particularly the forward velocity values.

The Chapter 2 studies showed that the Table 3.1 non-site specific forward approach velocity conditions does not provide reasonable expectations for what the Deformable BEAS would have to endure for the Markland site for the (wide) spectrum of barge train masses. Referring to the data contained in Figures 2.10 and 2.11, while higher velocities occurred (i.e., forward

Table 3.1 Ranges in non-site specific approach velocities, expressed in local barge coordinates for preliminary analyses (ETL 1110-2-563).

Load Condition	Forward Velocity V_x (fps)	Lateral Velocity V_y (fps)
Usual	0.5-2.0	0.01-0.1
Unusual	3.0-4.0	0.4-0.5
Extreme	4.0-6.0	>1.0

approach velocities above the Table 3.1 upper range of 6 fps for the extreme load case), these higher velocities were rare for this six months of data collection and usually involved barge trains that were not fully loaded. The design impact for Markland is envisioned to be a three-by-five, fully ballasted barge train. In this case, a maximum six feet per second approach appears to be reasonable.

3.3 Barge train

The efforts to model the barge train involved the modeling of lashings and of the barges themselves. Physical studies of lashing strength and finite element (FE) modeling of barges provided non-linear curves describing the properties that needed to be modeled.

3.3.1 Lashings

Tests were performed to find the Stress-strain relationship for individual lashings. These findings were discussed in Ebeling et al. (2010). Figure 3.1 shows the typical force-strain curve for a lashing, as recorded from pull test results. The vertical axis reports the force in the wire rope normalized by the maximum force of 115,690 lbs that was recorded during this pull test. This force-strain curve was recorded for one inch lashing cable. This lashing curve was used to determine forces between barges in the simulation as they pulled apart from each other.

As the cable was stretched, the force exerted by the cable grew until groups of strands or individual strands gave under the strain. This can be seen most effectively in Figure 3.1 at the approximate strains of 0.06, 0.095, and 0.108. Observe that after each strand ruptured, the cable then began to build force until the next separation. For the purposes of our simulations, we considered our lashing to be “damaged” at a strain of 0.06, and “broken” at a strain of 0.13.

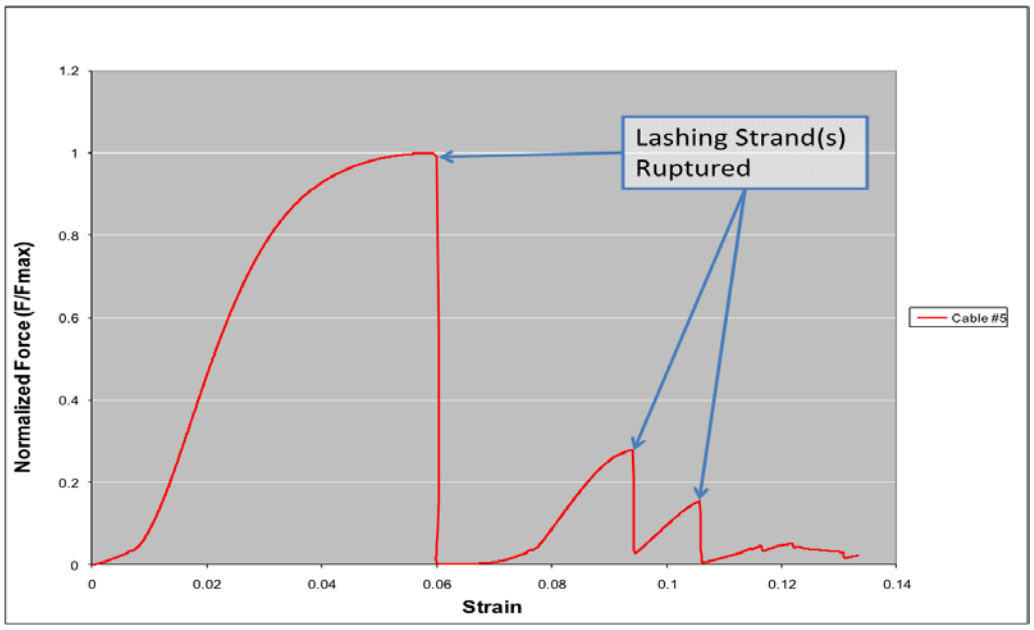

Figure 3.1 Normalized Force versus Strain Curve Recovered from a Pull Test for a 1-inch lashing cable. The maximum recorded force was 115,690 lbs.

3.3.2 Barges

Barges were initially modeled as rigid bodies that directly followed the laws of momentum over a single time step of the simulation. Because the time steps for the simulation would be very small by necessity, this model was unnecessarily stiff, and would lead to an extreme force when applied over a single time step. From Ebeling and Warren (2008, 2009), it is seen that these results are unrealistic, as the barge will deform over time. To more accurately model the impulse mechanics of the barge, a simplified deformable barge model was constructed that treated the sides of barges as springs connected to the center of mass of the barge (Figure 3.2b).

The springs of this simple deformable barge model were given a single K value corresponding to an approximation of the elastic deformation of the barge modeled using nonlinear finite elements by Ebeling and Warren (2008, 2009). The K values assigned to the barge model used in the current Deformable BEAS study were the same for the port and starboard of the barge, but were adjusted for the bow and stern based on the steel plate and steel angles supporting structural members of a barge and considering the cargo hold (open space) area. For Figure 3.3 (Ebeling and Warren, 2009), which measures head-on impact for the rake of a barge, the measured K value in the elastic portion of deformation would be about 1,440 kips per inch. From a similar (Ebeling and Warren, 2008) chart(s) for the side impact of the barge, the measured K value was given as 2,520 kips per inch.

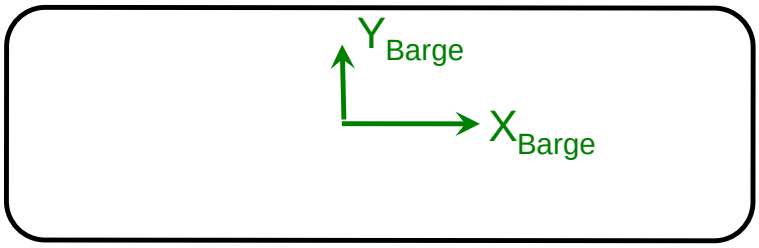

a) Rigid barge description

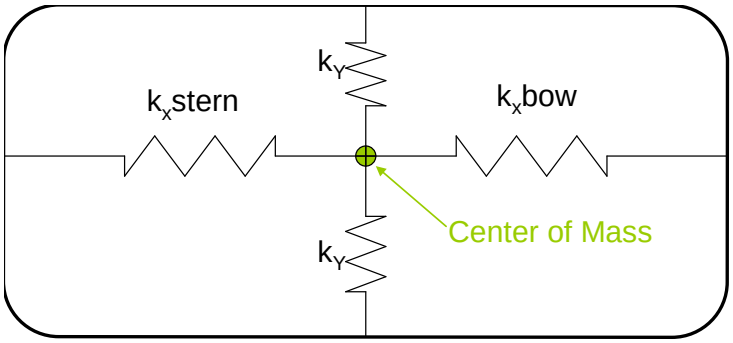

b) Spring barge description

Figure 3.2 Coordinate system and model for barge response.

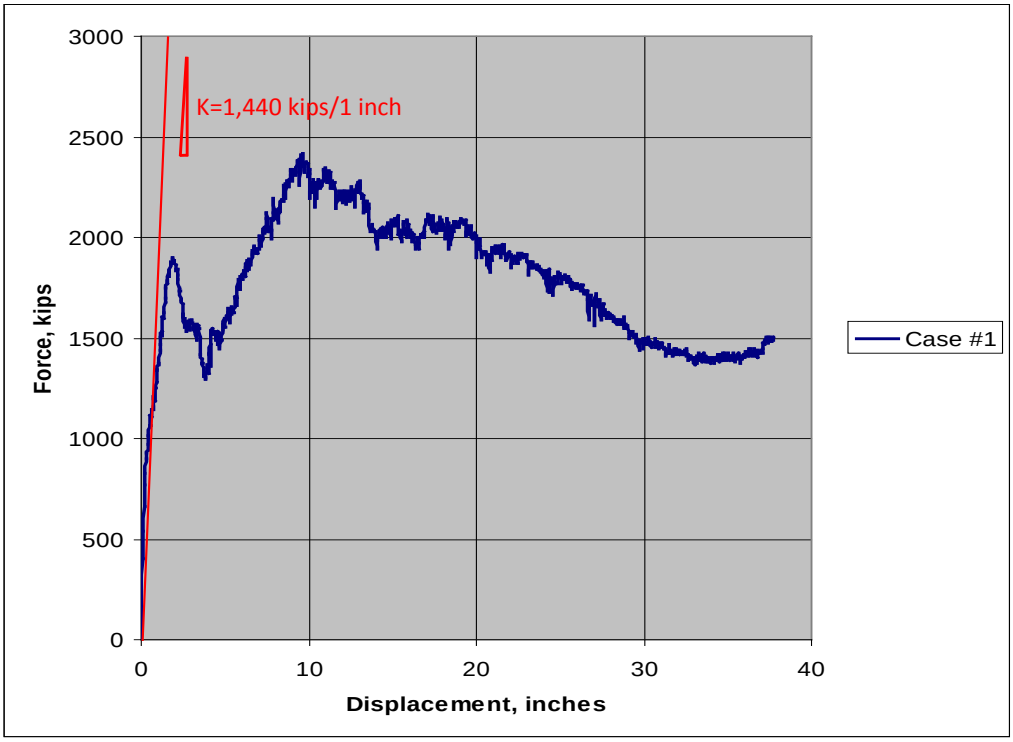

Figure 3.3. Force versus displacement of the initial contact point of the bow for the Ebeling and Warren (2009) Case No. 1 impact with a 20 feet diameter bullnose at 2 feet/sec. Overlaid in red is a K slope for the barge bow deformation.

The "stiffness" of cargo carried by the barge was also considered in determining the K values assigned to the different directions of the barge. By using the material properties of coal, which is the typical cargo for Markland barges, it was possible to approximate the stiffness of the cargo for the port/starboard, bow, and stern regions of the barge.

The estimate for a low-strain shear wave velocity (V_s) for coal is 400 feet per second and the unit weight (γ) is 90 pounds per cubic foot (American Institute of Steel Construction, 1989). From this, it was determined that the shear modulus (G) of the coal is 3.108 kips per square inch. Given the area (A) of the loaded sides of the barge (bow to center, stern to center, port to center, and starboard to center) and the shear modulus, it is possible, using the equations for shear stress(τ) and shear force(V), to determine the stiffness of the coal in that area. The relationships used are given by the following equations:

$$\tau = \frac{V}{A} = G\gamma = G\frac{u}{h} \tag{3.1}$$

and

$$V = GA\frac{u}{h} = ku \tag{3.2}$$

yields

$$K = \frac{GA}{h} \tag{3.3}$$

For example, for a Jeffboat open hopper barge with a rake bow that is loaded with coal, the shear modulus for the coal could be computed for the area of the coal in the bow region of the barge (i.e., from bow to centerline) using the dimensions given in Figure 3.4. Using the preceding equations, $K_{Coal,Bow}$ is computed to be 8,702.4 kips per inch.

$$K_{Coal,Bow} = \frac{GA}{h} = \frac{(3.108)(403{,}200)}{144} = 8702.4 \ kips/inch \tag{3.4}$$

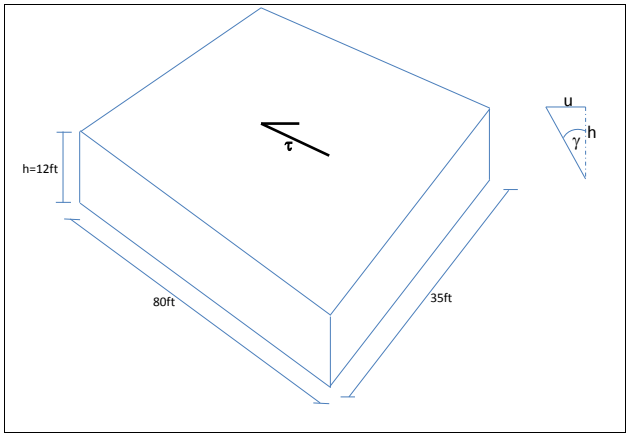

Figure 3.4 Determining the stiffness of the load in a loaded barge.

For a barge with a box bow, the length dimension from the bow to the centerline of the barge would be 90 feet instead of 80, and the calculation would have to be redone.

The cargo stiffnesses are then combined in parallel with the stiffness of the hopper portion of the barge structure in the direction (port/starboard, bow, and stern) to determine the combined stiffness of the hopper and cargo. The stiffness of the barge hopper is combined in series with the stiffness of the rake, if the barge has a rake in that direction. In this way, stiffness can be determined for each of the cardinal directions of the barge. Figure 3.5 shows how the stiffnesses are combined (and their equations) for the rake portion at the bow of a barge.

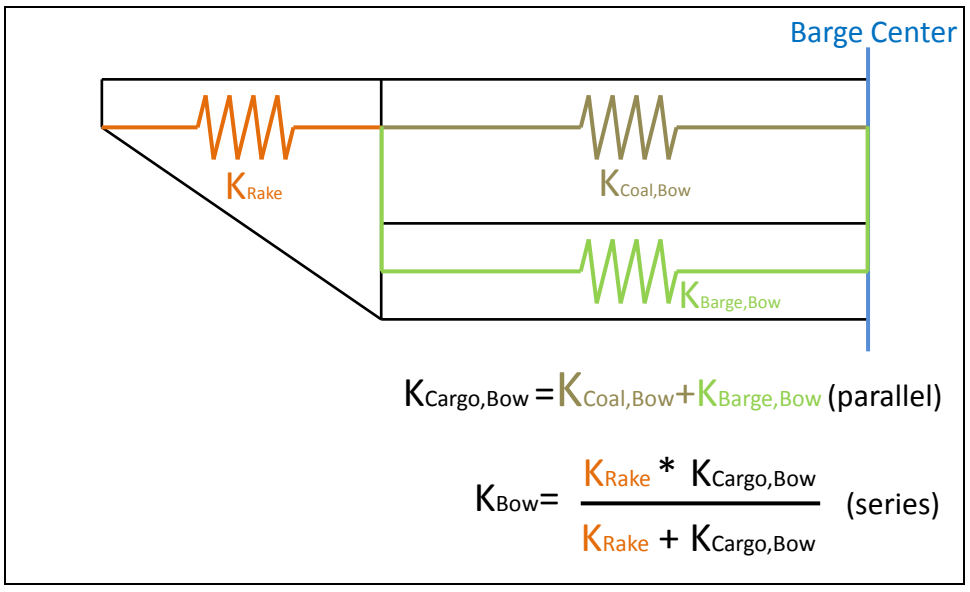

Figure 3.5 The spring model for the rake portion at the bow of the barge.

The stiffness of the barge in a box/hopper region, ($K_{Barge,Bow}$), was approximated as half the stiffness of the front rake section (K_{Rake}). This yields

$$K_{Cargo,Bow} = K_{Coal,Bow} + K_{Barge,Bow} = 8702.4 + 720 = 9422.4 \; kips / inch \quad (3.5)$$

$$K_{Bow} = \frac{K_{Rake} * K_{Cargo,Bow}}{K_{Rake} + K_{Cargo,Bow}} = \frac{(1440) * (9422.4)}{(1440) + (9422.4)} = 1249.1 \; kips / inch \quad (3.6)$$

These composite stiffness values indicate only a moderate change from the original stiffnesses for the barge alone. The default values assigned to the typical open hopper barge were stiffnesses (K) for the bow and stern of 1,440 kips per inch and for port and starboard of 2,520 kips per inch for the dBEAS program.

3.4 Base isolator properties

Figure 3.6 shows the bilinear curve that represents the base isolator response, interpreted from tests performed by Dynamic Isolation Systems and Bridgestone. In a phone conversation made on 28 April 2010, Dynamic Isolation Systems stated that base isolators could be made within a range +/-40% of this figure's stiffness.

3.4.1 Softening the effects of stiffness

Simulations, discussed later in this chapter, revealed that less stiff systems gave better results during the impact event. As a result, the stiffness relationship was lowered to 60% of the values shown in Figure 3.6, as recommended by Dynamic Isolation Systems. This "softened" base isolator material model was created by multiplying the force magnitudes of the Figure 3.6 curve by 0.6 but leaving the deflections unchanged. For instance, at the "hinge" point of 2.33 feet, instead of a force of 315 kips acting on the base isolator, the force would be 189 kips (= 0.6 * 315 kips).

3.4.2 Stacking base isolators

Base isolators can be stacked by bolting their retaining rings together. Stacked base isolators would have a lower stiffness because their overall displacement would be greater for the same lateral (i.e., shear) force. Stacked base isolators are modeled by multiplying the displacements of the curve in Figure 3.6 by the number of base isolators in the stack while

maintaining the same force value. For instance, for a stacked base isolator of height 2, the hinge point force of 315 kips would be acting at a displacement of 4.66 feet (= 2 * 2.33 feet), at the top of the stack.

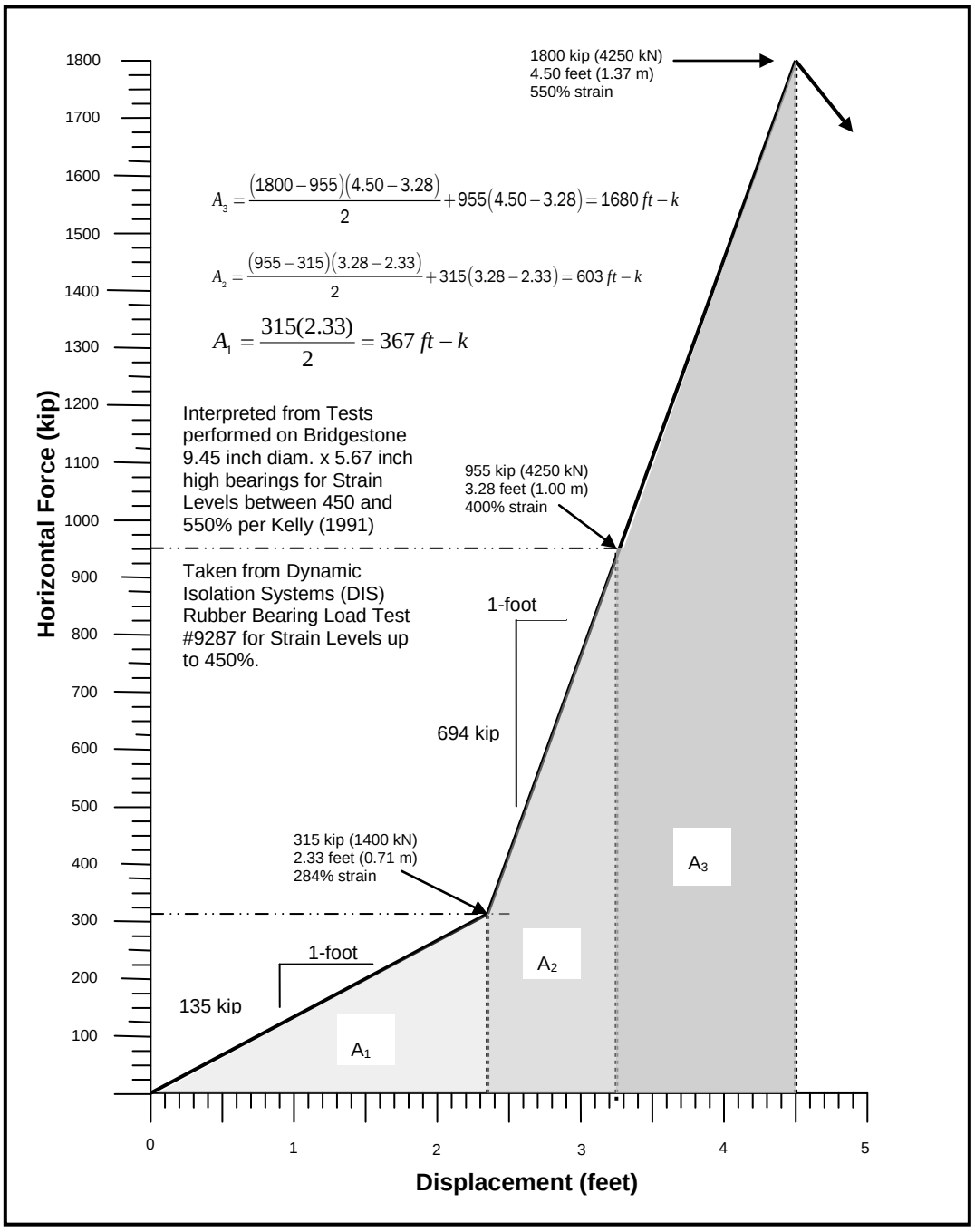

Figure 3.6 Single isolator spring stiffness – tri-linear approximation.

3.5 Deformable BEAS design

Figure 3.7 shows the Deformable BEAS design that is used in this chapter. It possesses a "stiff" concrete arch reinforced concrete structure at the front of the impact nosing of the Deformable BEAS. Observe in the section view that a top deck runs from the front of the arch to the last vertical wall and is 3 feet thick.

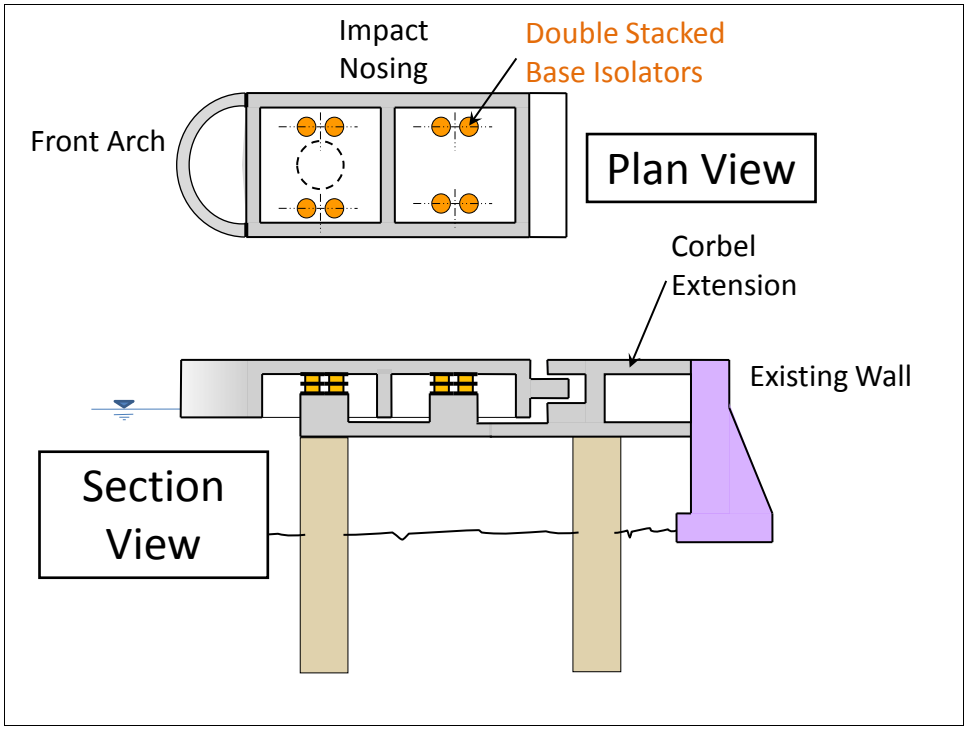

Figure 3.7 A single-part impact nosing with stacked base isolators.

Preliminary dimensions for an impact nosing being investigated using the analyses discussed in this chapter is presented in Figure 3.8. The total weight of this impact nosing monolith section would be 762 tons.

3.6 Testing and validation of dBEAS

To test and validate the simulation code for dBEAS, it was necessary to determine the range in impacts that the program would be primarily required to solve. Since most impacts would be of a glancing blow variety, it was determined that an appropriate test case would be of a barge train approaching the bullnose at a steep angle, based on the impact nosing geometry, relative to the steepest angle cited in the studies of Chapter 2. This angle for Markland was 9-16 degrees. The 9 degree impact is shown in Figure 3.9 (a). The lashing layout is shown in green, designating lashings

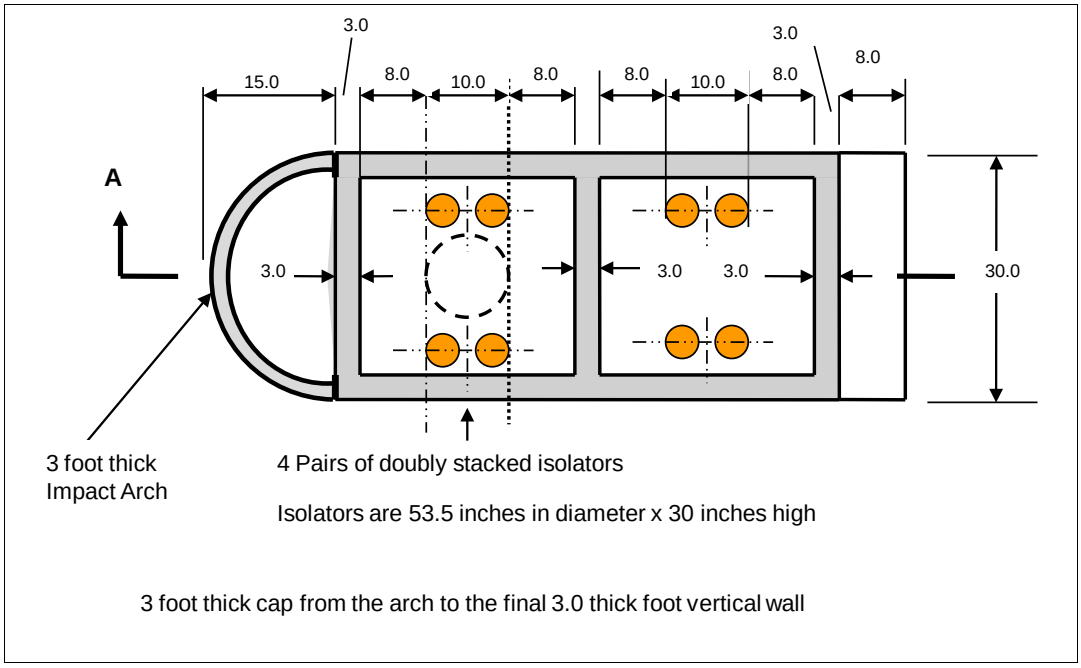

Figure 3.8 Dimensions (in feet) of a proposed impact nosing for a Deformable BEAS.

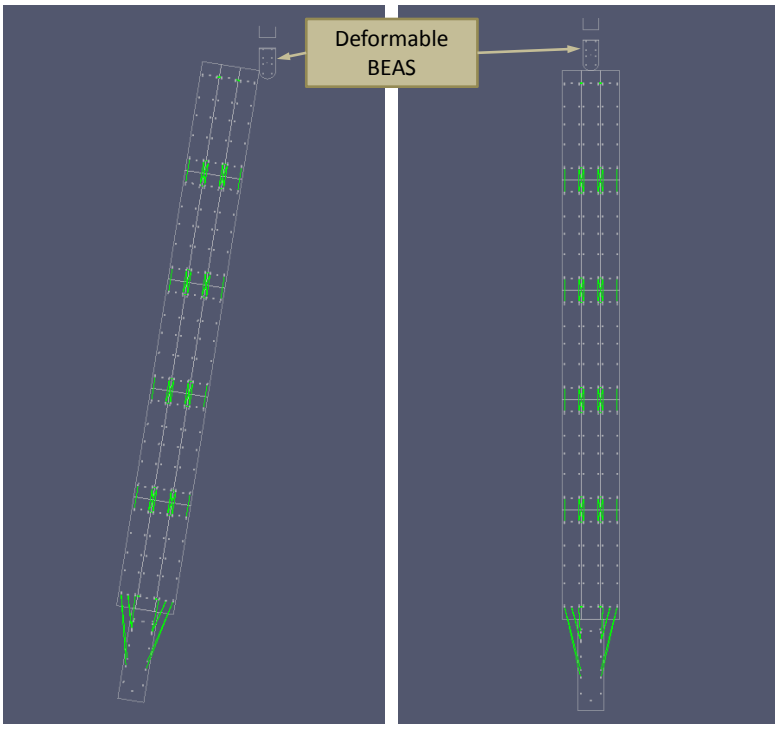

Figure 3.9 (a)Glancing Blow and (b)Head-on Impacts.

that are undamaged. The other case of focus would be the head-on impact of a barge along the center-line of the bullnose, as shown in Figure 3.9 (b). As simulations later in this chapter reveal, the head-on impact has the advantage that the maximum impact force against the Deformable BEAS is

correlated to the maximum lashing force due to symmetry of forces about the barge train. Simulations were also performed for barge train impacts where the impact was along the centerline of the bullnose but the points of impact on the barge train were at the center of the starboard barge and the corner of the starboard barge (Figures 3.19 a, b, and c).

Preliminary program executions showed that, even at high velocities, impacts at glancing blow angles on the sides of the impact nosing did not cause any "failures" to the barge train integrity (i.e., the barge train remained intact and under control by the tow boat). In a promising turn, it also showed a reduction in the peak forces between the barge train and the impact nosing. Head-on impacts also showed this reduction in peak forces, but these impacts were more likely to result in the loss of barge train integrity. Therefore, preventing the loss of barge train integrity for a head-on collision with a 3 x 5 fully-loaded barge train under the Usual, Unusual, and Extreme load cases became our goal.

Since dBEAS is a new software development effort, it was necessary to validate the engineering and numerical methods used for the model. The lashing model and the barge stiffness model were gathered from physical tests and FE analysis. The response of the impact nosing to the impact force time-history and the attached base isolators could be verified by comparing a simplified dBEAS 2-degree of freedom (2-DOF) analysis to the single degree of freedom (SDOF) system analysis using Impact-Beam.

3.6.1 Verification using Limit_Lashing

From a parametric study (Arroyo and Ebeling, 2005) using Limit_Lashing software (Arroyo and Ebeling, 2004), Figure 3.10 presents the variation of the maximum impact force normal to the wall for barge train systems 3 x 2, 3 x 3, 3 x 4, and 3 x 5 in a head-on impact. These results are computed using the values listed in Table 3.2 for a 1-inch diameter new wire rope. Pull tests conducted during the course of this research showed the breaking strength of the 1-inch new wire rope presented in the table to be conservative.[1]

Figure 3.10, based on simplified 2005 model studies, shows peak forces for a 3 x 5 barge train with a velocity of 2.7 fps to have a peak impact force of 4,200 kips. This simplified model contained within the Limit_Lashing

[1] The pull tests revealed that the breaking strength for 1-inch new wire rope was 145.45 kips rather than the 89.8 kips of Table 5.1.

Table 3.2 Mechanical properties of lashing – Case C (Arroyo and Ebeling, 2005).

Lashing layouts	As in the 1998 experiments	
Lashing diameter	1	in.
Breaking strength	89.8	kip
Nominal area	0.48	sq in.
Rupture strain	6	%

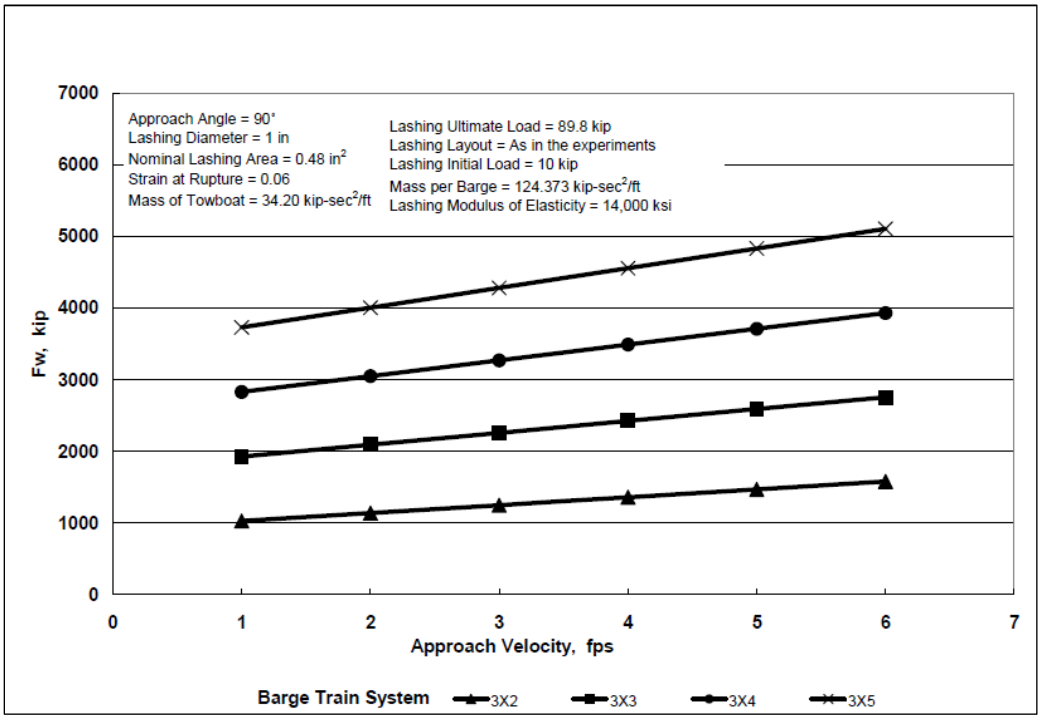

Figure 3.10 Maximum head-on impact force F_w – Case C (Arroyo and Ebeling, 2005).

software assumes yielding of lashings separating entire strings(s) of barges. In the dBEAS simulation for an impact by a 3 x 5 barge train with a rigid bullnose at 2.7 fps with higher tensile strength wire rope and more robust lashing layout (Table 3.5), the peak impact force with the rigid bullnose was 4,554 kips. The magnitude of the peak force at the rigid wall is comparable between the runs for the Limit_Lashing and more rigorous dBEAS software, providing additional verification of the dBEAS results.

3.6.2 Verification using Impact_Beam

Impact_Beam is a computer program used to determine deflection, strain, shear force and moment distributions along a simply supported (impact) beam given a force-time history at a given impact point. Its results have been verified using SAP-2000 (Ebeling et al. 2011).

To compare the 2-DOF dBEAS simulation with the SDOF calculations of Impact_Beam, a simplified 2-DOF scenario had to be constructed that applied an impact force at a single position and along a specific direction, thus providing an equivalent situation to match the SDOF free-body diagram (Figures 3.11 and 3.12). Because multiple lashed barges would be prone to add transverse forces during an impact at a point on the Deformable BEAS impact nosing (due to barge mass eccentricity relative to the line of impact), a single "super-barge" was constructed to collide with the impact nosing. The weight of the super-barge was equal to the weight of a barge train consisting of 15 barges plus the tow boat of 52,100 kips. This super-barge was set to collide along the center line of the super-barge and along the center line of the impact nosing. Then, the impact force-time history between the super-barge and the deformable bullnose was generated with dBEAS computer program.

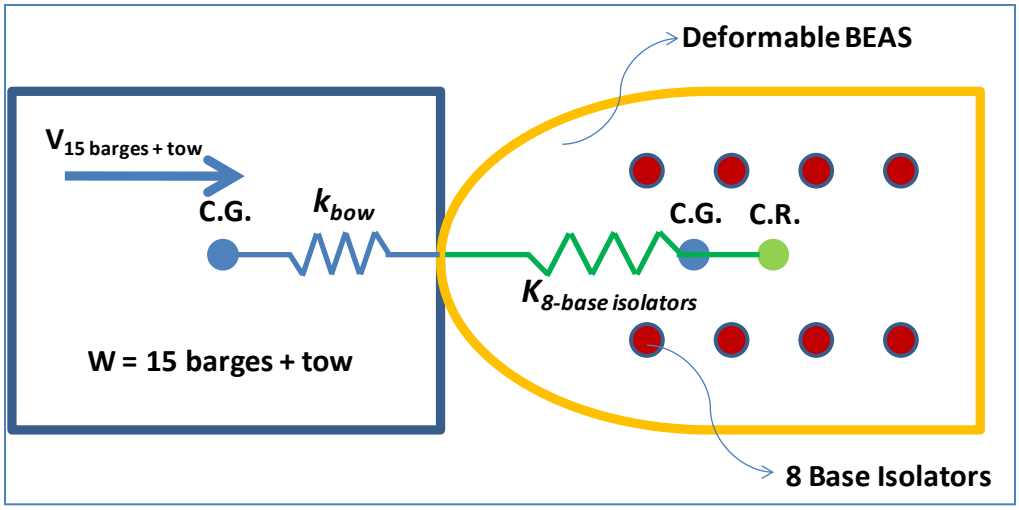

Figure 3.11 Plan view of the 2-DOF system of the super-barge dBEAS model (C.G. designates center of gravity; C.R. designates center of rigidity).

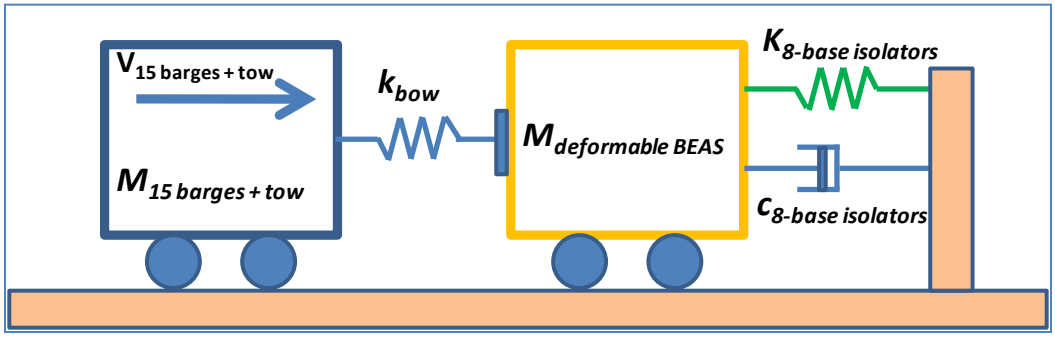

Figure 3.12 2-DOF system of the super-barge dBEAS model.

This impact force-time history was used as part of the input data for the SDOF model in Impact_Beam to calculate the response of the deformable bullnose and compared the results against the dBEAS computer program results. The bilinear spring stiffness curve for the base isolators (Figure 3.6) was modeled by Impact_Beam as a single curve multiplied by the number of base isolators, as the center of rigidity for the 2-DOF system would remain along the center line of the impact nosing due to symmetry.

For comparison purposes, multiple dBEAS runs were made varying two variables; the impact velocity of the super-barge, and the damping coefficient of the base isolators. The collected results can be found in Ebeling et al. (2011).

The results of the comparisons showed that the solution for the impact nosing mass and base isolators was virtually identical between dBEAS and the SDOF calculations of Impact_Beam in Ebeling et al. (2011). An example comparison is shown in Figures 3.13 and 3.14. The variation in values is quite small and well within the numerical tolerance for error in the simulation.

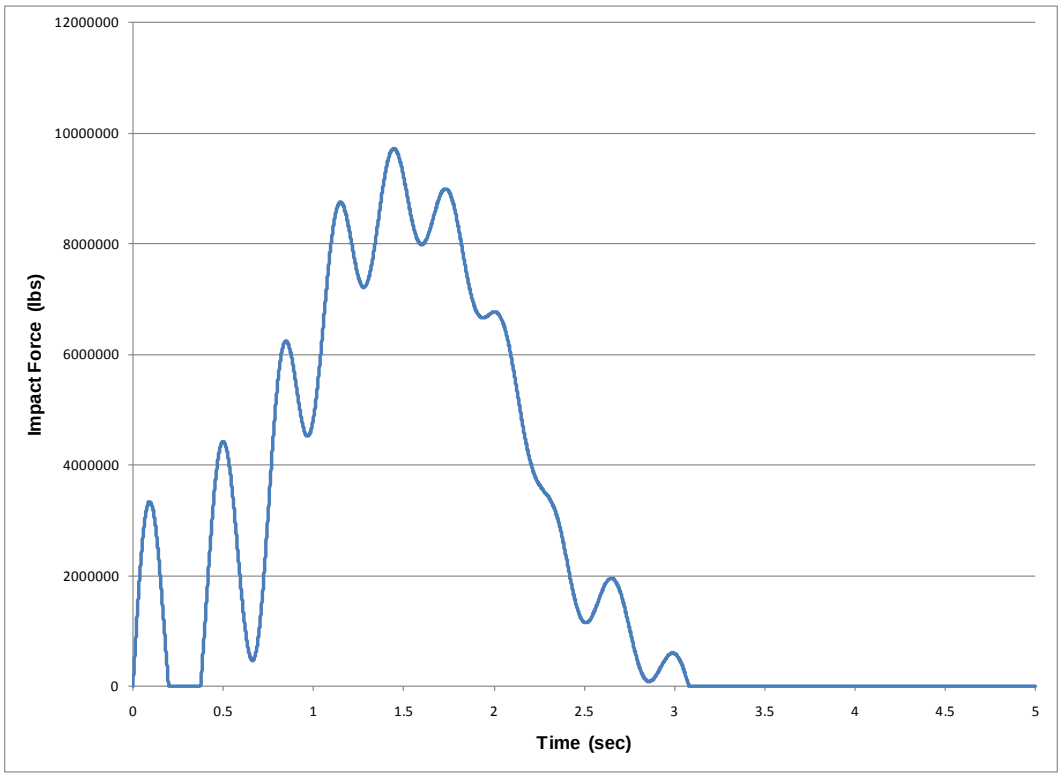

Figure 3.13 Dynamic external force for numerical example 5.2.5.5 – β = 15%, *v = 4 ft/s.*

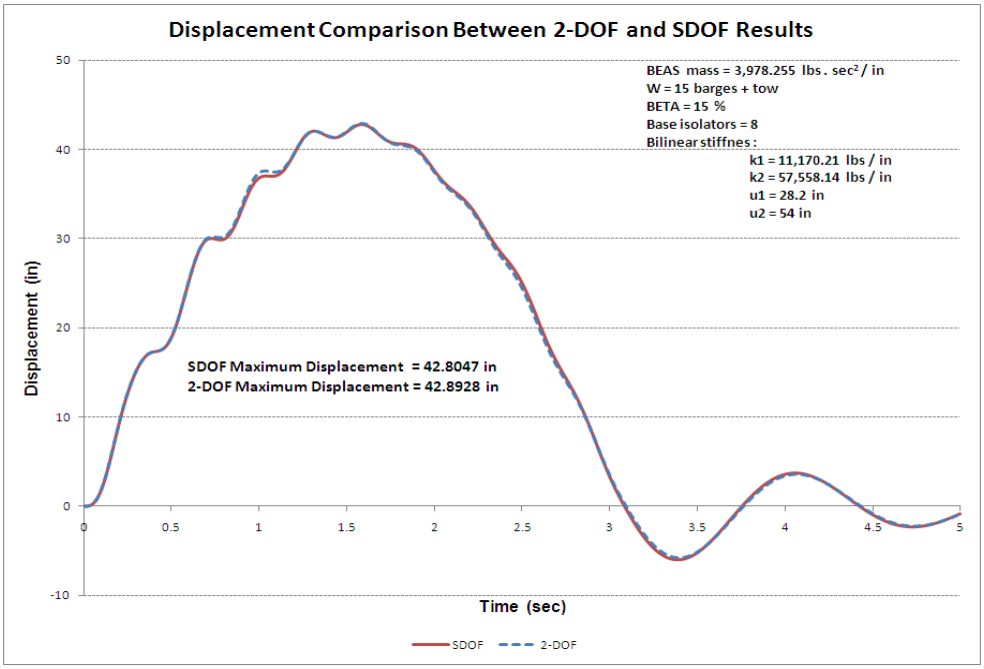

Figure 3.14 Response time history; dBEAS 2-DOF and Impact_Beam SDOF models, β = 15%, v = 4 ft/s.

3.7 dBEAS results

As the design of the Deformable BEAS progressed and as problems were identified, several simulation tests were performed. One of the criteria that had to be addressed was our "goal state" for the barge train. Figure 3.15 shows the states of the lashing under different strains, according to measurements. The colors of the three different states will serve as a legend to lashing integrity for the dBEAS result plots of barge train impact simulations. In these figures, blue lashings (see Figure 3.16) indicate that the lashing has no tension and is slack.

There are three states that barge lashings could be in after collision: no broken lashings, broken lashings but maintained barge train integrity, and lost barge train integrity. Barge train integrity was defined as the state where every barge in the barge train is connected to at least one other barge or tow by one or more undamaged lashing cables. For example, if three barges are connected to each other, but have only one damaged cable that connects them to the tow, then the barge integrity has been lost. For another example, if three rows of barges have separated from each other but each is held by one undamaged cable to the tow then barge train integrity has been maintained. Figure 3.16 shows examples of each state of barge train integrity.

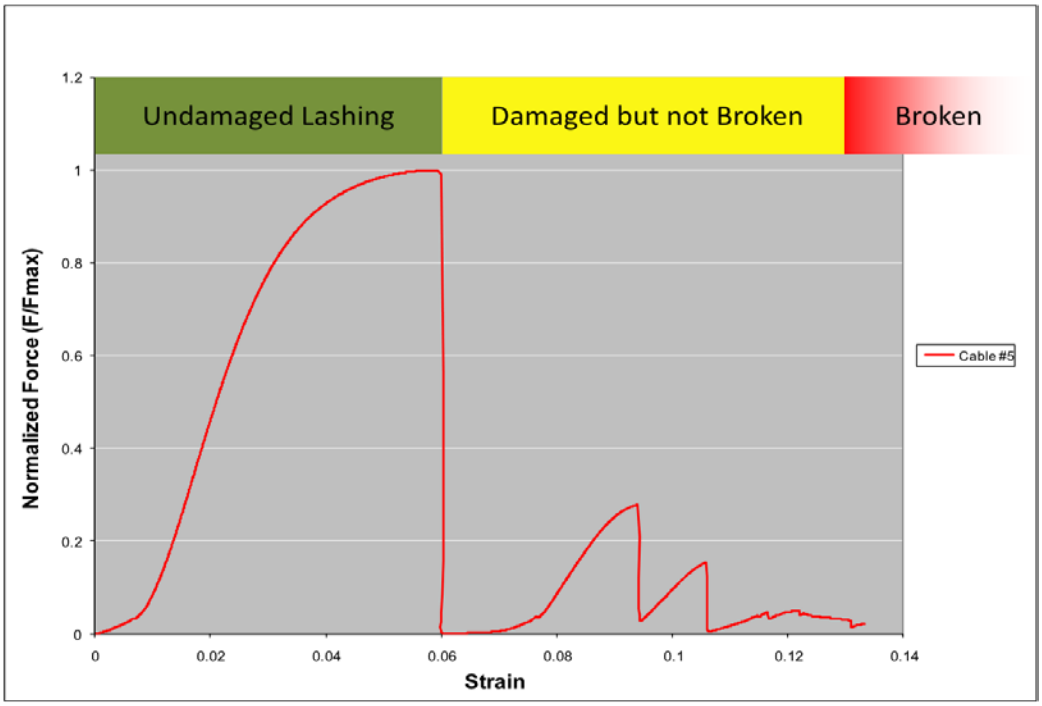

Figure 3.15 Three Lashing States Based on Strain with Normalized Force.

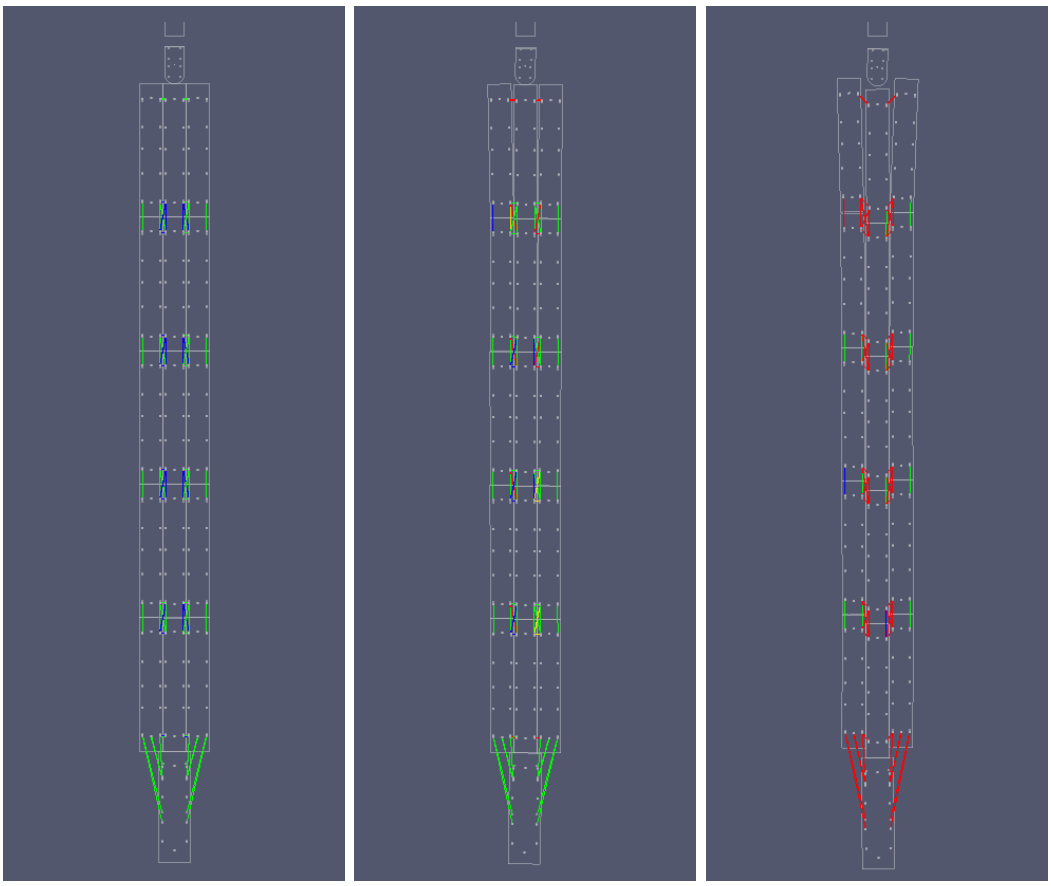

Figure 3.16 Barge train integrity: (a) no lashings broken, (b) lashings broken but barge train integrity maintained, and (c) barge train integrity lost.

3.7.1 Input variables

To understand the results of running the dBEAS program, it is important to understand the input variables involved in a run. For the impact simulations made, a single lashing force-deflection curve was used. This curve is from Ebeling et al. (2010) and is shown in Figure 3.1. The remaining input variables were; barge types for the barge train, lashing layout configuration, the number of barges in the simulation and their relative locations, individual barge weight, tow weight, initial velocity of the barge train, angle of approach for the barge train, pre-stress applied to each lashing, friction coefficient between barges, impact nosing weight, base isolator properties, the number of base isolator stacks, base isolator damping, and impact nosing friction.

To simplify the simulations, only barge families (rake barge, box barge, and reverse rakes) defined by the standard barges were used, as well as user-defined "super-barges" for verification of the program. Three barge families in particular were used, although they were chosen mainly for their ability to be connected with a certain lashing layout because of their bitt locations. These three barge families were the Jeffboat barges, CH barges, and Memco barges.

Lashing layout configuration was also chosen from a "standard." Although several lashing layouts were identified, two were tested to find out whether or not the selection of a lashing layout would have an effect on barge train integrity. The two that were used in the simulations are designated as the AEP lashing layout and the ACL lashing layout. The simulations are discussed below.

The number of barges and relative locations were selected to correspond to the typical barge train at the two sites that were being considered for installation of a Deformable BEAS structure, Markland and Newt Graham Lock and Dam 18 near Tulsa (to be discussed in Chapter 4). At Markland, the typical barge train consisted of three rows with five barges per row for a total of fifteen barges with a tow. At Newt Graham Lock and Dam 18 near Tulsa, the typical barge train had three rows with four barges per row for a total of twelve barges and a tow.

Barge weights were considered to be the weight of a barge with a maximum load. Initial tests gave this weight as 1,700 tons, but a modification made in

later tests gave this weight as 1,900 tons. The weight of the tow was set at 550 tons.

The initial barge velocity was given as a forward velocity only for these tests, as a head-on and glancing blow collision generally have much lower lateral velocities. Simulations for head-on collisions were performed first at the Usual, Unusual, and Extreme velocities of 2, 4, and 6 feet per second, respectively, and then varied around those values to find the limits of barge train integrity or loss of lashings. Glancing blow collisions were tested with much higher forward velocities to investigate the lateral deformation and rotation of the Deformable BEAS.

For the purposes of design, the barge train angle of approach only needed to have two angles. The head-on approach could be tested with an angle between the barge train and the impact nosing of 0 degrees. Because the glancing blow needed to test lateral deflection of the Deformable BEAS, the angle of attack was set to the maximum angle the barge train could make in the Markland channel for a three-by-five barge train, which was 15.8 degrees.

The pre-stress force that was acting on a lashing was set to reasonable limits of pre-stress discussed in the field. The force was set to either 500 or 2,000 pounds.

The inter-barge friction was set to the established steel-to-steel friction coefficient of 0.4. Initial tests revealed that not including inter-barge friction would lead to more damage of lashings, as discussed below.

The impact nosing weight for the Deformable BEAS system was computed based on a design that was meant to withstand over 4,500 kips of force. For the simulation tests, the weight of 768 tons was used. The resulting mass-moment of inertia was computed for this weight distributed per the design shown in Figure 3.8. Later tests were performed using fractions of this weight but, because the only collision considered was a head-on symmetric collision, the mass-moment of inertia was not altered.

There were several options for the base isolator properties. The bilinear curve, shown in Figure 3.4, was used for individual base isolators as well as a softened bilinear curve using force values scaled by 60% as specified by the DIS base isolator suppliers. To represent stacked base isolators, the

bilinear displacement could be multiplied by an integer value for the number of base isolators in a stack.

Using the design for the impact nosing discussed in Section 3.5, 8 stacks of base isolators were used for the simulations. This configuration of base isolators proved to work well in simulated impacts with various sizes and configurations of barge trains.

Damping could be added to base isolators as a lead core at the center of the base isolator that would resist the motion of the base isolator. Damping values from 0.02 to 0.15 were typical and these limits were used.

The impact nosing armor friction was originally set to the value of 0.2 as the lower end of the steel-to-steel friction coefficient. Low friction materials for armor were discovered and the impact nosing armor friction was reduced to 0.09.

3.7.2 Lashing layout differences

Table 3.3 shows the results of a comparison between an ACL lashing layout and AEP lashing layout. The input files for these tests varied only in the barge type and lashing layout. The barge train was three-by-five with barges loaded to 1,700 tons. Combined with the tow, the barge train weighed 26,050 tons. The barge train velocity was 2.7 feet per second, and the approach was at 0 degrees for a head-on collision. The inter-barge friction was 0.4, and lashing pre-stress was 500 pounds. For this test, the base isolators were given such a high K value as to be rigid, negating the effects of weight and base isolator number and damping. The friction between the nosing and impacting barge was set to 0.2. The collision was centered down the midline of the impact nosing and the barge train.

Table 3.3 Lashing layout comparison for 2.7 fps collision with a rigid bullnose.

Barge type	Lashing layout	Peak force (kips)	Peak deflection (ft)	Impulse (kips-ft)	Time of peak force (sec)	Time of first lashing failure (sec)	Time of peak deflection (sec)	Notes
CH	ACL	4554	0.0032	5384	0.561	0.74	0.561	Maintains barge train integrity
Jeffboat	AEP	3937	0.0028	4049	0.53	0.48	0.53	Complete loss of barge train integrity

The barge types vary only in the bitt positions that are required for the lashing layout. Notice that the ACL lashing layout has additional scissor wires as compared to the AEP lashing layout, as shown in Figure 3.17.

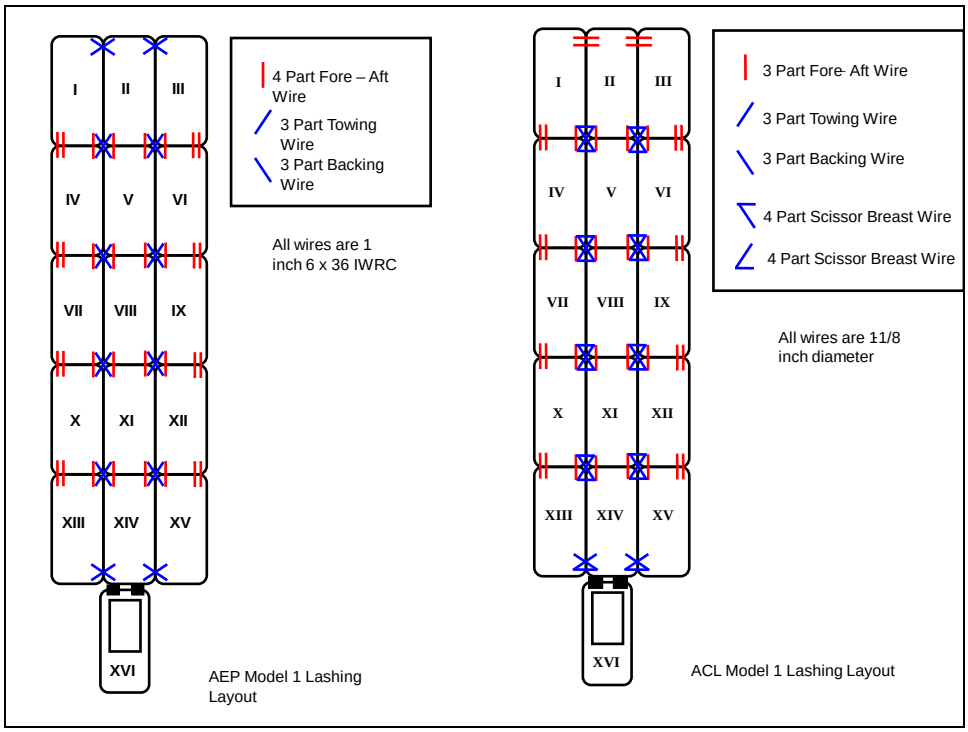

Figure 3.17 Comparisons of AEP and ACL Lashing Layouts.

While the ACL lashing layout does show a higher peak force in the table, the most telling numbers are in the Impulse and the Time of first lashing failure. Given equivalent barge train masses, the impulse should be equivalent between the barge trains (with small differences due to numerical inaccuracies). The Time of first lashing failure completes the picture by showing that lashing cables began to break earlier on the AEP lashing layout. In fact, the AEP lashing layout did not maintain barge train integrity whereas the ACL lashing layout did maintain the barge train integrity, which explains the difference in the values for the impulse for the two impact simulations. This set of simulation runs demonstrates that lashing layout alone can make a difference in the survivability of barge train integrity.

3.7.3 Parametric tests of base isolator response

For another set of tests, the number of base isolators per stack was varied to determine what conditions would ensure that not a single lashing failed for a three-by-five barge train at different velocities. Each barge was

loaded to 1,900 tons. Combined with the tow, the barge train weighed 29,050 tons. The barge train velocity was varied at 2, 3, 4, 5, and 6 feet per second, and the approach was at 0 degrees for a head-on collision. The inter-barge friction was 0.4, and lashing pre-stress was 500 pounds.

The impact nosing weighed 768 tons, with standard strength base isolators that were scaled as if they were stacked up to a 9 high. The damping coefficient for the base isolators was 0.15 and the armor friction was 0.09.

Table 3.4 shows the results of the testing. Because the kinetic energy in the system increases with the square of the velocity, i.e.,

Table 3.4 Base isolator stack response for barge train integrity with no lashing damage.

Barge train initial velocity	Base isolator stack height	Deflection of the impact nosing (feet)	Peak force at the impact nosing (kips)
2	1	2.2283	2632
3	2	4.9091	3271
4	4	9.71	3009
5	6	14.9117	3559
6	9	22.2238	4266

$$KE = (1/2m)v^2 \tag{3.7}$$

it makes sense that the (minimum) number of required base isolators in a stack would increase in an exponential fashion, as well as the deflection of the impact nosing (Figure 3.18). The peak force is affected by the time that that the barge train is in contact with the impact nosing, and how close a lashing is to breaking. This set of test runs was important to determine what conditions were required to slow the barge train and how those conditions changed with the initial velocity of the barge train.

3.7.4 Comparison of rigid bullnose versus Deformable BEAS

As a proof of concept, the effects of a rigid bullnose needed to be compared to a deformable structure supported by base isolators. For these tests, the only variable would be the stiffness of the base isolators. To model a rigid bullnose, the stiffness of the base isolators was set to a value based on the maximum force and maximum deflection of the flexible beam in the Winfield Tests discussed in Ebeling et al. (2011). The Deformable BEAS base isolator stiffness was given by the normal stiffness curve from

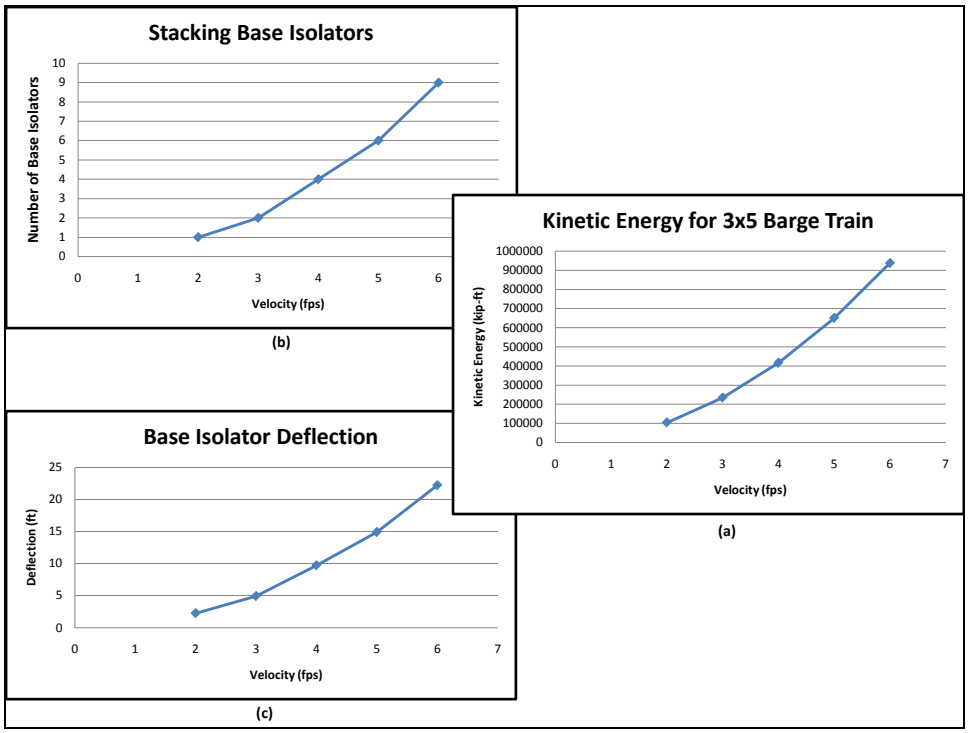

Figure 3.18 Exponential response of (a)kinetic energy, (b)deflection, and (c)stack heights versus velocity.

Figure 3.4, but stacked 2 high. The base isolator fraction of critical damping was 0.15 and the impact nosing armor friction was given as 0.2. The impact nosing weight was 768 tons.

For the other parameters, a three-by-five barge train with CH barges and ACL lashing layout was used. Each barge had a weight of 1,700 tons, giving the full barge train a weight of 26,050 tons. The barge train forward velocity was 2.7 feet per second, which was the point where collision with the rigid bullnose broke the first lashing in the barge train. The inter-barge friction was 0.4, and the lashing pre-stress was 2,000 pounds.

The collision was a head-on collision with the center-line of the barge train coinciding with the center-line of the bullnose. The results are given in Table 3.5.

By using a stacked set of base isolators, the peak force was reduced to nearly 55% of the peak force encountered by the barge train impacting the rigid bullnose. The reduction of the impulse encountered by the rigid bullnose was accounted for by the fact that barge train integrity was not maintained. It is noteworthy to see that the impact-nosing was deflected 4.3 feet in this simulation.

Table 3.5 Comparison of rigid bullnose to Deformable BEAS.

BI stack	Peak force (kips)	Peak deflection (ft)	Impulse (kips-ft)	Time of peak force (sec)	Time of first lashing failure (sec)	Time of peak deflection (sec)	Notes
Rigid	4554.08	0.0032	5383.965	0.561	0.74	0.561	Loss of Lashing Integrity
8-Double	2417.4	4.2963	8757.821	2.913	NA	3.059	No lashing failures

3.7.5 Comparison of base isolator stiffnesses

Given (in subsection 3.7.3) that less stiff base isolator systems provide better protection for barge train and lashing integrity and (in subsection 3.7.4) that a rigid bullnose does not provide the same protection as a Deformable BEAS, the next logical set of simulations was to vary the stiffness of the base isolators used for the Deformable BEAS to reveal how the maximum lashing forces would change with the lower stiffnesses. To change the stiffnesses of the base isolators, the Deformable BEAS was given eight base isolators in (a) a single stack, (b) a double stack, and (c) a double stack with 60% stiffness, as discussed in subsection 3.4.1. The base isolator fraction of critical damping was 0.15 and the impact nosing armor friction was given as 0.2. The impact nosing weight was 768 tons.

A three-by-five barge train with CH barges and ACL lashing layout is used in all simulations. Each barge had a weight of 1,700 tons, giving the full barge train a weight of 26,050 tons. The barge train forward velocity was 2.0 feet per second, which was guaranteed to not break any lashings in the barge train so that an accurate force could be measured. The inter-barge friction was 0.4, and the lashing pre-stress was 2000 pounds.

The barge train approached in a head-on collision. The results are shown in Table 3.6.

Table 3.6 Comparison of base isolator stiffness.

Base isolator parameters	Peak impact nosing force (kips)	Peak impact nosing deflection (ft)	Peak lashing force (kips)
Single stack	2448	2.1346	120.7
Double stack	1825	3.1816	96.2
Double stack – 60%	1483	4.2184	81.4

The peak lashing force is measured by finding the maximum individual lashing force that was experienced by any lashing in the barge train. Both impact nosing and lashing force values decreased as the base isolator system stiffness was reduced, providing more protection for the lashings, which seemed to indicate a "relationship" between the Deformable BEAS force and lashing integrity.

3.7.6 Off-center impact tests

All of the simulations performed to this point were performed for head-on collisions where the impact point and barge train velocity was along the line through the center of gravities of the impact nosing and barge train and the barge train and impact nosing were symmetric about that line. To verify that peak force at the impact nosing was related to the peak lashing force in the system, it was decided that simulations with an off-center impact with the barge train impacting the impact nosing would need to be performed. These simulations would still have the initial impact point and velocity along the center-line of the impact nosing, but the barge train center of gravity would not be in line with the impact point and velocity. The impact points for the simulations would be the in-line impact (Figure 3.19a), along the centerline of the starboard bow barge (Figure 3.19b), and at the starboard bow corner of the barge train (Figure 3.19c).

The results are shown in Table 3.7. For the off-center impacts, the peak lashing force shows an inverse correspondence to the increases or decreases of the peak impact force acting at the Deformable BEAS impact nosing. This is because there is more mass, and therefore more inertia, acting against the lashings of the starboard string of barges. This is exacerbated by the additional moment induced to the barge train by the off-center hit location. This reveals that the peak impact force occurring at the impact nosing is an indicator of barge train integrity only for a head-on impact due to symmetry of the impact relative to the Deformable BEAS and the barge train.

3.7.7 Head-on parametric velocity tests

With an adequate proof of concept, it became necessary to test the velocities at which a Deformable BEAS could prevent a barge train from losing barge train integrity. Tests were performed at 2, 4, and 6 feet per second. This corresponds roughly to the top end of the ETL 1110-2-563 non-site specific Usual, Unusual, and Extreme approach velocity ranges listed in Table 3.1.

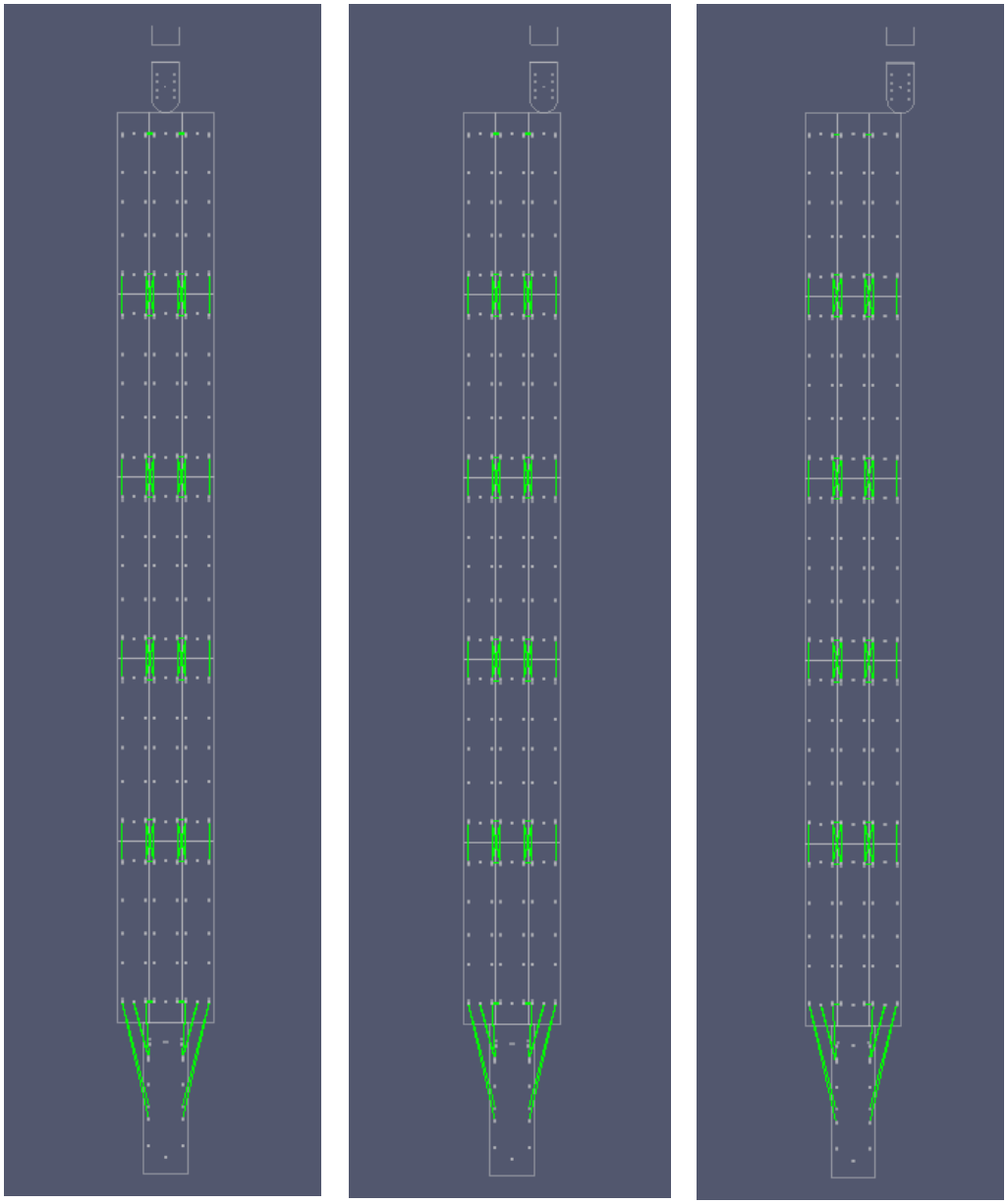

a) Head-On b) Starboard Barge c) Starboard Corner

Figure 3.19 Barge train impact locations for off-center impact simulations.

Table 3.7 Comparison of off-center impacts.

Impact conditions	Peak impact nosing force (kips)	Peak lashing force (kips)
Inline	1483	81.4
Starboard barge	1451	107.9
Starboard corner	1397	111.9

The Deformable BEAS base isolator stiffness for this test was given by the stiffness curve from Figure 3.4, scaled by 60% on the force axis and stacked 2 high. The base isolator fraction of critical damping was 0.15 and the impact nosing armor friction was given as 0.09. The impact nosing weight was 768 tons.

For the barge train parameters, a three-by-five barge train with CH barges and ACL lashing layout was used. Each barge had a weight of 1,700 tons, giving the full barge train a weight of 26,050 tons. The inter-barge friction was set to 0.4, and the lashing pre-stress was 500 pounds.

Each simulation run was performed with an ending simulation time of 10 seconds to allow for the full interval of the impact, with separation of the barge train from the Deformable BEAS impact nosing. Because barges did not separate from the barge train, the peak force at the highest velocity would be the maximum force acting on the Deformable BEAS structure.

When it was discovered that barge train integrity could be maintained at 4 feet per second and that it could not be maintained at 6 feet per second, the tests were performed at 0.1 foot per second intervals, starting at 4 feet per second, to determine the speed at which barge train integrity was lost. Barge train integrity for the conditions described was maintained up to a maximum velocity of 4.5 feet per second, with a peak force of nearly 5,950 kips and a maximum impact nosing deflection of slightly over 7 feet. Additional tests are described in Chapter 4 for different barge train sizes and changes in design for the Deformable BEAS. Figures 3.20 (a)-(d) show the different ending states of the barge train for the collisions at the different (approach) velocities of 2 fps, 4 fps, 4.5 fps and 6 fps.

A similar set of simulations were performed with a rigid bullnose to establish a base-line for comparison. The results are shown in Table 3.8.

3.7.8 Glancing blow tests comparison between flexible and rigid approach walls

For design purposes, the lateral deflection of the base isolators had to be taken into account, as well as the deflection along the Deformable BEAS. An oblique impact (glancing blow) test was performed to see the response of the base isolators to impacts along the side of the Deformable BEAS. Given the data from Chapter 2 concerning the maximum angles possible by a three-by-five barge train at Markland, the barge train angle of attack was given at 16 degrees. The colliding barge was the forward, starboard barge.

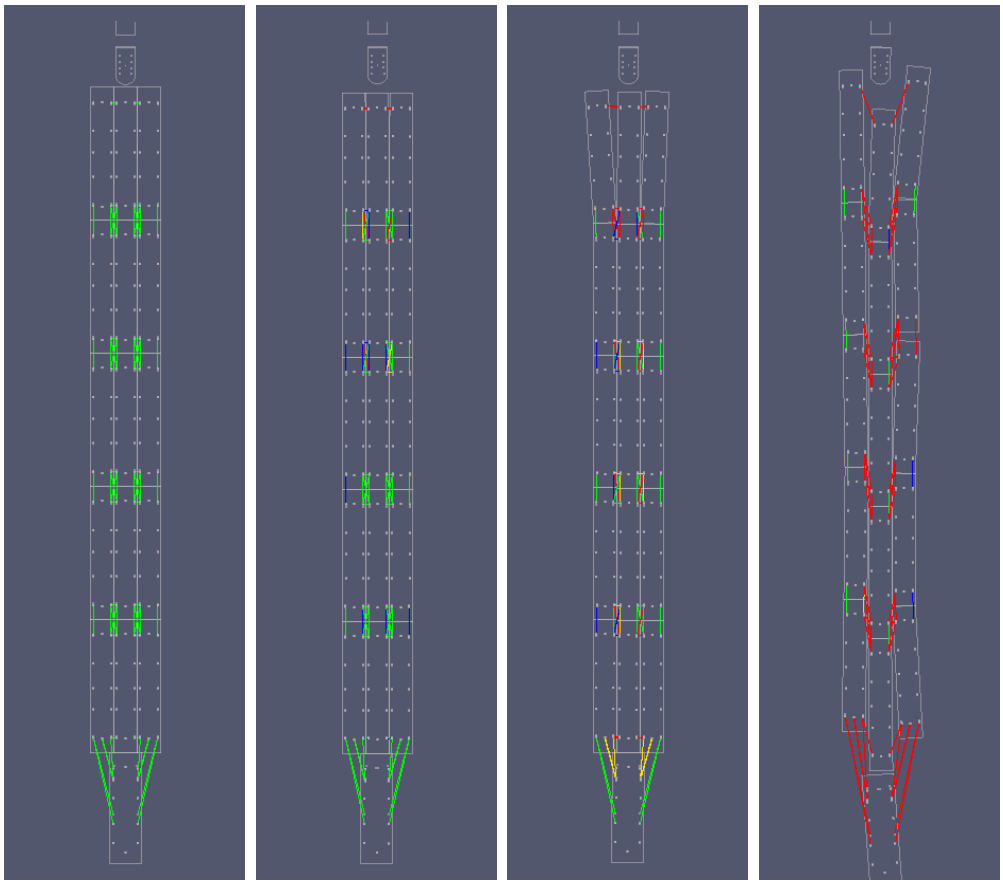

Figure 3.20 Barge train velocity tests at time=10 sec: (a) 2fps - no lashings broken, (b) 4fps -lashings broken (c) 4.5fps – strained but barge train integrity maintained, and (d) 6fps - barge train integrity lost.

Table 3.8 Comparison of max velocity without losing barge train integrity.

Type of bullnose impacted	Maximum velocity with which barge train integrity was maintained (fps)
Rigid	3.2
Deformable BEAS with 8 double-stacked, 60% force base isolators	4.5

The forward velocity of the barge train was set to the extreme velocity of 7.6 feet per second discussed in Chapter 2 for Markland flow velocities at which navigation terminates. This setup is shown in Figure 3.21.

The Deformable BEAS base isolator stiffness for this test was given by the stiffness curve from Figure 3.4 scaled by 60% on the force axis and stacked 2 high. The base isolator fraction of critical damping was 0.15 and the impact nosing armor friction was given as 0.09. The impact nosing weight was 768 tons.

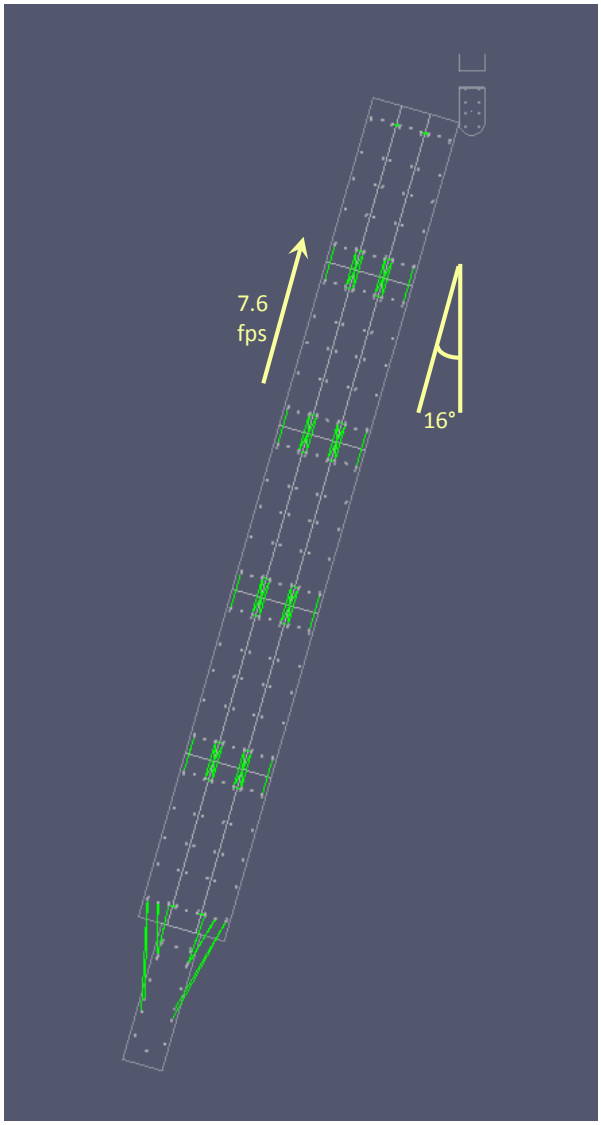

Figure 3.21 Three-by-five barge train with an approach of 16 degrees.

For the barge train parameters, a three-by-five barge train was used with CH barges and an ACL lashing layout. Each barge had a weight of 1,700 tons, giving the full barge train a weight of 26,050 tons. The inter-barge friction was set to 0.4, and the lashing pre-stress was 2,000 pounds.

For these simulations with an approach velocity of 7.6 feet per second, the barge train had broken lashings across the first row of barges for the impact with a rigid bullnose (Figure 3.22a). The barge train that impacted the Deformable BEAS had no lashing damage or breakages (Figure 3.22b). (Recall that damaged lashings will be shown in yellow and broken lashings are shown in red in the figure).

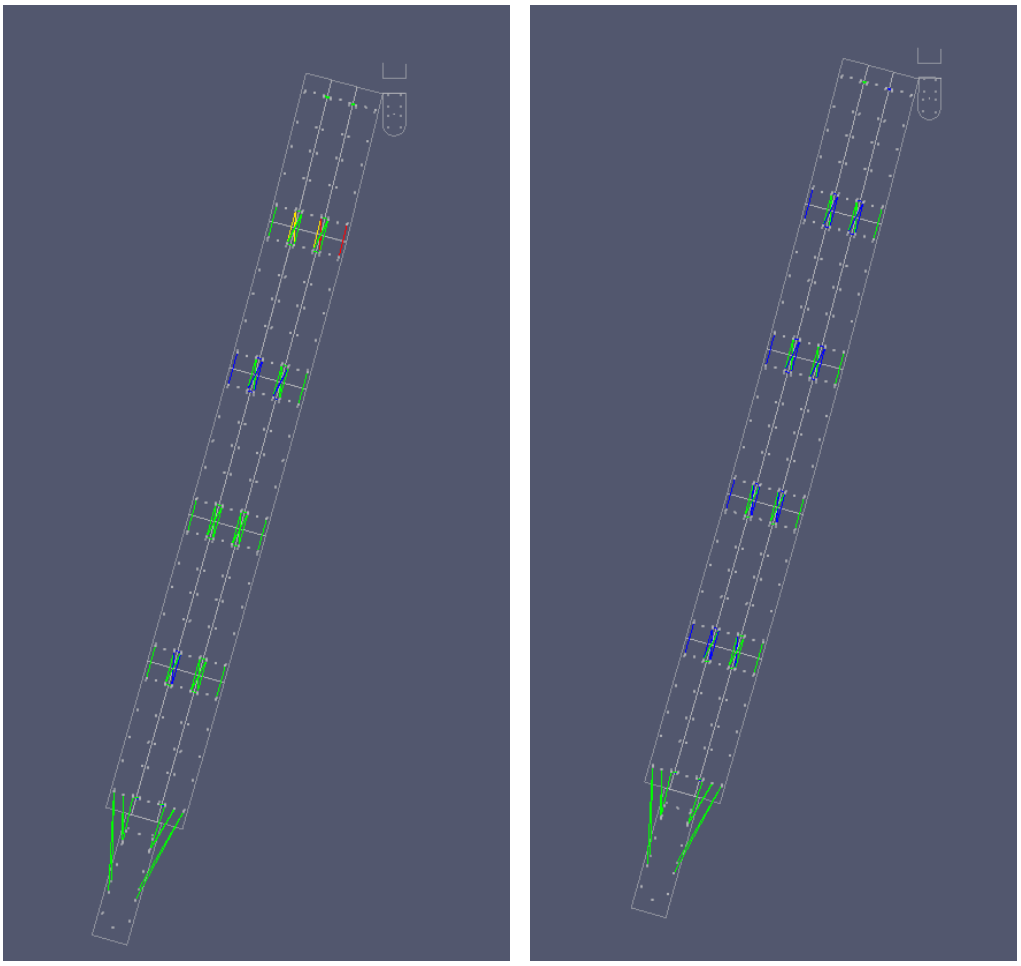

(a) (b)

Figure 3.22 Final state of high-velocity, glancing blow simulation for (a) rigid bullnose and (b) Deformable BEAS.

For the glancing blow impact with a velocity of 7.6 feet per second, the lashing integrity was maintained for an impact with the Deformable BEAS. This same glancing blow impact resulted in broken lashings for the rigid bullnose. The peak force at the impact nosing for the deformable system is comparable to that of the rigid system. The deflection of the Deformable BEAS is nearly two feet, which can be handled easily by a double stack of base isolators.

Figures 3.23 (a and b) show the total impulse characteristics for the collision of the three-by-five barge train with the rigid and deformable bullnose systems. The rigid bullnose impact is comprised to two impulses. The deformable bullnose impact is comprised of several shorter duration impulses. Between each impulse is a “respite” time, when the barge train and the impact nosing are under only internal forces. During these respite

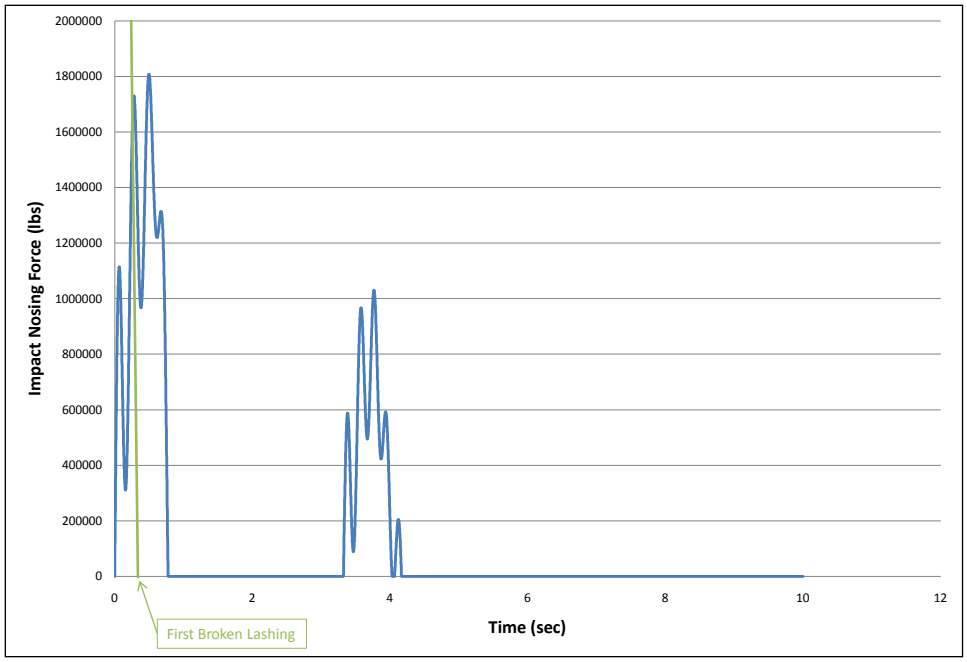

(a) Impulse for 3x5 barge train with rigid impact nosing – 16 degrees, 7.6fps.

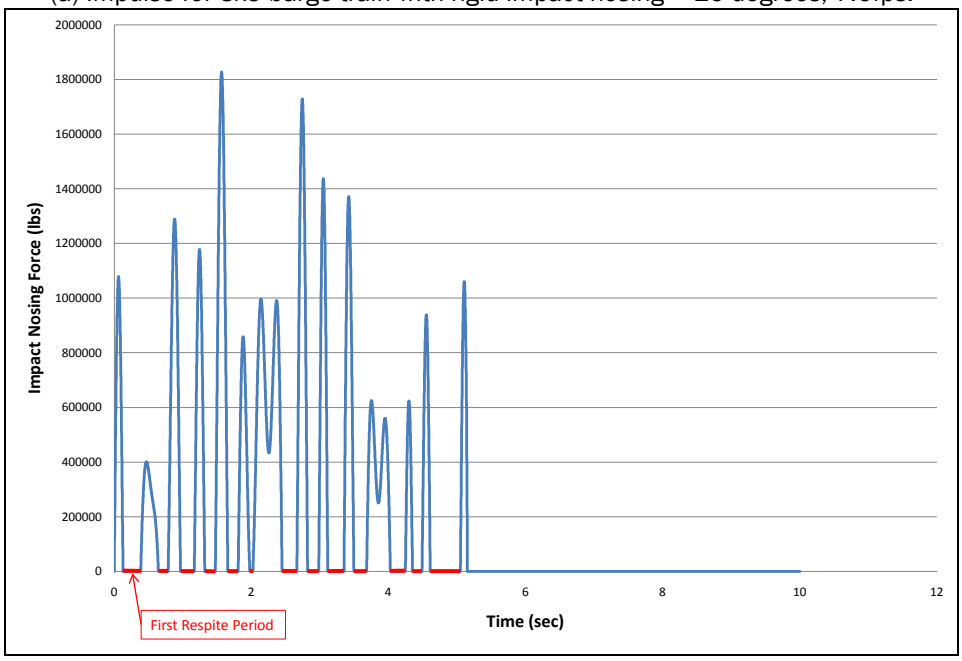

(b) Impulse for 3x5 barge train with deformable impact nosing – 16 degrees, 7.6fps.

Figure 3.23 Impulses for impacts with a (a) rigid bullnose and (b) Deformable BEAS.

times, the lashing forces can act to relieve the tensile strain that the lashings have been under due to the collision, effectively "resetting" the lashings and pulling the barge train back towards its "at-rest" position for the next impulse. In this way, the Deformable BEAS preserves the lashing integrity for higher velocity, glancing-blow impacts.

Further simulations were then performed to discover the velocity at which the barge train impact with the rigid wall first damaged a lashing and when the barge train impact with a Deformable BEAS first damaged a lashing. The velocity was decremented by 0.1 feet per second from 7.6 feet per second for the rigid wall, and incremented by the same amount for the flexible system. The rigid wall had its first damaged lashing with an impact at 7.1 feet per second, and the flexible wall had its first damaged lashing with an impact at 8.0 feet per second. Looking at Table 2.8 for flow-based, site specific load conditions, the rigid wall could maintain barge train integrity for part of the Usual load condition at Markland. The Deformable BEAS would be able to maintain barge train integrity into the Extreme load condition for Markland. Observe that the comparable approach velocity for head-on impacts with a Deformable BEAS with initial lashing damage is less than 4.0 feet per second (Figure 3.20b). This is much lower than the approach velocity of 8.0 feet per second for first lashing failure with a Deformable BEAS, which implies that a structure could be more optimally designed for glancing blow impacts while maintaining lashing integrity. Recall the Deformable BEAS design is controlled by the head-on impact event.

It's important to recognize that the structural system defining the Deformable BEAS is based upon design for high energy, head-on impact. These demands are much higher than for glancing blow impacts that would be sustained by an approach wall system. This implies that a flexible approach wall could be more optimally designed to withstand high energy, glancing blow impacts while maintaining barge train integrity. These glancing blow impacts have lower peak forces than a head-on collision, which will change the structural design of the wall to be smaller and lighter. The wall also can be designed to lower the amount of rotation for impact beams that are simply supported.

3.8 Conclusions

For three-by-five barge train collisions that would be typical for an impact event at Markland, the simulations using the dBEAS software package were able to prove that a Deformable BEAS structure using base isolators would be able to reduce the peak forces at the impact nosing during the impact. By extending the time of impact and lowering the peak forces, barge train integrity can be maintained, especially for the demanding head-on impacts. By altering the base isolator properties and stacking the base isolators, barge train integrity could be maintained at velocities in the

extreme range for head-on collisions. Unfortunately, because the amount of kinetic energy that would need to be absorbed by the system increases according to the square of the velocity, the amount of deflection (during the impact event) grows to a distance that would be hard to design for. The number of base isolators that would need to be stacked becomes prohibitive, also.

Positive features of the Deformable BEAS for head-on collision:

- Extends the time of impact.
- Lowers peak forces of the impact.
- Reduces lashing failures.
- Maintains barge integrity for impacts of up to 4.5 feet per second with only 16 base isolators. By the listed ETL 1110-2-563 non-site specific approach velocities, the Deformable BEAS would successfully accommodate these Usual and Unusual load cases.

Negative features of the Deformable BEAS for head-on collision:

- The number of base isolators increases exponentially for higher velocity designs.
- The peak deformation for extreme velocities is prohibitive (>7 feet at 4.5 fps).
- Cannot maintain barge train integrity with 16 base isolators for impacts with a three-by-five barge train at >4.5 feet per second, which is less than the ETL 1110-2-563 maximum of 6 feet per second for extreme conditions.

However, for glancing blow impacts the Deformable BEAS, base isolator system works well for Usual, Unusual and Extreme velocity impacts. Lashings can be saved from damage and breakage that would occur for rigid walls during Unusual to Extreme velocity impacts by lengthening the time for the full impact and providing “respite” times for the lashings between shorter impulses. In fact, the Deformable BEAS can maintain complete lashing integrity for a barge train with a 7.6 feet per second approach velocity at 16 degrees, corresponding to the Chapter 2 Markland upper range flow estimate and maximum possible approach angle for a three-by-five barge train. This also corresponds to the lower bounds of the Markland site-specific extreme velocity event (Table 2.9). The rigid bullnose system cannot maintain lashing integrity for the barge train under these conditions.

Positive features of the Deformable BEAS for glancing blow collision:

- Extends the time for the full impact event. Reduces lashing failures.
- Minimal deflection.
- By the listed ETL 1110-2-563 non-site specific approach velocities, the Deformable BEAS would successfully accommodate these Usual, Unusual and Extreme load cases.
- Deformable BEAS maintains complete lashing integrity for a barge train into Markland site-specific Extreme approach velocity events. The rigid approach wall could only handle Markland site-specific Usual approach velocity without broken lashings.

Negative features of the Deformable BEAS for glancing blow collision:

- None.

Trends suggested by the Deformable BEAS research:

- An entirely different structural system is envisioned for approach walls that deal exclusively with glancing blow impacts.
- Approach walls can be designed for impact events with much lower peak forces and impulse, thereby reducing the size and cost of the structural system, and optimizing the system to maintain barge train integrity under glancing blow impacts.

4 Three-by-Four Barge Train Impacts with Deformable BEAS Containing a Collapsible Front Arch

4.1 Introduction

In this chapter, the focus is on the typical barge train for an impact at Newt Graham Lock and Dam 18 on the Verdigris River near Tulsa, Oklahoma. This three-by-four barge train was discussed in Chapter 2. Again, focus will be placed on the impact load cases that we expect a Deformable BEAS to operate under should it be constructed at this lock. Recall that Table 3.1 lists the ETL 1110-2-563 non-site specific approach velocity conditions for the Usual, Unusual and Extreme design events.

4.2 Barge train and deformable bullnose properties

The typical barge train for the Newt Graham Lock and Dam 18 tests was similar in its parameters to the Markland barge trains described in Chapter 3. Lashings and barge properties were not changed, but the standard barge train size was defined to have three strings of barges with 4 barges per string.

Likewise, the base isolator properties and impact nosing changed very little from the information of Chapter 3, with one exception. To provide additional “softness” for the Deformable BEAS, a collapsible front arch was designed for the Deformable BEAS. One notable point to recognize is that these tests were working with the impact nosing mass for an impact nosing designed to handle the peak stresses of a three-by-five barge train impact.

Because of the robustness of the Markland barge trains under a glancing blow impact, it was decided that these tests would focus primarily on head-on impacts, like those shown in Figure 3.9(b).

4.3 A collapsible arch for the impact nosing

The results of the testing of the Markland conditions, especially the tests in Section 3.7.3, showed that when the stiffness of the Deformable BEAS structure was lowered, the barge train velocity could be increased and still

maintain barge train integrity. However, the lower stiffness would mean that a rigid impact nosing of the Deformable BEAS would have a higher deflection for an impact (or more precisely, impulse) of the same magnitude. This led to the suggestion that the impact nosing of the Deformable BEAS would not need to be rigid, leading to the design of the collapsible arch for the front of the impact nosing.

The collapsible arch was designed to be engaged when the Deformable BEAS had yet to reach the peak force discovered for a three-by-five, 26,050 ton barge train travelling at 4.5 feet per second. At that point, the collapsible arch would start to collapse, giving a lower stiffness that would act in series with the base isolators. Each time that one of these extreme events occurred, the collapsed arch would need to be replaced.

Figure 4.1 shows a possible design for a Deformable BEAS with a collapsible front arch. The collapsible front arch would be designed to collapse when the force between the barge train and impact nosing reached a specified maximum force, which was calculated as the maximum peak impact force determined for a three-by-five barge train that had maintained integrity at the greatest velocity with a double-stacked, softened base isolator system under the impact nosing, as tested in section 3.7.5. At that point, the arch would start to collapse causing the stiffness of the impact nosing to be lower. A free-body diagram of the single degree of freedom head-on collision between the barge train and the bullnose with the collapsing arch can be seen in Figure 4.2. The impact nosing stiffness is in series with the stiffness of the base isolators, so the entire system stiffness would be lowered, according Equation 4.1.

$$K_{\text{Deformable BEAS}} = \frac{K_{\text{Base Isolators}} * K_{\text{Collapsing Arch}}}{K_{\text{Base Isolators}} + K_{\text{Collapsing Arch}}} \tag{4.1}$$

Because the collapsing arch would exhibit different characteristic force-deformation curves based on the position along the arch of the impact, the dBEAS program was designed to accept specific curves for response calculations at different arcs along the arch of the impact nosing.

A pushover analysis was performed that assumed head-on impact loads in the range of 4000 – 4500 kips on a steel bullnose arch with an outside radius of 15 feet. The arch sections for fully loaded impact were three of the eight W 14 x 398 sections. These are heavy steel sections with shallow

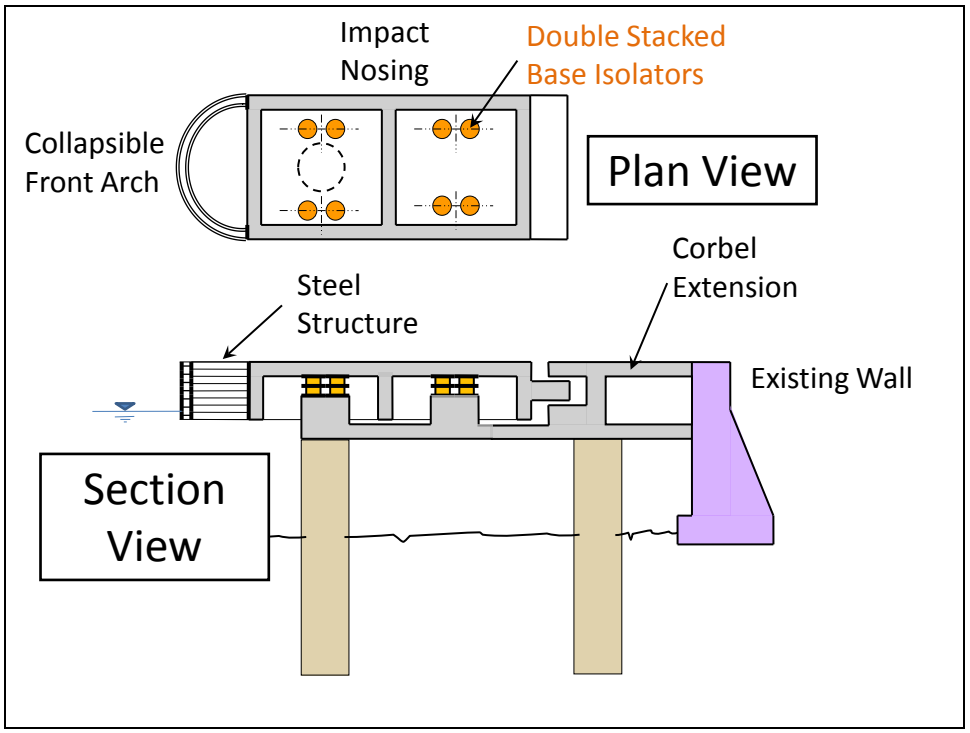

Figure 4.1 A single-part impact nosing with stacked base isolators and collapsible front arch.

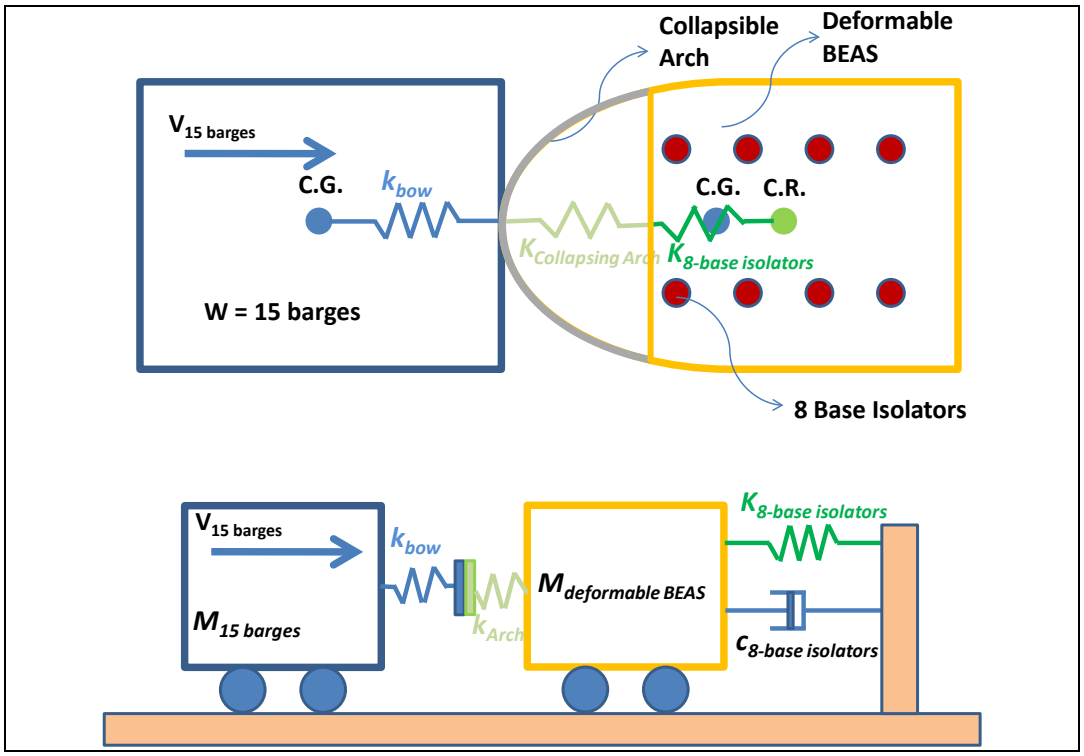

Figure 4.2 A state diagram of the single degree of freedom impact between a barge train and the Deformable BEAS with a collapsible front arch (C.G. designates center of gravity; C.R. designates center of rigidity).

beam “depth” (relative to the arc dimension for the arch) were used to maximize displacement response. It will be assumed that 50 grade steel with a yield of 50 ksi will be used and that full plastic hinging develops at 60 ± ksi (partially into the strain hardening range). The pushover analysis, performed using the element program SAP-2000, generated the response curve of forces acting for a head-on collision, as shown in Figure 4.3.

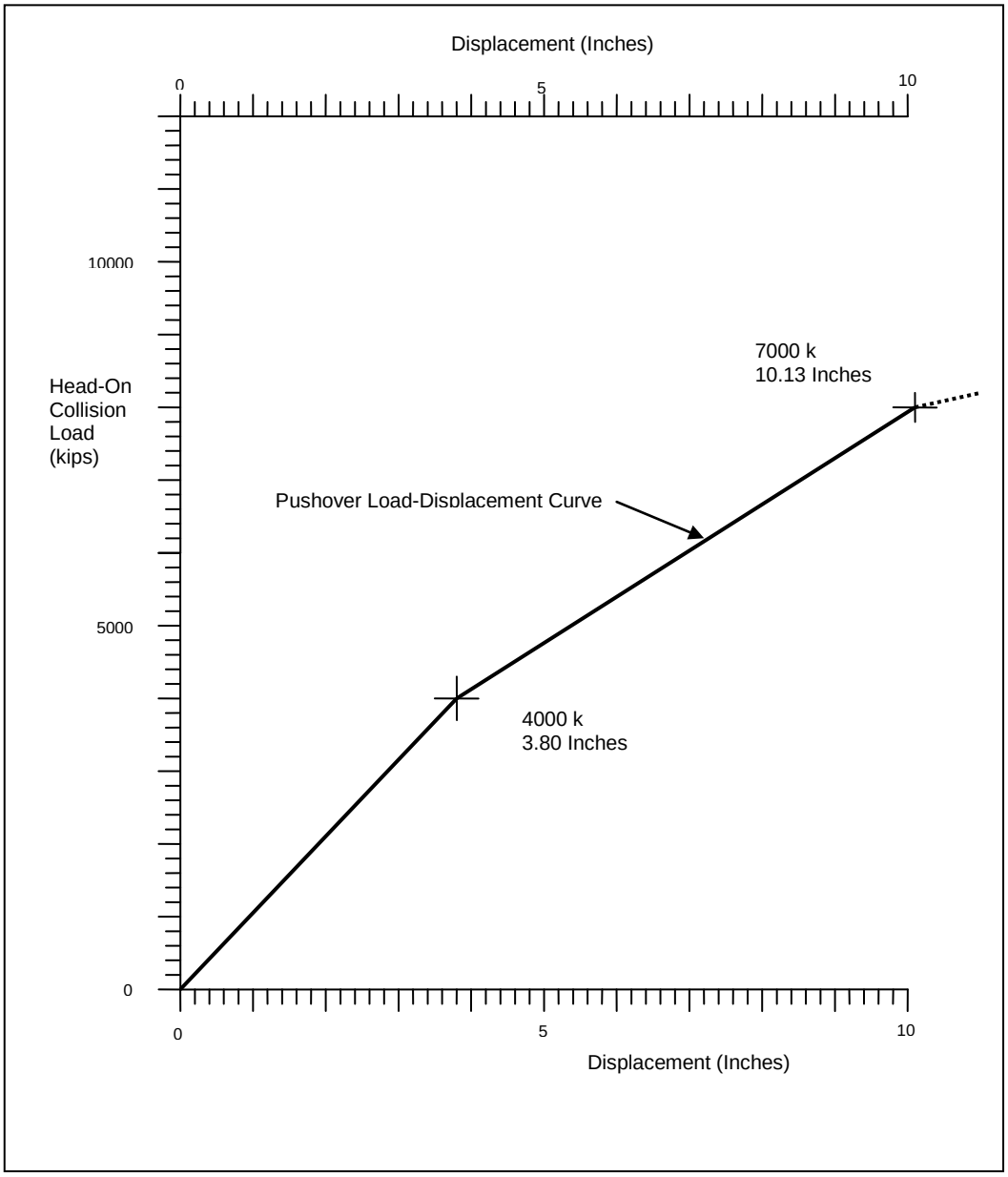

Figure 4.3 Pushover load displacement curve at the center of a collapsing steel arch.

The dimensions of the impact nosing would be changed to account for the new front arch, but the mass and moments of inertia for the structure would be nearly identical since these values are dominated by the

reinforced concrete structural features, including the top deck, of the impact nosing. Figure 4.4 shows the very minor differences in design compared to the Chapter 3 design with a reinforced concrete arch structural system.

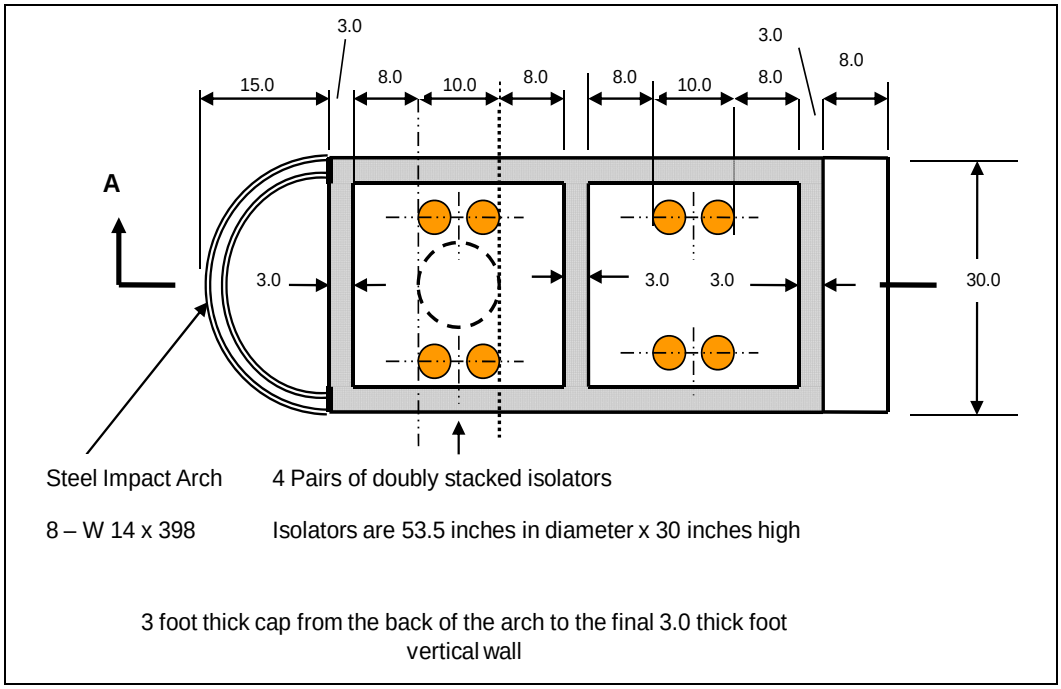

Figure 4.4 Dimensions (in feet) of the impact nosing of the Deformable BEAS with a collapsible front steel arch.

4.4 Implementation and validation of collapsing arch

To implement the collapsing arch system, it was necessary to recognize that once the response curve for the direction of impact had reached the peak force values, the deformations became permanent. This was accomplished as it was with the lashings, using an unload/reload slope for repeated loads. For impacts with forces below 4,000 kips the arch remains elastic; the Young's modulus for this unload/reload slope would give a consistent spring force of the same magnitude as during initial loading, i.e., elastic response.

While the validity of the collapsing arch structure curve could be verified with SAP-2000, additional validation tests would be required for the collapsing arch code in the dBEAS program. Rigid and non-rigid bullnose impact tests would need to be performed.

4.4.1 Input variables

The input variables for the Newt Graham Lock and Dam runs are essentially the same as the variables defined in Section 3.7.1 of the previous chapter. The primary change to the barge train was (1) the use of a three-by-four barge train, using differing (2) barges and (3) lashing layouts. The lashings were pre-stressed with 2,000 lbs of force. Each barge was given a weight of 1,900 tons, as compared to the 1,700 tons typically used for testing the three-by-five barge trains. The total weight of the barge train was 23,350 tons.

While the dBEAS program could accept different displacement/load curves for collisions along different directions of the collapsing arch (full modeling of the collapsing arch would have been prohibitive), the primary case that was of interest was the head-on collision. The inputs for the collapsing arch used the curve shown in Figure 4.3 for any impact within 30 degrees of the center-line of the arch, measured from the center of the semicircle defining the arch.

4.4.2 Validation test I; rigid bullnose

The first validation test for the collapsible arch was performed on a rigid bullnose. That is to say, the impact nosing was placed on base isolators that were given an arbitrarily high stiffness. In this test, the variation was in using a rigid front arch or the collapsing arch to determine if the arch would make a difference in the response of the structural system. The approach velocity of the barge train at the time of impact was 2.0 feet per second. This low approach velocity was specified to prevent break-away barges from affecting the impulse calculations. (Recall that analyses cited in Chapter 3 showed that the "mass shedding" of break-away barges reduced the impulse of the barge train during the impact event.) Table 4.1 summarizes results taken from these calculations.

Table 4.1 Results for impact of a 3 x 4 barge train against a rigid bullnose without and with a collapsible front arch.

Collapsing arch	Peak force (kips)	Peak impact nosing deflection (feet)	Time to peak force (seconds)	Time to peak deflection (seconds)
Rigid	4,643	0.0037	1.034	1.034
Flexible	3,594	0.0029	1.172	1.172

Significantly, the use of the collapsible front arch reduced the peak force that was shared between the wall and the barge train by nearly 1,100 kips. Because the collapsing flexible arch did not reach 4,000 kips and begin plastic deformation, the arch would spring back into its original position after the impact event concluded. Although the magnitude of the impact force numbers were small (due to the low 2 fps approach velocity used in these calculations), it is still noticeable that the collapsing arch kept the impact nosing from moving as far as if it were rigid. This was because the front of the impact nosing deflected in serial with the base isolator deflection(s). The times to peak force and deflection indicate that the duration of impact was extended.

4.4.3 Validation test II; Deformable BEAS

A second validation test for the collapsible arch was performed on a Deformable BEAS. The impact nosing was placed on double-stacked, softened base isolators, as discussed in Chapter 3. In this test, the variation was in using a rigid front arch in place of a collapsing arch to determine if an arch structure would make a difference in the response of the structure. The approach velocity of the barge train at the time of impact was 4.0 feet per second. Table 4.2 shows the results for this calculation.

Table 4.2 Results for impact of a 3 x 4 barge train against a Deformable BEAS without and with a collapsible front arch.

Collapsing arch	Peak force (kips)	Peak impact nosing deflection (feet)	Time to peak force (seconds)	Time to peak deflection (seconds)
Rigid	4,636	6.3541	2.679	2.791
Flexible	4,122	6.2646	3.037	2.806

Although not as big as the peak force drop in validation test I, the peak force drop was still significant at 500 kips. The difference in the impact nosing deflection is less significant, being nearly $1/60^{th}$ of the total deflection. The times to peak force and deflection again show that with the softer system, the impulse will take place over a longer interval.

Observe that the values for maximum peak impact force computed for a rigid collapsing arch mounted on a rigid bullnose (Table 4.1) and mounted on a Deformable BEAS (Table 4.2) are nearly the same value when the barge train approach velocity is doubled. Doubling of the approach velocity to 4 fps for a barge train impacting a flexible collapsing arch mounted on a rigid bullnose (Table 4.1), compared to the case for one mounted on a

Deformable BEAS (Table 4.2), results in an increase in the maximum impact force by 528 kips, to 4,122 kips.

4.5 Velocity tests I; standard mass impact nosing

Once the model had been validated, velocity tests were performed to see how the newly designed Deformable BEAS with collapsible arch, which had much the same mass as the fixed arch model, would perform for impact with a three-by-four barge train weighing 23,350 tons that would be the typical case at Newt Graham Lock and Dam 18 near Tulsa, Oklahoma. These tests followed the form as the tests in Chapter 3, Section 3.7.5, with approach velocities of 2, 4, and 6 feet per second. When barge train integrity was lost for an impact at 6 feet per second, the velocity was increased in increments of 0.1 feet per second from 4 feet per second, to investigate the maximum approach velocity at which barge train integrity had been maintained.

It was pre-supposed that this Chapter 4 barge train, of lesser mass by three barges than the three-by-five barge train used in the Chapter 3 analyses, would be more likely to maintain barge train integrity for impacts with higher velocity against the same Deformable BEAS structure, and even higher velocities when the collapsible front arch was appended to the impact nosing. This was not the case. In fact, the three by four barge train performed almost identically to the results from Section 3.7.7. Barge train integrity was maintained until the barge train reached an approach velocity of 4.5 feet per second, as shown in Figure 4.5. The peak force of the impact was 4,873 kips and the impact nosing deflected by 6.621 feet.

4.6 The effect of impact nosing mass

It was assumed that, since the Deformable BEAS without a collapsible front arch could handle a three-by-five barge train with a weight of 26,050 tons without losing barge train integrity, a Deformable BEAS design with a collapsible front arch should be able to handle a smaller barge train (i.e. three-by-four barge train with a gross weight of 23,350 tons) at higher velocities without loss of barge train integrity.

Unfortunately, this assumption was not substantiated by the calculations, which led to the idea that the relationship of the mass of the Deformable BEAS to the barge train mass was affecting the conservation of momentum. If this was true, the mass of the impact nosing structure could be tuned to the mass of a specific, design barge train to achieve better results.

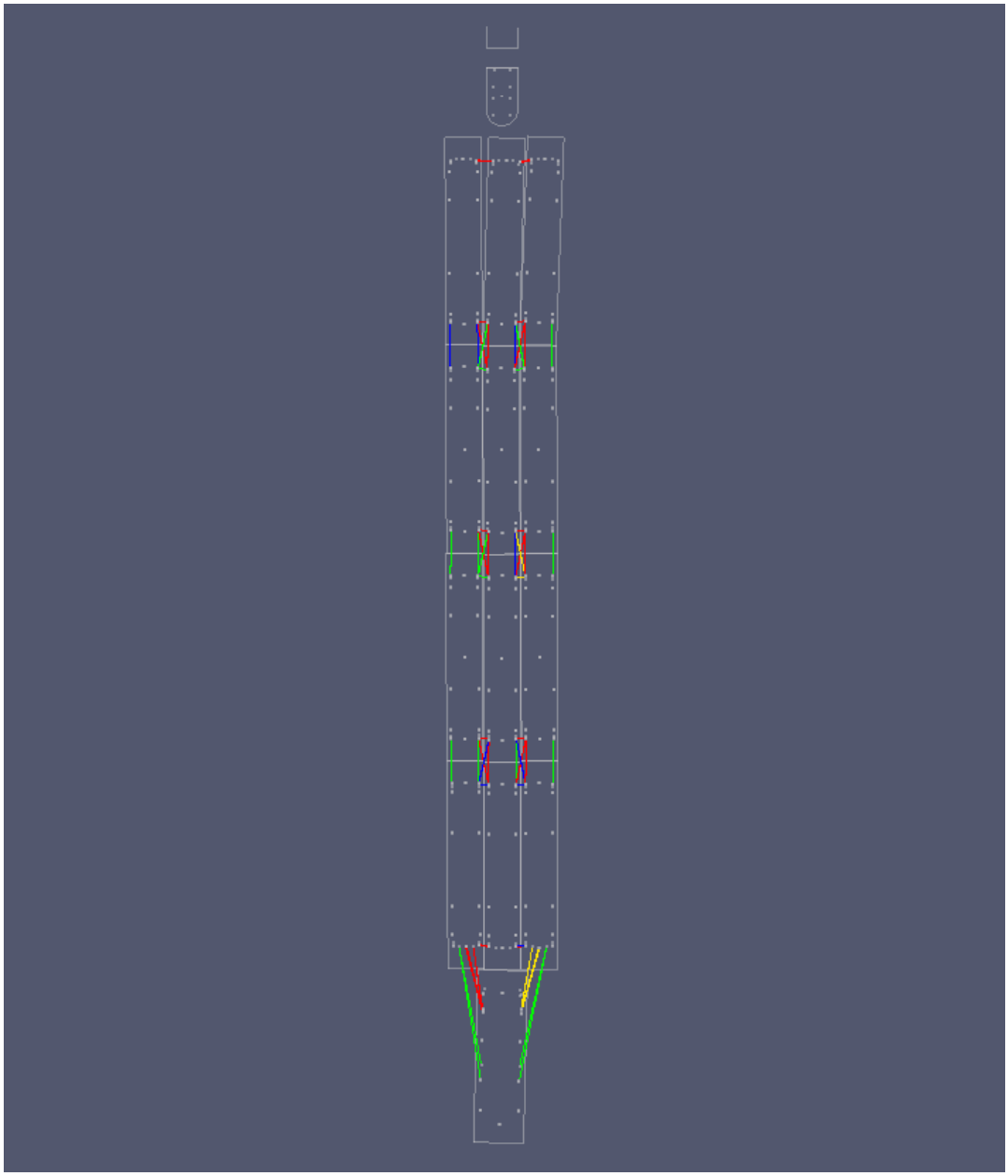

Figure 4.5 Results from an impact of a 3 x 4 barge train with a Deformable BEAS with a collapsible front arch and impact nosing weight of 762 tons at 4.5 feet per second.

Tests to verify this theory were established. The total weight of the impact nosing was varied from the initial fully designed weight at 762 tons to fractions of that weight; at 80%, 60%, and 40% of the total initial design weight. The barge train was a three-by-four barge train weighing 23,350 tons and approached for a head-on collision. Tables 4.3, 4.4, and 4.5 show the results of the testing.

Table 4.3. Results for impact of a 3 x 4 barge train travelling at 2fps against a Deformable BEAS with different masses.

% Mass	Peak force (kips)	Peak impact nosing deflection (feet)	Time to peak force (seconds)	Time to peak deflection (seconds)
100	1,374	3.9792	2.491	3.589
80	1,314	3.9843	4.140	3.463
60	1,363	4.0018	3.155	3.688
40	1,352	4.0344	3.564	3.710

Table 4.4. Results for impact of a 3 x 4 barge train travelling at 4fps against a Deformable BEAS with different masses.

% Mass	Peak force (kips)	Peak impact nosing deflection (feet)	Time to peak force (seconds)	Time to peak deflection (seconds)
100	3,921	6.1934	2.556	2.835
80	3,859	6.1741	2.649	2.882
60	4,044	6.1799	2.828	2.953
40	4,141	6.2030	2.719	2.881

Table 4.5. Results for impact of a 3 x 4 barge train travelling at 6fps against a Deformable BEAS with different masses.

% Mass	Peak force (kips)	Peak impact nosing deflection (feet)	Time to peak force (seconds)	Time to peak deflection (seconds)
100	5,644	7.1797	2.210	2.255
80	6,052	7.5405	2.119	2.207
60	5,715	7.2470	2.247	2.014
40	5,918	7.4157	1.918	2.006

For impacts at 2 and 4 feet per second, the results show that slightly better performance could be expected for peak force if the impact nosing weight was reduced to 80% of the original design weight of 762 tons. For a 2 foot per second impact, it seems that the greater mass impact nosing has a lower displacement than the lower mass impact nosings, but for 4 foot per second impacts, the displacement follows roughly the same curve as the change in peak force.

The data was also collected for 6 feet per second impact events. Analysis of the simulation results revealed that barge train integrity was lost for every

test at this approach velocity. Because barge train mass was shed due to run-away barges, these tests do not give us a good indication of expected peak forces or deflections, other than to tell us that, if barge integrity was maintained, the peak forces would be greater than 5,600 kips and the deflection would be greater than 7 feet.

4.7 Velocity tests II; reduced mass impact nosing

Once it was determined that a lower mass impact nosing for the Deformable BEAS structure could provide some amount relief during an impact by lowering the peak force, the velocity tests were performed following the procedure outlined in Section 3.7.7. Under the new tests, the barge train integrity was held until the barge train exceeded 4.7 feet per second, as shown in Figure 4.6. Tuning the mass of the impact nosing to the expected mass of the barge train seems to provide some improvement for maintaining barge train integrity at higher velocities. The peak force of the impact was 4,977 kips and the impact nosing deflected by 6.799 feet.

After this second set of simulations was performed, a similar set of simulations were performed with a rigid bullnose to establish a base-line for comparison, in much the same manner as was done in subsection 3.7.7. The results are shown in Table 4.6.

4.8 Conclusions

In this chapter, we focused on the design of a Deformable BEAS for Newt Graham Lock and Dam 18 on the Verdigris River near Tulsa, Oklahoma. After identifying features for improvement within the original Deformable BEAS design, we attempted to add a new structural feature, the collapsible front arch, to enhance energy absorption capabilities at higher velocity impacts.

Positive features of the Deformable BEAS with collapsible front arch for head-on collision:

- Lowers peak impact forces.
- Reduces lashing failures for higher velocity impacts of 3 x 4 barge train.
- Maintains barge integrity of three-by-four barge trains for impacts of up to 4.7 feet per second for a Deformable BEAS with only 16 base isolators.

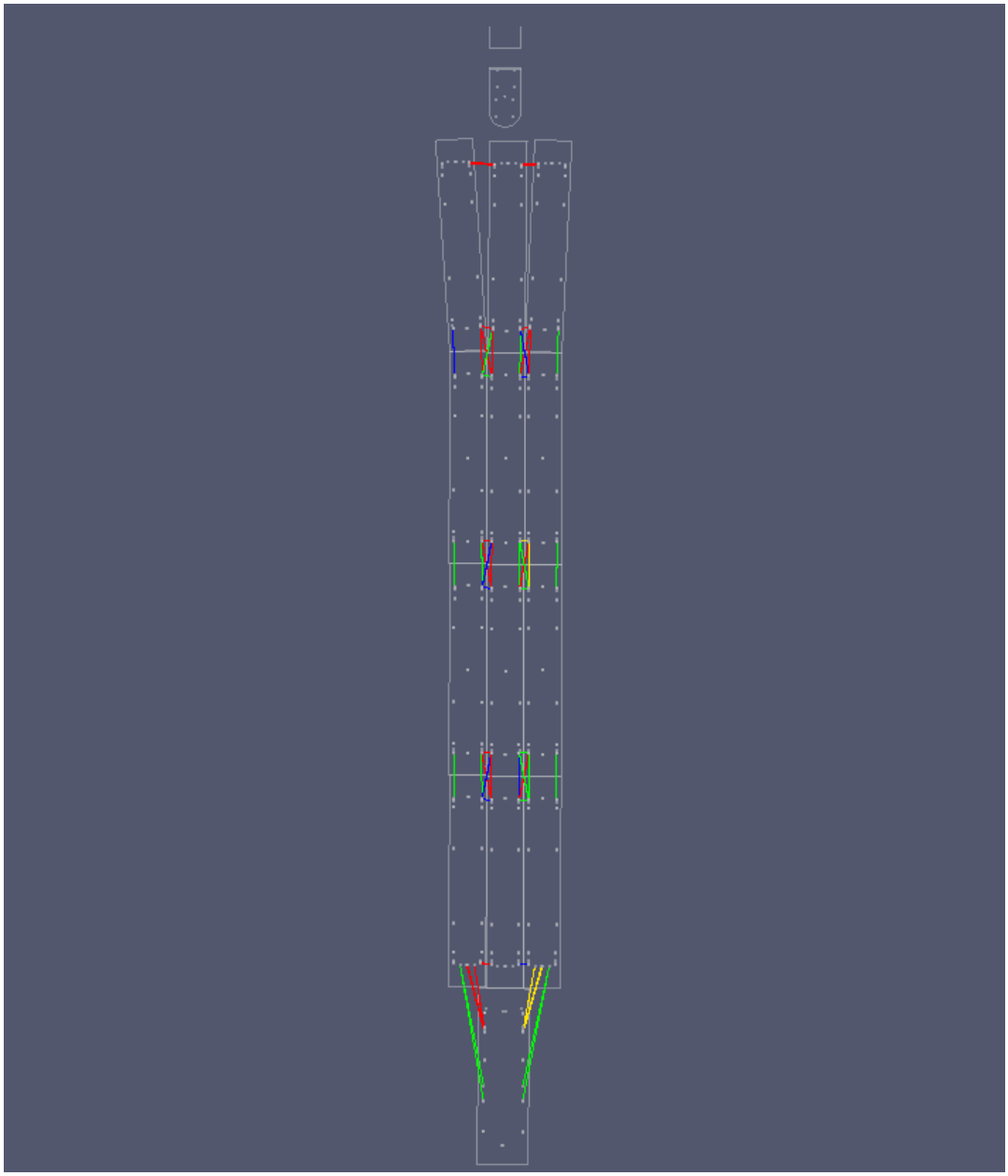

Figure 4.6 Results from an impact of a 3 x 4 barge train with a Deformable BEAS with a collapsible front arch and impact nosing weight of 80% of 762 tons at 4.7 feet per second.

Table 4.6 Comparison of max velocity without losing barge train integrity.

Type of Bullnose Impacted	Maximun velocity with which barge train integrity was maintained (fps)
Rigid	3.0
Deformable BEAS with collapsible front arch and 8 double-stacked, 60% force base isolators	4.7

Negative features of the Deformable BEAS with collapsible front arch for head-on collision:

- The peak deformation for extreme velocities, while lower, is still prohibitive (>6.79 feet at 4.7 fps).
- Still cannot maintain barge train integrity with 16 base isolators for impacts with a three-by-four barge train at greater than 4.7 feet per second, which is less than the ETL 1110-2-563 maximum non-site specific approach velocity of 6 feet per second for the extreme load case.

It is notable that the magnitude of the impact nosing mass of the Deformable BEAS, relative to the mass of the barge train, has such an effect on the overall impact response characteristics for the two bodies. By tuning the mass of the impact nosing to the mass of the "design" barge train, a more responsive system can be designed. However, performance may degrade if the mass of the approaching barge train does not conform to the mass for which the design was developed.

The collapsible front arch for the Deformable BEAS does aid in maintaining the barge train integrity during higher velocity impacts. It does this by reducing the stiffness of the Deformable BEAS when the collapse condition is triggered by exceeding a designed value of force. This suggests that a less stiff bumper system (perhaps aided by base isolators again) could raise the approach velocities that the barge train could achieve before losing barge train integrity.

5 Conclusions and Future Enhancements

5.1 Introduction and assumptions prior to simulations

Several assumptions were made as we came into the simulations in this second phase of research:

1. A head-on impact event has a higher severity than a glancing blow impact event, and therefore is more likely to cause a barge train to lose integrity through the primary threat of the failure of a sufficient number of lashings so as to result in "break-away," out-of- control barges.
2. A Deformable BEAS provides for time to decelerate the barge train, thereby reducing peak forces within the lashings contained in a barge train.
3. The Deformable BEAS should be designed most specifically to deal with the peak force at the impact nosing, which would be at a maximum for a head-on impact.
4. The Deformable BEAS peak force would be an indicator of barge train integrity.
5. A Deformable BEAS would relieve peak forces by extending the duration of the impulse for the barge train against the impact nosing.
6. Base isolators would be the best method to facilitate deformation during an impact event due to their use for massive (building) structures during earthquake loading and the amount of deformation that they make possible.

5.2 Recommendation for site-specific guidance criteria

Results of the investigation to design a Deformable BEAS for the Markland Locks and Dam Project have shown that there appears to be a discrepancy between the probabilistic non site specific criteria given in ETL-1110-2-563 guidance for Usual, Unusual and Extreme load condition criteria and the actual flow and approach tow velocities at Markland. According to the guidelines for Markland Project operations, the maximum locking stage is el 463. This upper pool stage corresponds to a discharge of 540,000 cfs. The estimates of flow velocity based on the 1953 flow model indicate that with a discharge of 540,000 cfs the velocity in the vicinity of the guard wall bullnose is around 7.6 ft/sec. If the discharge were 540,000 cfs, a tow

would approach the bullnose at a velocity less than 7.6 ft/sec in order to maintain control.

The approach velocity data collected from April through September 2010, and shown in Figures 2.10 and 2.11, for three-by-five tows show that an approach velocity of 6 ft/sec is not uncommon. Non site-specific criteria suggests than an approach velocity of 6 ft/sec is extreme. This difference or discrepancy demonstrates the need for site specific studies to collect approach velocity data and better define the load conditions for a specific project.

5.3 Establishing a base-line for determination of fundamental factors influencing barge train integrity

To assess the improvement made by inclusion of the Deformable BEAS and addition of other energy absorbing devices, two questions needed to be answered: “What is the influence of lashing layout on barge train integrity?” and “what is the influence of the size of the barge train on barge train integrity?” These questions need to be answered for the Corps lock that is being analyzed because the lashing layouts and design barge train size vary with lock capabilities and river properties. The answers to these two questions establish a baseline at a specified Corps lock for the assessment of improvement due to the inclusion of a Deformable BEAS.

In the simulations, it was determined that the choice of lashing layout could have a strong influence on simulation results for impacts of a barge train with a bullnose for head-on impacts (Table 5.1). Simulations of a head-on collision between a three-by-five barge train with an AEP lashing layout with a rigid bullnose revealed that the barge train integrity was lost for approach velocities of 2.7 fps and above, while the same barge train with an ACL lashing layout would maintain barge train integrity for approach velocities up to 3.3 fps.

The design barge train size also has a strong influence on the simulation results. Larger barge trains have more mass, more surface area, and more lashings. More mass means greater demands on barge train integrity due to inertial effects. More surface area means that there are more opportunities for sliding friction as one barge moves relative to another, resulting in a force that is found to be favorable for maintaining barge train integrity. More lashings means that there is more resisting forces to maintain barge train integrity. In simulations, it was discovered that a three-by-five barge

Table 5.1 Comparison of Deformable BEAS to base-line simulations.

Bullnose type	Barge train size	Barge train lashing layout	Limiting velocity for maintaining barge train integrity (fps)
Rigid	3x5	AEP	2.7
Rigid	3x5	ACL	3.3
Deformable BEAS with 8 double-stacked, 60% stiffness base isolators	3x5	ACL	4.5
Rigid	3x4	ACL	3.0
80% Mass Deformable BEAS with 8 double-stacked, 60% stiffness base isolators and Collapsible Front Arch	3x4	ACL	4.7

train could withstand a higher velocity impact (3.3 fps) with a rigid bullnose than a three-by-four barge train (3.0 fps). This implies that the effects of friction and additional lashing for a larger barge train dominate the inertial effects due to the increased mass.

For either size barge train, the performance could be improved using a Deformable BEAS. Adding a Deformable BEAS with 8 double-stacked, softened base isolators allowed the limiting approach velocity for a 3 x 5 barge train using an ACL lashing layout to be increased to 4.5 feet per second. For a 3 x 4 barge train with an ACL lashing layout, the limiting approach velocity could be increased to 4.7 feet per second with the addition of other energy absorbing features and by “tuning” the impact nosing mass to the design barge train mass.

5.4 dBEAS results

From the results of the empirical data gathering and simulations we can ascertain certain facts:

- Site-specific approach velocities must be determined from empirical data gathered through (complete) seasonal cycles.
- Pull tests on wire ropes revealed that the actual breaking strength is much greater than the value cited in Table 3.2.
- The choice of lashing layout for same size barge trains affects the magnitude of the limiting velocity for maintaining barge train integrity.
- The size of the design barge train affects the magnitude of the limiting velocity for maintaining barge train integrity.

- A Deformable BEAS with an impact nosing founded on base isolators will reduce lashing failures due to impact and therefore preserve barge train integrity for higher velocity events than a rigid bullnose.
- The reason that the Deformable BEAS preserves lashing integrity is because the flexibility of the base isolators causes the impact nosing to make several short duration sub-impulses with the impacting barge with intervals between each sub-impulse allows the wire rope to relieve tensile strain. This interval is referred to as a "respite interval".
- Compared to a base group of single base isolators, a base group of stacked base isolators lower the stiffness of the Deformable BEAS and provides sufficient deflection to provide protection for barge train integrity.
- Because the kinetic energy of a barge train varies with the square of the velocity, the deflection necessary to protect barge train integrity with higher velocity barge trains is shown to increase in a nonlinear fashion with velocity.
- The effectiveness of a Deformable BEAS for maintaining barge train integrity is found to be sensitive to the mass of the barge train. Therefore the Deformable BEAS should be designed for the site-specific, fully-loaded "design" barge train.
- For a head-on allision, the Deformable BEAS with a base group of double-stacked base isolators will perform better than the rigid bullnose, but will not achieve the desired protection of barge train integrity for the entire range of the non-site specific Extreme load velocities specified in ETL-1110-2-563.
- It is proven that the collapsing arch added to the front of an impact nosing provides additional protection of barge train integrity when combined with the base group of double-stacked base isolators for even higher velocity barge trains.
- The collapsing arch combined with the double-stacked base isolators will not achieve the desired protection of barge train integrity for the entire range of the non-site specific Extreme load velocities specified in ETL-1110-2-563.
- For glancing blow impacts between the barge train and the Deformable BEAS with Markland site-specific data, the Deformable BEAS maintained lashing integrity into the site-specific Extreme load case velocity range. The rigid bullnose did not maintain lashing integrity into the Unusual load case velocity range.

5.5 Conclusions

The Deformable BEAS without a collapsible front arch is capable of maintaining barge train integrity for head-on three-by-five barge train impacts up to approach velocity of 4.5 fps which is in the non-site specific Extreme load case approach velocity range. For Markland, this approach velocity corresponds to the Usual load case range. For head-on collisions, it will harder to design a bullnose to meet site-specific velocity criteria for locks with greater flow capacity.

For Newt Graham Lock and Dam 18, a Deformable BEAS with a collapsible front arch is capable of maintaining barge train integrity for head-on three-by-four barge train impacts up to approach velocity of 4.7 fps which is in the non-site specific Extreme load case approach velocity range. The smaller barge train had lower mass (favorable), but also fewer lashings (unfavorable). Because of these changes in the barge train, it was necessary to lower the mass of the impact nosing and lower the stiffness of the BEAS (now with the collapsible nosing) to "tune" the dynamics of barge train to that of the impact nosing structural system for optimal response characteristics.

For glancing blow impacts, the Deformable BEAS with double-stacked base isolators was capable of maintaining lashing integrity for the non-site specific Extreme load case approach velocity range, as well as the site-specific Extreme load case approach velocity at an extreme site-specific angle for Markland. This implies that structures that are only subjected to glancing blows (i.e. approach walls) could benefit from the addition of these flexible structural features.

5.6 Future research

Future research with regard to the Deformable Bullnose would seem to require that we continue to reduce the stiffness of the impact nosing relative to the barge train. To achieve the desired goal for maintaining barge train integrity for a head-on Extreme impact event, additional energy absorbing feature(s) will be required. Concepts for the next stage of research into additional energy absorbing devices to be added on are discussed in this section.

5.6.1 Frangible section

One of the issues not considered in the research to this point has been contact between the impact nosing of the Deformable BEAS and the supporting end of approach wall structural feature for the Deformable BEAS. In the event of an extreme impact, the impact nosing may be "pushed" to a point that the rigid section of the impact nosing may come in contact with the continuing wall section or supporting platform vertical face, introducing higher forces due to a "rigid" impact within this zone. To further "soften" this collision, bumper systems composed of frangible system(s) are being proposed for investigation during the next phase of research. Figure 5.1 shows a possible configuration of a frangible structural system internal to the impact nosing. The rigid pedestals that support the base isolators for the Deformable BEAS would be equipped with one of the frangible systems discussed below. These frangible systems could also be appended to a corbel extension for the existing approach wall, behind the impact nosing. Under extreme conditions, the frangible sections would crush, providing a soft response in much the same way as the collapsible arch does. This provides the advantage that a system configuration can be proposed so that the frangible sections would need to be replaced when a rare Extreme design load case impact occurs without damaging the impact nosing and its base isolators.

The structural configuration shown in Figure 5.1 was selected to provide space for the following frangible wall options:

- Axial loaded high strength steel tubes with accordion type bucking behavior (Tai et al., 2009).
- Axial loaded concrete-filled steel tubes (Schneider, 1998).
- Multi-cell steel braced-frame system (Celik et al, 2006 and AASHTO, 1991).
- Rubber super arch delta and super cone fender energy absorbing system (AASHTO, 1991).

These four options would be investigated during the next stage of research. The attractive features for these options are discussed in the following four subsections.

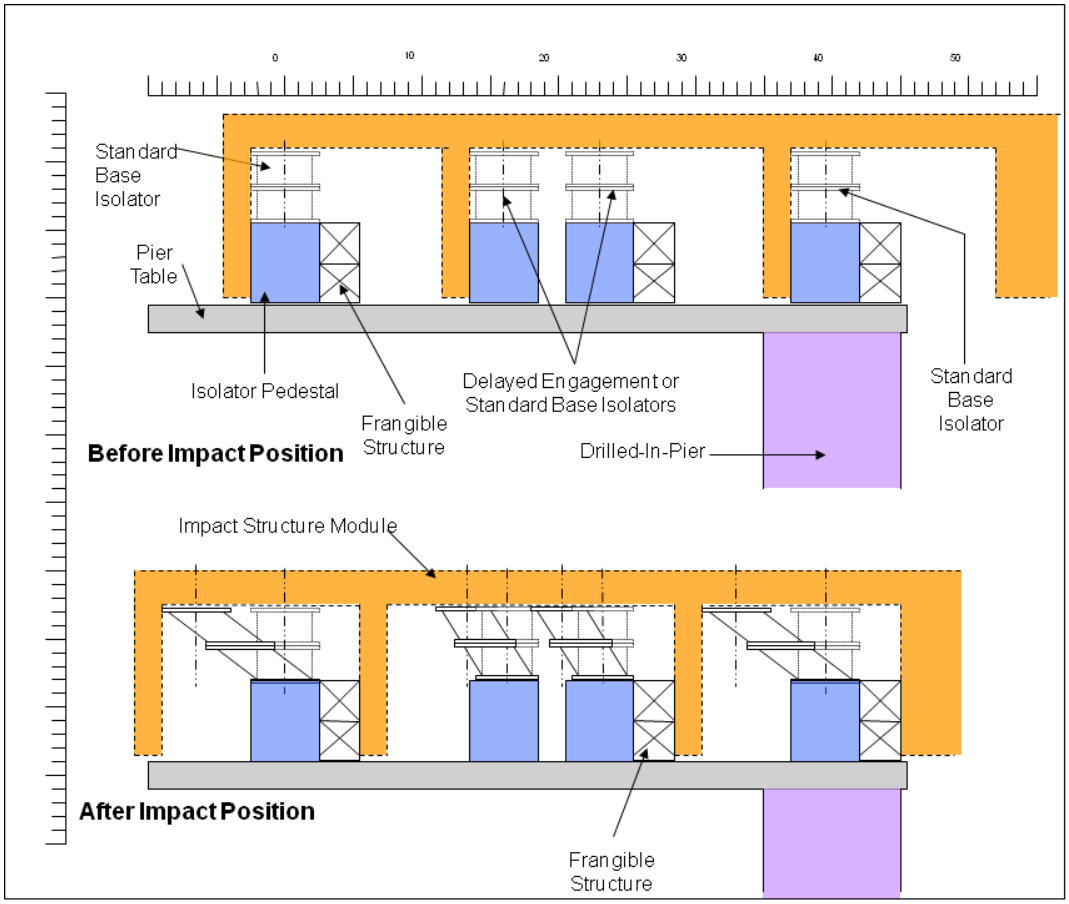

Figure 5.1 The internal addition of the frangible sections to the Deformable BEAS.

5.6.1.1 Axial loaded High Strength Steel Tubes (HST)

Barge impact loading and other types of impact loadings are different from cyclic loading such as those associated with earthquakes. Impact loadings are a following type loading where the displacements continue to increase with time and energy dissipation occurs as the impacted structure continues to deform. Earthquake loadings are cyclic loadings where energy dissipation is achieved through hysteretic behavior. The HST system will require testing and/or analysis consistent with impact loading. The behavior of a good impact energy dissipating system is illustrated in Figure 5.2.

The HSTs of Tai et al. (2009) were small, having a diameter of 31mm (1.25 inch) with lengths of 90mm (3.5 inch), 120mm (4.75 inch), and 200mm (8-inch). The average energy absorption of the 22 specimens tested was 3.3 joules (2.34 ft-kips) with an average peak load of 106 kN (24 kips) and an average displacement of 60mm (2.36 inch). An exorbitant number of small HSTs would be required to dissipate the extra energy associated with an Extreme barge impact hit. Assuming the demand in terms of kinetic

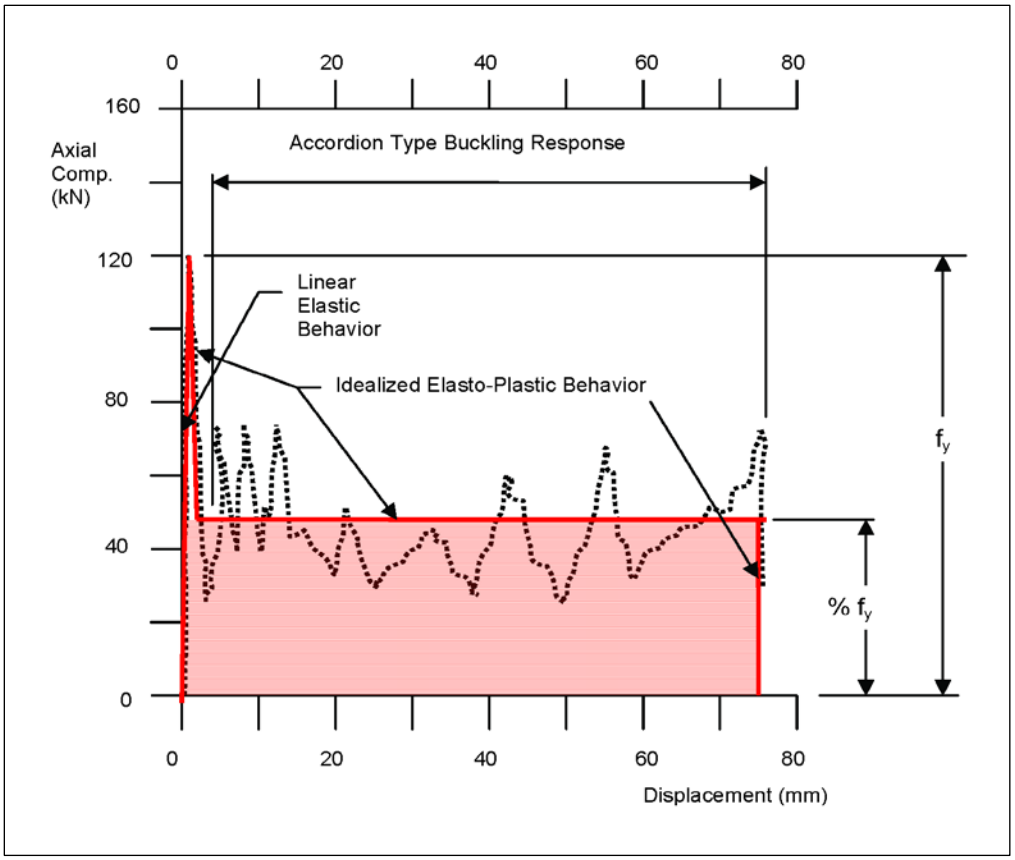

Figure 5.2 Energy dissipation of HST (after Tai et al. 2009).

energy was 20,000 ft-kips, a total of 20,000 / 2.34, or 8550 HSTs would be required. Keeping the diameter to length ratio at 120 / 30, or equal to 4, it may be possible to use 6 inch diameter x 24 inch long HSTs with a thickness of 0.125 inch and dissipate a much greater quantity of energy. The type of behavior sought is illustrated in Figure 5.3. Obtaining this type of behavior would require a non-linear finite element (FE) analysis with plastic buckling capabilities. This research team has extensive experience in nonlinear finite element analyses of complex structural systems, with the latest examples being shown in Ebeling and Warren (2008, 2009).

5.6.1.2 Axial loaded Concrete Filled Steel Tubes (CFT)

Cylindrical CFTs have excellent displacement ductility and should perform well under earthquake type cyclic loading. However, the displacement at buckling is only about 20 mm (1-inch) and the total displacement capacity at failure is only 32 mm (1.25 inch). It is not known what kind of energy dissipation could be expected under impact type (following load) conditions. Typical load-displacement behavior of a CFT is illustrated in Figure 5.4.

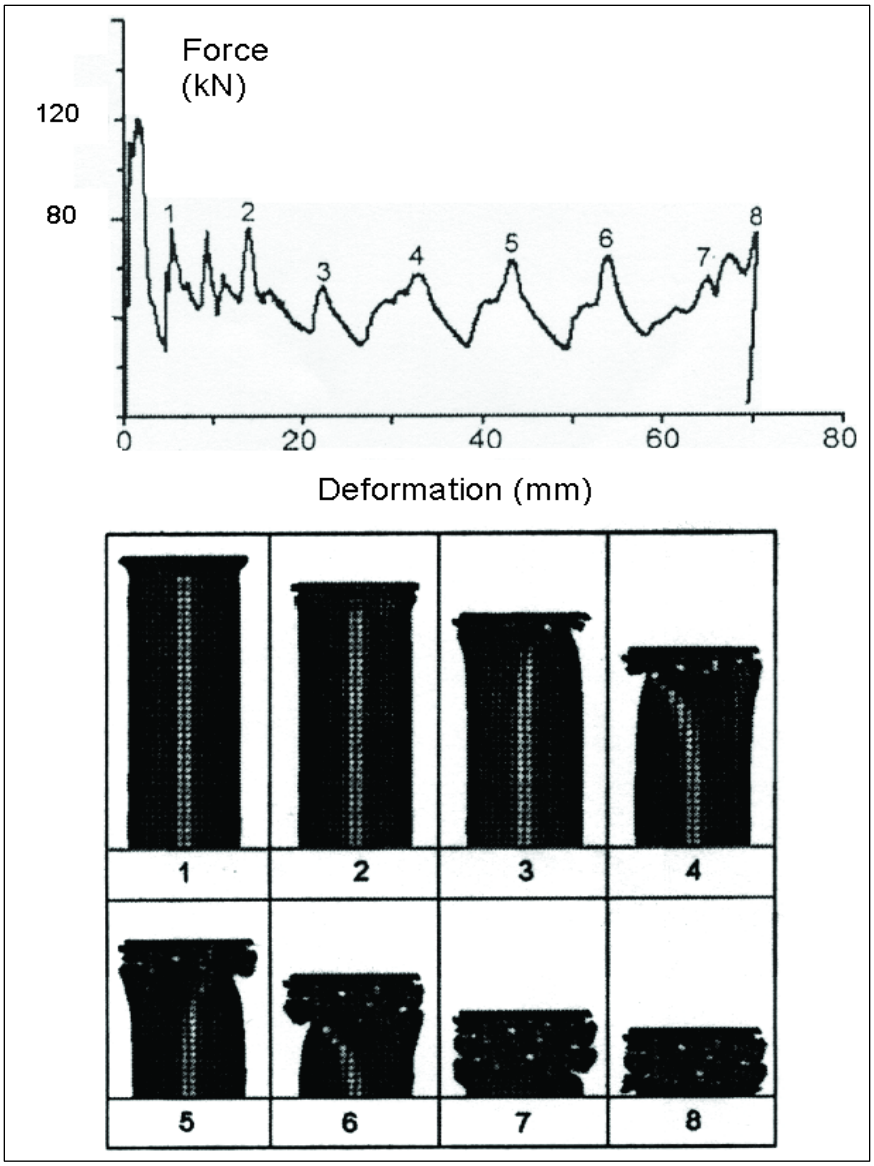

Figure 5.3 HST behavior (after Tai et al. (2009)).

Testing of CFTs in Schneider (1998) indicated buckling behavior of the nature shown in Figure 5.5.

Both HST and CFT systems have the potential to dissipate large amounts of energy; however, this would require as a minimum a non-linear finite element analysis with plastic buckling capabilities. A large number of CFTs would be required to dissipate the extra energy associated with an Extreme barge impact hit. Assuming the demand in terms of kinetic energy was 20,000 ft-kips, a total of 20,000 / 35.4, or 565 CFTs would be required. Again, nonlinear FE analyses would be proposed to further define the required characteristics.

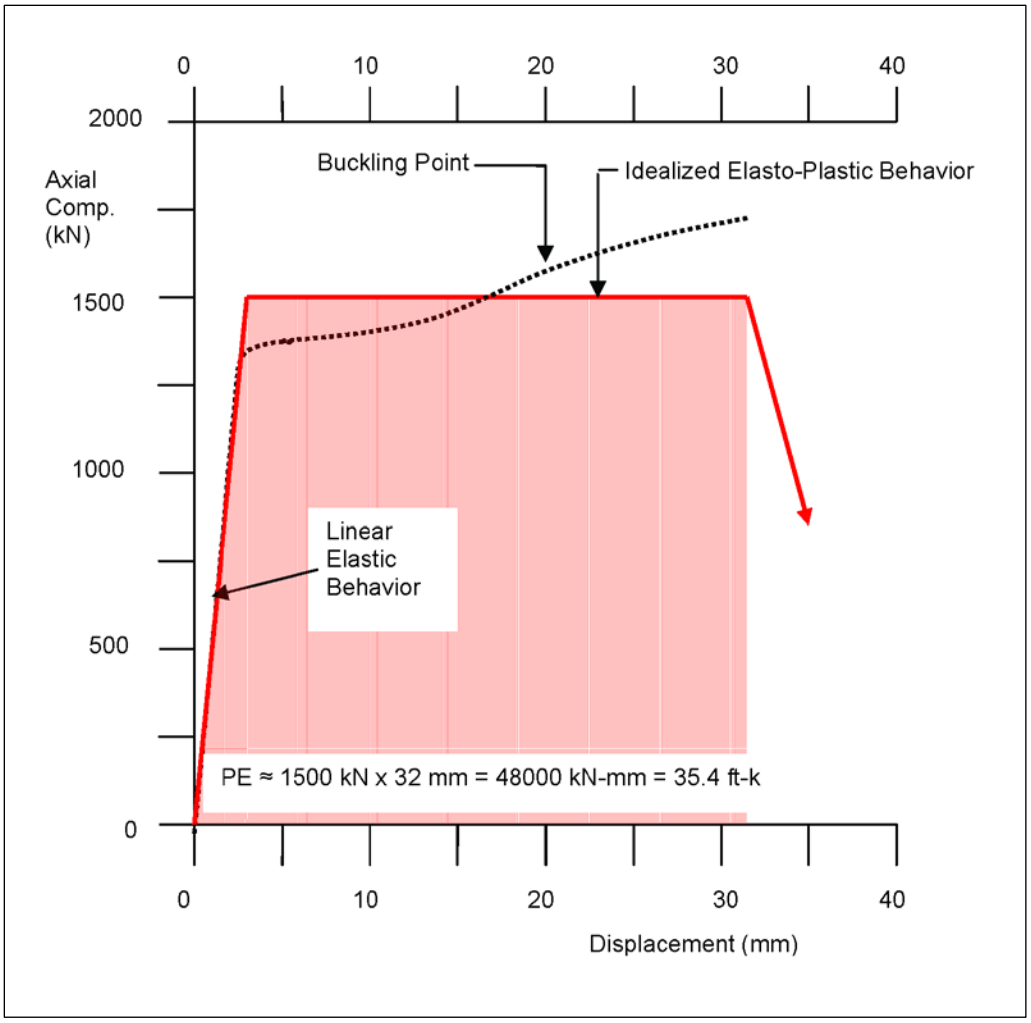

Figure 5.4 Energy dissipation of CFT (after Schneider, 1998).

5.6.1.3 Framed Steel Systems (FSS)

A FSS has been developed in Japan for protection of the Bisan-Seto Bridge piers. The research described in AASHTO (1991) suggests that the FSS could withstand an impact force of 800 kips, with the impact energy dissipation capacity of 7500 ft-kips. The steel frame system consisted of a series of a vertical impact plates, a series of horizontal plates (diaphragms) that apparently dissipate energy through buckling, and a series of cross frames, cross bracing, and ribs. The load-displacement performance of the system was elasto-plastic, similar to that indicated for the CFT system. It is indicated in AASHTO (1991) that additional energy dissipation could be achieved by filling the frame with dense foam. The number of frames required in a collision to achieve the 7500 ft-kips of energy dissipation cannot be determined from the information contained in AASHTO (1991). The displacement under a load of 800 kips would be 7500 ft-kips / 800 kip,

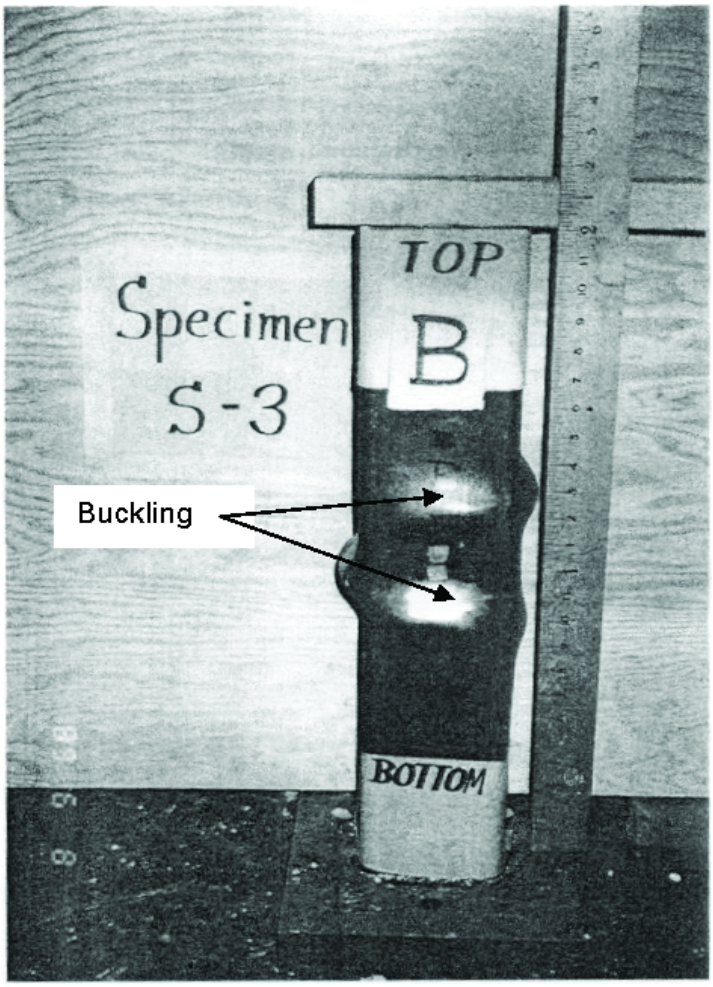

Figure 5.5 CFT behavior (after Schneider, 1998).

or a little over 9 feet. This type of framing system would be best appended to a corbel extension for the existing approach wall, behind the impact nosing. Other framing techniques are discussed in Celik et al (2006). The steel frame system consisted of a series of a vertical impact plates, a series of horizontal plates (diaphragms) that apparently dissipate energy through buckling, and a series of cross frames, cross bracing, and ribs (Figure 5.6).

5.6.1.4 Super Arch Delta (SAD) and Super Cone Fender (SCF) energy absorbing systems

The Super Arch Delta and Super Cone Fender energy absorbing systems are part of a family of fendering systems that have been used for mooring ships and other large marine vessels. There are several companies that manufacture these types of energy absorbing devices. The information that follows is after Trelleborg, and fairly represents this family of fendering systems.

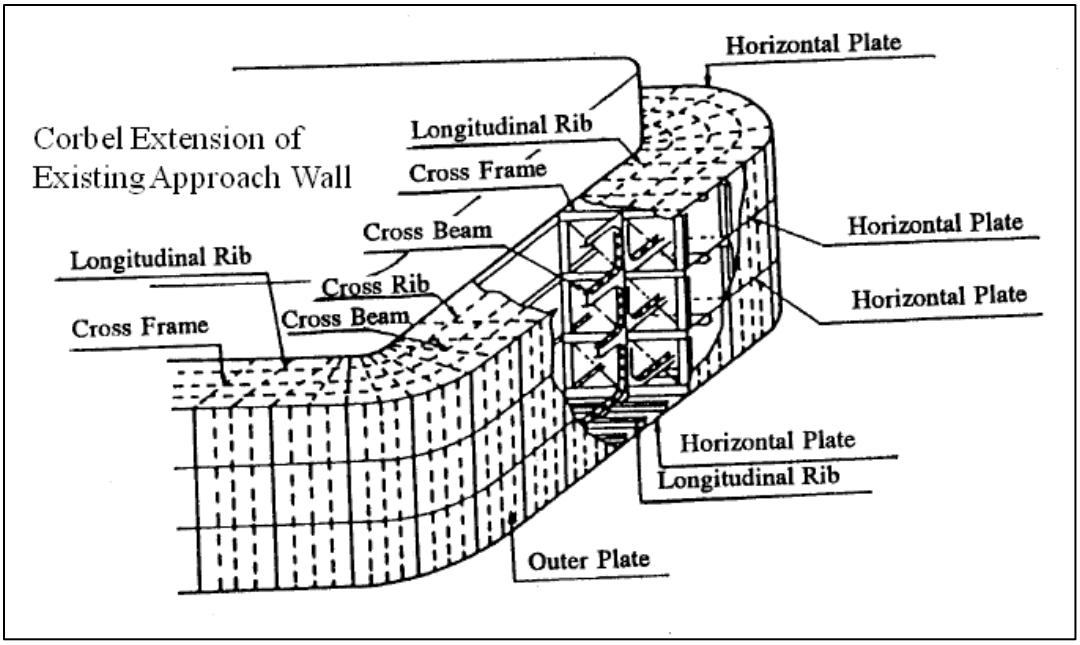

Figure 5.6 An example of a Framed Steel System (after AASHTO, 1991).

Super Arch Delta energy absorbing systems (Figure 5.7) are a proven system for absorbing energy during the mooring of large marine vessels. They are stable even at high compressive strains. They are designed to deform along their primary axis of symmetry (Figure 5.8). Super Cone Fender load-displacement and energy absorption is illustrated in Figure 5.9.

Figure 5.7 A Super Arch Delta energy absorbing system (after Trelleborg, 2007).

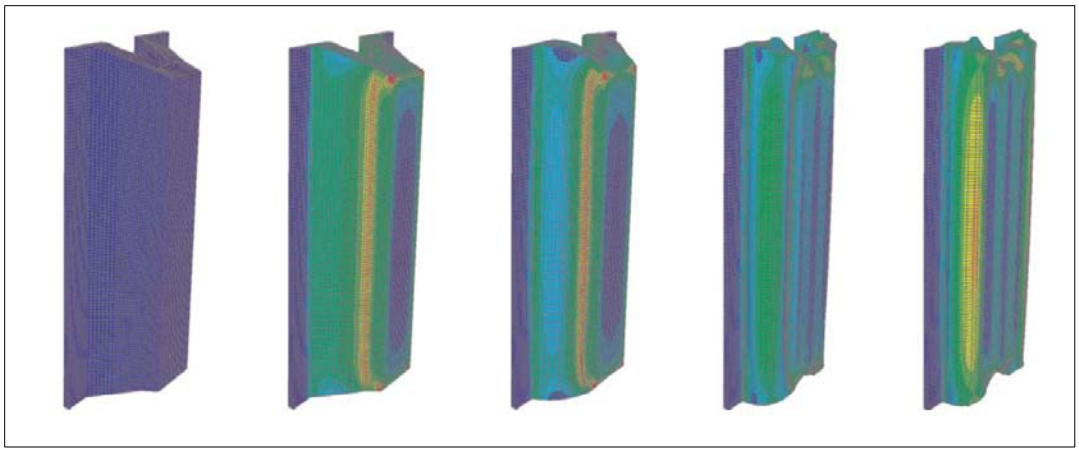

Figure 5.8 Deformation of a Super Arch Delta (after Trelleborg, 2007).

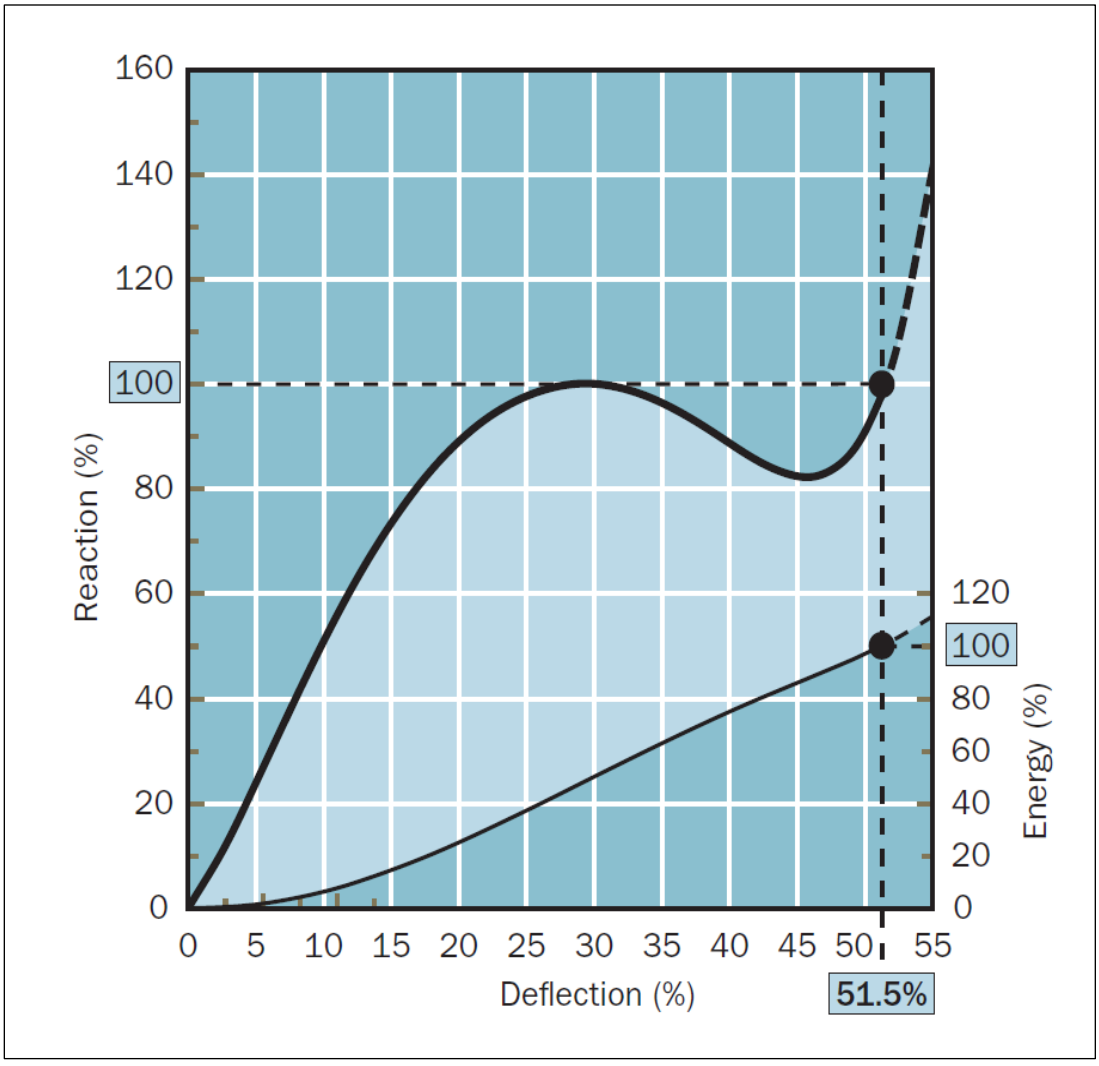

Figure 5.9 Super Arch Delta reaction versus deflection curve (after Trelleborg, 2007).

Super Cone Fenders are the latest generation of fenders used for the mooring of large marine vessels. They are stable even at high compressive strains. They deform axially, where base isolator systems deform in shear. Doubling the cones, as illustrated in Figure 5.10, would provide a workable energy absorption system that could work in combination with base isolators when high energy head-on collisions take place. A portion of the impact energy may be absorbed prior to engaging the base isolators, thereby keeping barge trains intact while preventing damage to the base isolators. Super Cone Fender load-displacement and energy absorption is illustrated in Figure 5.11.

Figure 5.10 Double Super Cone Fenders (after Trelleborg, 2007).

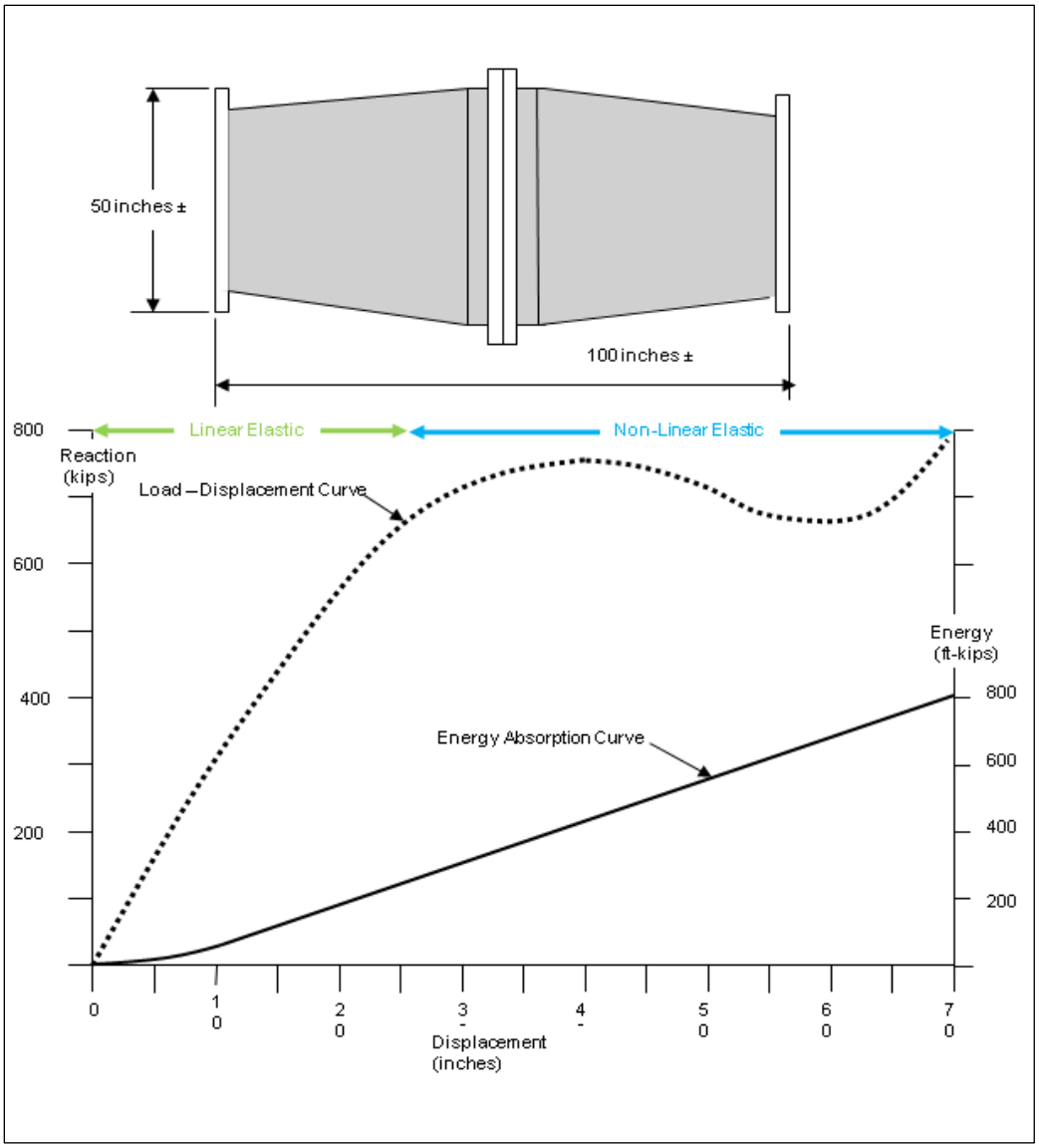

Figure 5.11 Double Cone Fender performance (after Trelleborg, 2007).

5.6.2 Deformable nose cone

It was shown in Chapter 4 that a Deformable BEAS with a collapsible front arch would provide more protection for barge train integrity, mainly due to the fact that its stiffness would act in series with the stiffness of the base isolators supporting the impact nosing. It was also shown in Chapter 3 that glancing blow impacts between a barge train and the Deformable BEAS are less damaging to barge train and lashing integrity at much higher velocities than for a head-on impact. This suggests that a less stiff collapsible or frangible system would only need to be installed at the smaller "head-on impact region" of the impact nosing, as shown in Figure 5.12. This system could be modified to provide even lower stiffnesses for a head-on collision.

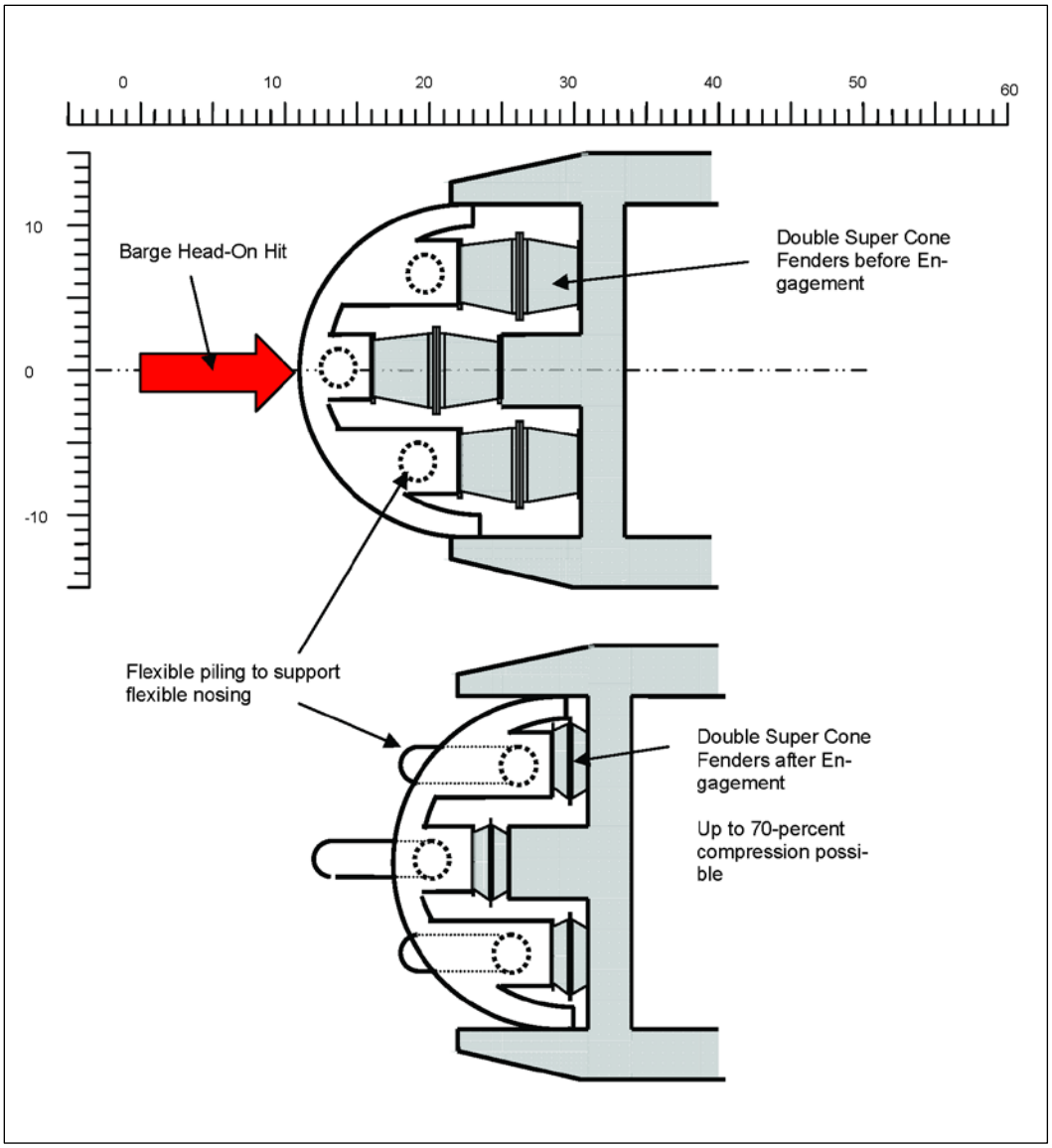

Figure 5.12 Concept of a Deformable BEAS impact nosing designed specifically for head-on impact using Super Cone Fenders.

The stiffness curve for a head-on collision with a collapsible arch is shown in Figure 4.3. The collapsing arch showed the energy absorbing capability of 3,535 kip-feet for 10 inches of deflection. From the double super cone energy absorption curve of Figure 5.11 and the proposed design for head-on impacts in Figure 5.12 with 3 sets of double super cone energy absorbing devices, it can be shown that 2,400 kip-feet of energy absorption can be performed over 70 inches of deflection in an entirely elastic manner. The stiffness is much less for the super cones than for the collapsible arch system. Acting in series with the base isolators will provide a lower overall stiffness for the Deformable BEAS.

A preliminary investigation was performed using an approximation of the stiffness curve of the double super cone fenders for the stiffness of the leading arch for the Deformable BEAS impact nosing. The results were promising, showing that barge train integrity was maintained for a head-on collision between a fully-loaded, 3-by-4 barge train and the Deformable BEAS at velocities up to 6.1 feet per second. This result was obtained in a parametric study where the number of double super cone fenders used for the impact nosing was increased from 3 to 7 (see Table 5.2). "Stopper blocks" were to be added to the structure so that after 70 inches (5.83 feet) of deformation of the double super cone fenders the front arch would be stopped (becoming rigid) to prevent destruction of the fenders. For 3 to 5 double super cone fenders the front arch reached the 70 inch deformation limit, and the peak force acting at the point of contact between the barge train and the Deformable BEAS was greater than the maximum force that the fenders could withstand with 70 inches of deformation. For 6 double super cone fenders, the structure did not reach the 70 inch deformation limit, and therefore the peak BEAS force was lower. With 7 double super cone fenders the system became too stiff, and barge train integrity was lost at less than 5.5 feet per second.

Figure 5.13 shows the force response over time of the 6.1 fps barge train collision with the Impact Nosing with a deformable front arch with 6 double super cone fenders. The peak force is 4,814 kips as noted in Table 5.2

Table 5.2 Preliminary Double Super Cone Fender Front Arch Results

Number of Double Super Cone Fenders	Peak Force at 70" Deformation (kips)	Maximum Velocity to Maintain Barge Train Integrity (fps)	Peak BEAS Force (kips)	Impact Nosing Deflection (ft)
3	2400	5.5	4814	6.47
4	3200	5.8	4676	6.53
5	4000	6.2	5003	6.66
6	4800	6.1	4148	6.42
7	5200	<5.5	n/a	n/a

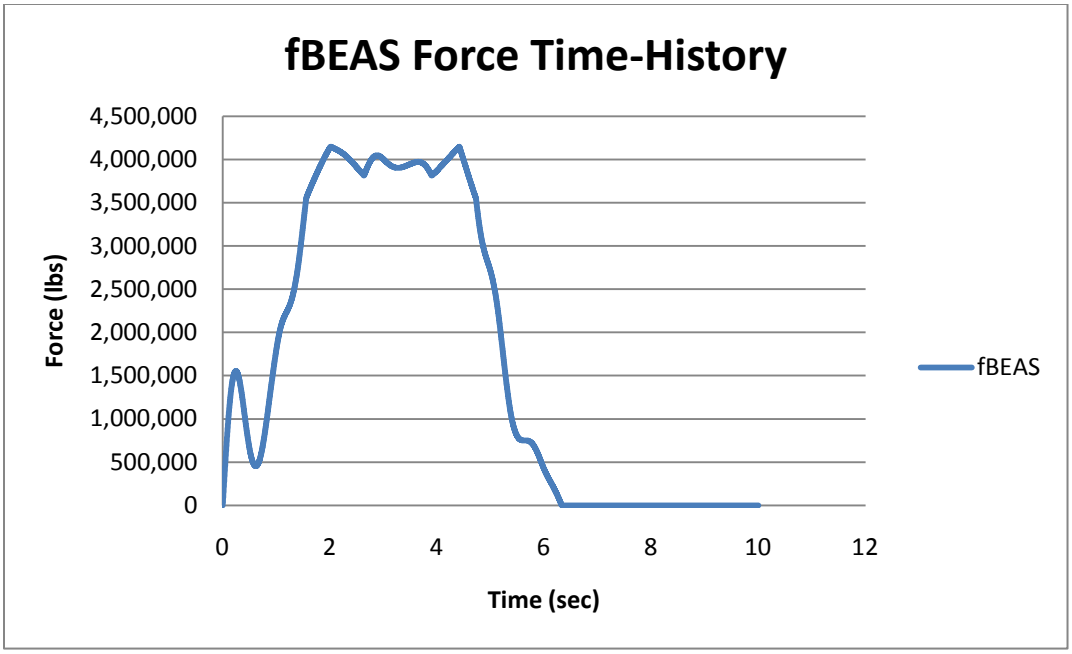

Figure 5.13 Results for Impact of 3-by-4 Barge Train with Deformable BEAS

5.6.3 Structures to maintain contact between impact nosing and barge train

It was originally assumed at the start of this second phase of research that a Deformable BEAS system would stay in contact with the impacting barge train for a longer period of time and with lower peak forces due to the acceleration of the impact nosing mass in conjunction with the deceleration of the barge train. The dBEAS simulations discussed in this report show that the interaction between the barge train and the Deformable BEAS impact nosing is sensitive to the relative masses of the barge train and the Deformable BEAS impact nosing, the collective stiffness of the base isolators and the collapsible front arch for the impact nosing, and the position and angle of approach for the barge train. The interactions of the barge train and the Deformable BEAS impact nosing will be sensitive also to the stiffness of proposed frangible systems located between the impact nosing and its supporting structure. As shown in Subsection 3.7.8, the interaction between the impact nosing and the barge train is a series of short duration impulses with high peak forces. This is due to the dynamic interaction between the barge train and the impact nosing, as expected due to the conservation of momentum, and the dynamic interaction between the impact nosing and its base isolators. The conservation of momentum propels the lower-mass impact nosing from the higher-mass barge train followed by the base isolators pulling the impact nosing back into the barge train. The returning impact nosing has a high velocity relative to the still on-

coming barge train. Each of the short duration impulses reflects an energy transfer between the barge train and the impact nosing due to the conservation of momentum. The shorter impulses are beneficial to maintaining barge train and lashing integrity because of the 'respite' time between impulses, when the lashings can relieve strain energy because the barge train has no external forces applied to it.

Despite the fact that these 'respite' times enable the maintenance of barge train and lashing integrity, the fact that the peak forces are comparable to the forces in a rigid approach wall impact implies that the impact nosing will need to be designed for these peak forces contained within the short duration impulses. Preliminary tests show that this phenomenon may change with the addition of other types of energy absorption devices (e.g., super cones and/or super arch fendering systems) that soften the impact nosing structural system. Additionally, it may be possible to design an impact nosing with damped motion using a frictional device. A frictional damper could enable the impact nosing to remain in contact with the barge train for longer duration impulses with lower peak forces, as the impulse was originally envisioned for the Extreme head-on impact events. Research into rolling friction devices that would provide the drag for the damping of the impact event would be need to be performed, followed by dBEAS simulations with the appropriate mechanical model and properties to reflect the frictional system being investigated.

5.6.4 Deformable approach wall systems for glancing blow impacts

Given the results of Subsection 3.7.8, where a Deformable BEAS outperformed the rigid bullnose at maintaining barge train and lashing integrity for higher velocity glancing blow impacts, it is logical to assume that the lessons learned from these results may be applied to guide and guard walls. Because the approaches to these walls are limited, glancing blow impacts make up the majority of events that occur at these approach walls. Using the deformable structures discussed in this report and the possible future research discussed in Subsection 5.6.3, approach walls could be engineered to protect barge train and lashing integrity over multiple events. This topic is currently being researched by members of this team under the work unit for the Navigations Systems R&D program "Innovative Lock & Approach Walls Structural System Features".

5.7 Stage 3 research

The addition of the collapsible front arch to an impact nosing with double stacked, soft base isolators combined with its subsequent improvement in the performance of the Deformable BEAS to extend the maintenance of barge train integrity to 4.7 feet per second for a head-on collision implies that other innovative energy absorbing features could allow for even higher approach velocities. Also, energy absorbing features could provide more protection for the impact nosing during Extreme (design) impact events.

The next stage of research will include the investigation of:

- super cones and/or super arch fendering systems,
- fendering systems for the supporting structure for the base isolators and impact nosing (i.e., corbel extension or base isolator pedestals),
- super cones for a deformable front arch of the impact nosing, and
- rolling friction devices.

5.8 Costing of a Deformable BEAS Structural System

This subsection discusses the costing of a Deformable BEAS using the structural system configuration shown in Figure 5.14. The site assumed is at the upstream end of the landside guide wall at Newt Graham Lock 18, on the Verdigris River, near Tulsa, Oklahoma (Tulsa District). To reduce construction costs and the impact of construction activities on lock traffic during construction, the fixed pier table and drilled in piles foundation support structure to the impact nosing and base isolators (shown in Figures 1.4 and 3.7) are replaced by a two 28-ft diameter steel sheet pile cells filled (by tremie method) with concrete. This maximizes construction from barges and avoids dewatering. It also avoids the need for a lowered pool at select time intervals during construction. A third, smaller, 24-ft diameter steel sheet pile cell filled with concrete is used to support the precast impact beams extending the guide wall and the back-side “stopper” block shown in the figure. It is envisioned that the steel sheet piles can extend above any pool elevation anticipated during construction and excess sheet pile can be cut off when construction of the base isolator pedestal is complete. Considering the shale (moderately hard, carbonaceous) foundation, a set of four six-foot diameter, drilled in place piles are included below each of the three cells to assist with bearing and shear loadings. Two simply-supported, stacked, precast, post-tensioned concrete impact beams are also added that extend the existing guide wall into the Deformable BEAS. All lock-side surfaces are to be armored.

5.8.1 Deformable BEAS cost for Newt Graham Lock 18

Mr. Richard Femrite and Mr. Kent Hokens of MVP developed a cost estimate using the "rudimentary" Figure 5.14 sketch of the structural system. Because no detail, site-specific design for the foundation system was made at this stage of Deformable BEAS Research & Development (R&D), they state that the cost estimate is to be considered "a rough order of magnitude type estimate and should not be used for final funding purposes." The unit prices used in this costing exercise is based on March 2010 unit pricing for Lock & Dam 22 and MVP costing work at other locks on the Mississippi. These 2010 prices were then indexed to midpoint of October 2013 for the Construction and Construction Management estimates. The 2010 unit pricing for Planning, Engineering and Design were indexed to February 2012. Given these caveats, a midpoint 2013 construction cost estimate is approximately $10 million for the Figure 5.14 Deformable BEAS structural system (including the foundation system and the pair of post tensioned impact beams tie-in), with an additional $2.5 million for Planning, Engineering and Design as well as Construction Management.

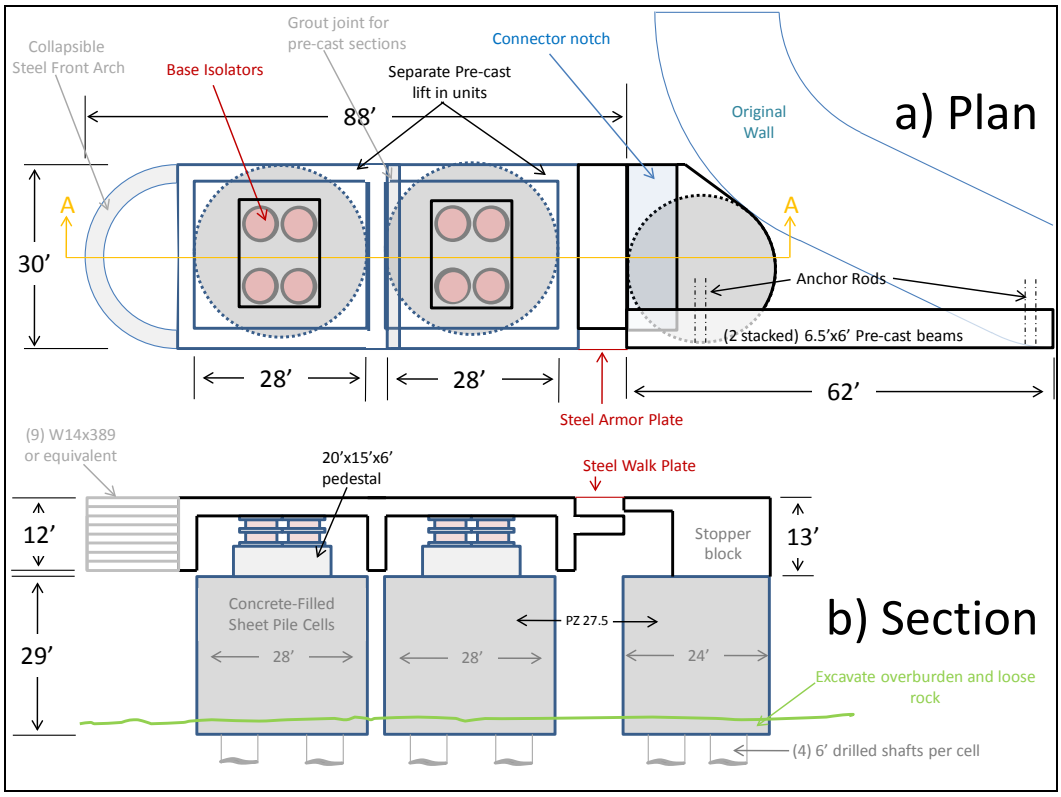

Figure 5.14 Costing design for a Deformable BEAS as proposed at Newt Graham Lock and Dam 18

5.8.2 Rigid Bullnose costs

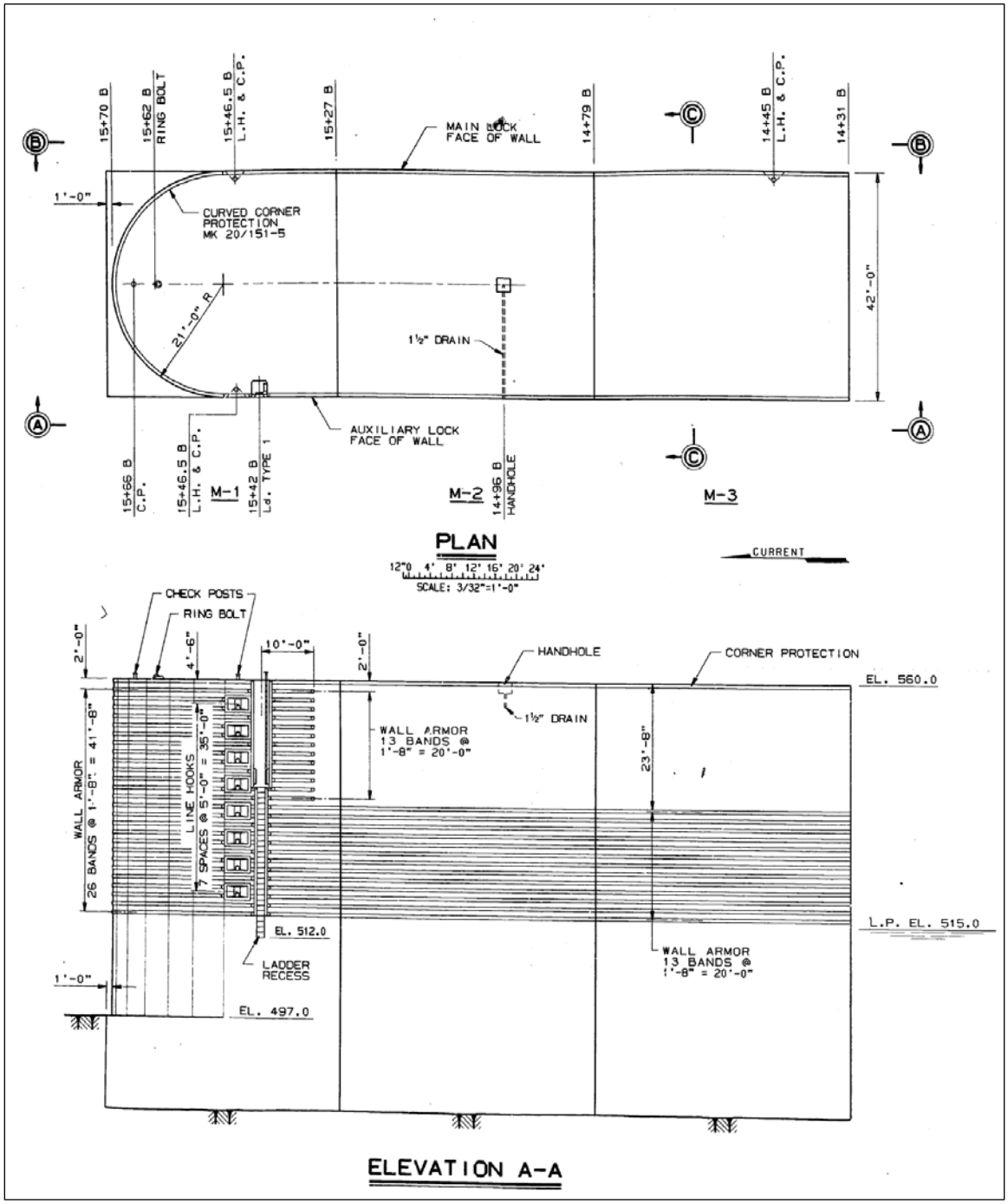

Figure 5.15 Downstream design for the R.C.Byrd center wall

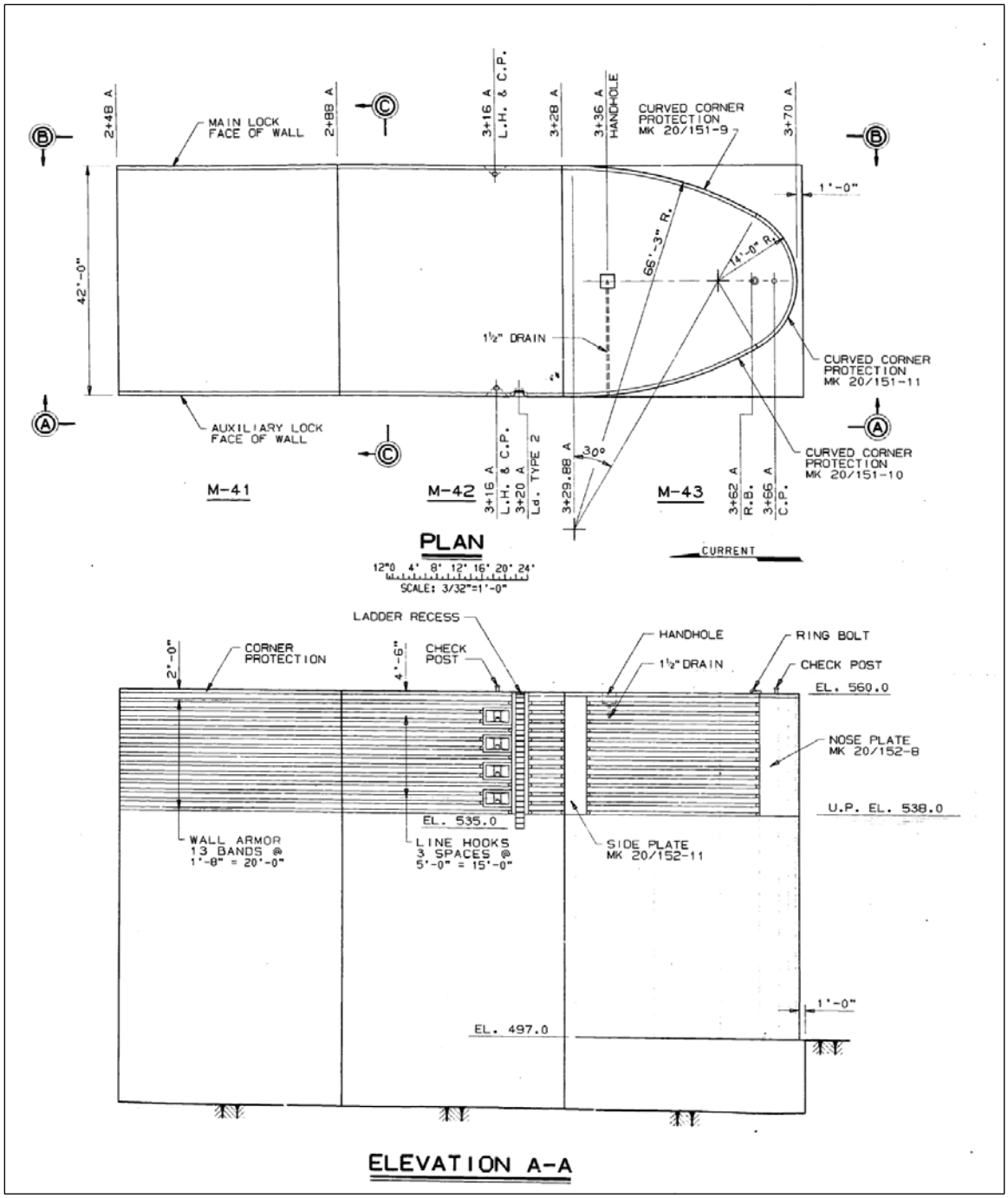

Figure 5.16 Upstream design for the R.C.Byrd center wall

Mr. Bryan Bledsoe and Mr. David Sullivan of Huntington District developed a cost estimate for a rigid bullnose using Figures 5.15 and 5.16. These figures show designs for downstream and upstream cast-in-place walls at the end of the common wall between two parallel locks at the R.C.Byrd Locks and Dam. The downstream bullnose (Section M-1) has a 21 feet radius with a 43 feet length. The width of the wall section is 42 feet and the height of the

wall is 80 feet, including the 17 foot depth of embedment into rock. This gives a total volume of 129,909.43 cubic feet. The upstream bullnose (Section M-43) is slightly more curved and has a length of 36 feet. The width of the wall section is 42 feet and the height of the wall is 76 feet, including the 13 foot depth of embedment into rock. The upstream bullnose has a total volume of 111,680.15 cubic feet. The estimated total costs for these bullnoses are $2.5M and $2.2M for downstream and upstream, respectively. These costs cover the material, formwork, construction labor, ancillary placement costs, the Engineering/Design (END) and Supervision/Administration of construction contract (SA) costs.

Figure 5.17 Marmet Lock and Dam with Cellular Bullnose

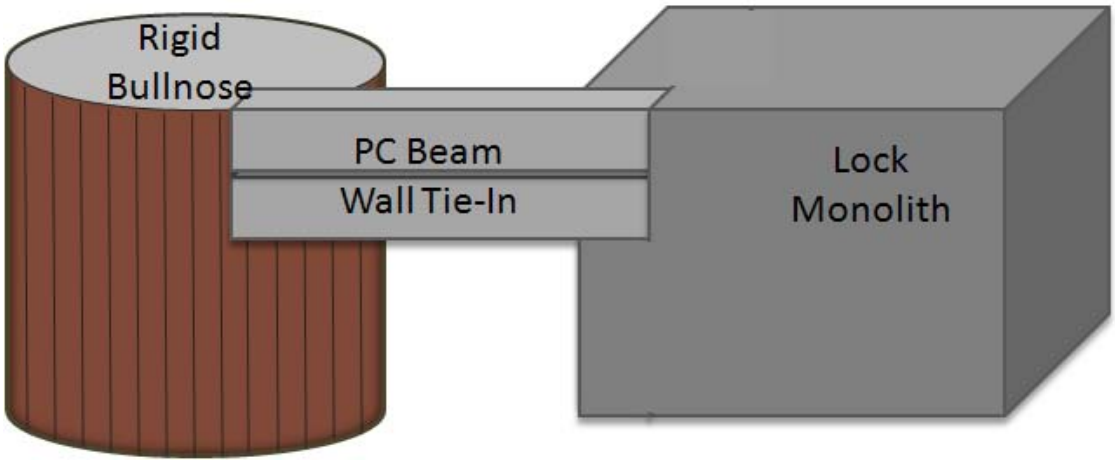

Figure 5.18 Hypothetical Concrete-filled Cellular Bullnose with Precast Beams Tied to the Lock Monolith

Mr. Derek Maxey and Mr. David Sullivan of Huntington District developed a cost estimate based on a hypothetical situation that closely matches the Marmet Lock Replacement Project (Figures 5.17 and 5.18). The rigid bullnose design was a sheetpile cell filled with tremie concrete. Two precast concrete beams connected the bullnose to the lock monolith. The hypothetical cell had a diameter of 60 feet and was constructed of 45 foot long PS27.5 sheet-piles. Approximately 4,920 cubic yards of tremie concrete filled the cell. The estimated total cost of this bullnose is $4.5M. This cost covers the material, formwork, construction labor, ancillary placement costs, the Engineering/Design (END) and Supervision/Administration of construction contract (SA) costs.

Mrs. Kathy Feger and Mr. Larry Dalton II of Louisville District estimated costs for cell-based cellular bullnoses, upstream and downstream, at McAlpine Lock and Dam through Mr. Byron McClellan (retired Chief of Structures from Louisville District). The McAlpine bullnose cells were both 50 foot in diameter. One cell was 76 feet tall and the other cell was 43 feet tall. The total costs for both cells was estimated to be $4.7M. This cost covers the material, formwork, construction labor, ancillary placement costs, the Engineering/Design (END) and Supervision/Administration of construction contract (SA) costs.

According to these examples and discussions with other district engineers, the estimated cost for constructing a conventional, rigid bullnose can be in the range of $2M to $5M.

5.8.3 Cost for shutdown related to loss of barge train integrity

To get an estimate of the total worth of a Deformable BEAS, it is important to see the possible consequences that may be ameliorated with the addition of the deformable structure in front of a rigid bullnose. It has been shown through simulation that, in a head-on allision with a rigid bullnose, a fully-loaded barge train with 15 barges travelling at 2.7 feet per second will lose barge train integrity, separating barges from the tow.

On January 6, 2005, the M\V Jon J. Strong was heading north out of Belleville Lock and Dam when strong currents, due to flooding on the Ohio River, caught the lead barges, broke lashings, and led to loss of barge train integrity. Nine of the twelve barges broke away from the tow and were drawn to the open gates of the dam by the flood waters. Of the nine barges, three sank, two were drawn completely through the fully-open tainter

gates, and four lodged in the dam. Figure 5.19 shows barges trapped on the Belleville Lock and Dam.

Figure 5.19. Barges blocking dam gate operations at Belleville Locks and Dam.

With the four barges lodged in the dam, the tainter gates for the Belleville Lock and Dam were unable to be closed leading to a loss of the upper pool when the flood receded. On January 20, the area between Belleville Lock and Dam and Willow Island was declared unnavigable. Shortly thereafter, the loss of pool was felt downstream of the lock and dam, resulting in further closures downriver. Plants along the river, such as DuPont and Kraton Polymers, had to bring in pumps to provide water from the lowered river to their water intakes. The gates were inoperable until the last barge was removed on February 1, 2005. The River Salvage Rig "Large Marge" was brought in to remove the barges. By that time, the Ohio River had been declared unnavigable for 12 days.

According to the Corps spreadsheet giving the cost per closure of locks and dams from Navigation Economics PDT (2011), using 2010 dollars, the cost for a total closure of the Belleville Lock and Dam for 10 days is $7.87 million - this cost represents only the delay cost to the towing companies while the system is either shut down or operating inefficiently. Bob Willis, retired Chief of Operations for the Great Lakes and Ohio River Division who was on

site during this closure, estimated the costs for the incident at Belleville to be closer to $100 million, based on information gathered by the Corps of Engineers which accounted for costs to shippers and end users of the products. Additional costs (not included in the cited cost) would also include the cost of lost and damaged barges as well as cargo lost, not to mention the potential for loss of life during the initial accident or during salvage operations.

These types of incidents are not isolated. A similar incident occurred at the Montgomery Lock and Dam on the Ohio River in PA on January, 2005, with loss of life.

There are also examples of barge train integrity being lost due to allisions with Corps structures. In March 31, 2005, the M/V Amber Brittany collided with the 2nd Street Bridge upstream from the McAlpine Lock. The tow lost control of his barge train and required the assistance of three other tows, the Sharon M., Glenn R., and Richard Baker to gather the barges before they could end up on the dam wall in an incident similar to the Belleville Lock and Dam incident.

These types of incidents could also be exascerbated if the barges were carrying hazardous materials. For example, Newt Graham Lock and Dam #18 at Tulsa, OK, discussed in this report regularly locks through barges carrying nitrogen rich fertilizer, which is highly explosive. Barges carrying petrolieum products are regullarly passed through most of the Corps locks.

Table 5.2 contains a representative portion of a Corps spreadsheet giving the cost per full closure of locks and dams, using 2010 dollars. Mr. David Sullivan supplied the Corps Navigation Economics PDT tabulation of transit costs over time for full closure at the Corps lock and dam structures. This table gives the cost of delay to towing companies while the (river) system is either shut down or operating inefficiently. This spreadsheet contains all Corps maintained locks. The list of lock sites in this chart is sorted from maximum to minimum on full closure costs to the industry for closures of 5 days. The sites for this chart were chosen based on their representation as sites of accidents in this Deformable BEAS report and in the first Deformable BEAS report [Ebeling, et al., 2010]. According to this spreadsheet, Smithland Lock and Dam has the highest industry cost for a full closure of all the Corps maintained locks.

Table 5.3 Costs Over Time for Full Closure at Particular Corps Structures

Division	District	River	Project	Costs per ($K)				
				1 day	3 days	5 days	10 days	15 days
LRD	LRL	Ohio	Smithland L&D	282	2,025	4,887	13,774	24,969
LRD	LRL	Ohio	Cannelton L&D	165	1,580	3,618	10,291	20,007
LRD	LRL	Ohio	Markland L&D	110	1,340	3,008	8,973	16,959
LRD	LRH	Ohio	Belleville L&D	123	1,173	2,985	7,870	15,720
SWD	SWT	McClellan-Kerr Arkansas	Newt Graham L&D	10	120	232	571	1,053

The authors of this report observe that the transit costs for full closure in the Table 5.3 data increases exponentially for longer periods of time (Figure 5.20). This is because scheduled barge traffic that has been stopped accumulates along the river.

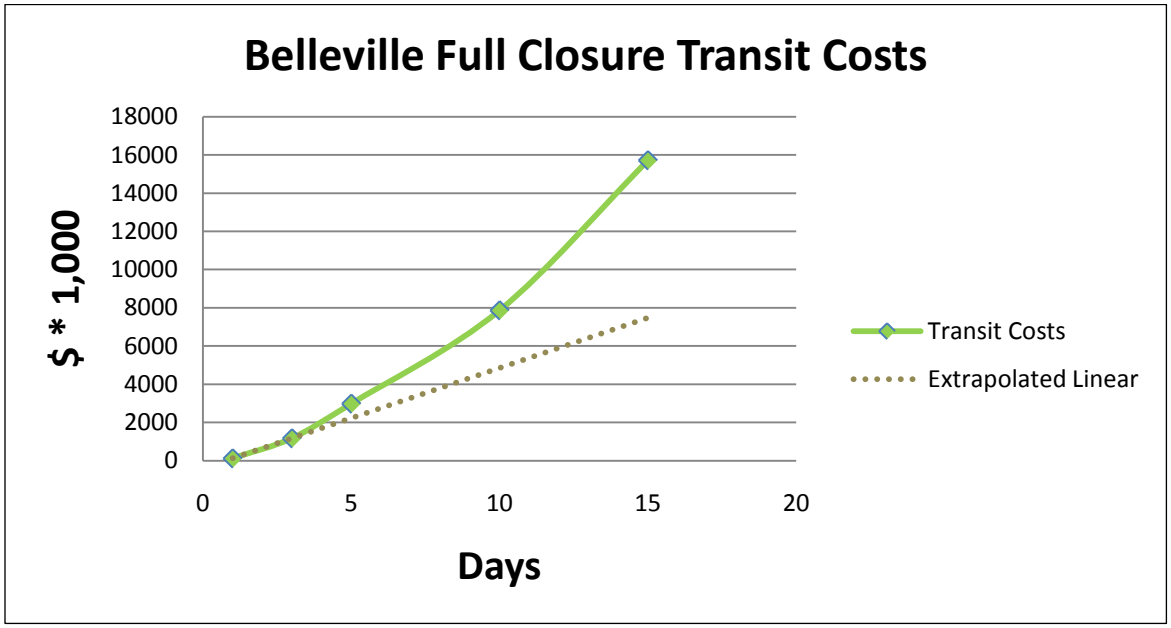

Figure 5.20 The non-linear costs for full closure of the locks and dam at Belleville

The Deformable BEAS can remove a cause for loss of barge train integrity, thereby reducing the likelihood of lock and dam closure. Barge train integrity can be maintained for head-on impacts with bullnoses in up to extreme non-site specific conditions; up to 4.7 fps for a 3-by-4 fully loaded

barge train and 4.5 fps for a 3-by-5 fully loaded barge train. Corps estimates for closure costs over time combined with the Corps experiences of the time of closure for specific examples of out of control barges in dam gates shows that these incidents have a significant impact in terms of cost to industry. Anecdotal experience shows that the cost for a single, noteworthy incident can range from tens to hundreds of millions of dollars. The magnitude of these closure costs present a basis for arguing for the additional up-front cost of constructing a deformable bullnose.

5.8.4 Costing Conclusions

Mr. Bob Willis, retired Chief of operations for the Great Lakes and Ohio River Division, observes that material, construction and engineering costs may not be the only basis for evaluating the usefulness of a Deformable BEAS as compared to a rigid bullnose. An estimate of the construction and engineering costs of a Deformable BEAS was given as $12.5 million. With the objective that the Deformable BEAS mitigate/eliminate the potential for rupture of the lashings during a glancing blow or a head-on impact with a bullnose that would then allow “break-away” barges to occur, costs other than construction costs may be considered during a total worth assessment for a Deformable BEAS. For example, there are transit costs over time for full closure at the Corps lock and dam structures resulting from a shut-down of a lock and dam due to an incident involving break-away barges. For the four Ohio river lock and dams at Smithland, Cannelton, Markland and Belleville, these 10 day full closure transit costs range from $8 million to $14 million. This cost does not include the costs that shipper may incur due to finding alternative ways to ship their products, or other costs associated with conducting business along the river. For the 12-day incident at Belleville, the transit costs (according to Figure 5.20) would be on the order of $10.75M. The “total” cost data gathered by the Corps of Engineers for the 2005 Belleville incident (involving barges in the dam gates), supplied by Mr. Bob Willis, was $100 million. This reveals that the total cost for a full closure at a lock and dam is much greater than just the Navigation Economics PDT tabulation of costs. The “total” cost to industries along the river and businesses that depend upon river transportation of materials and products during a full closure at a lock and dam site dwarfs the construction costs for a

Deformable BEAS, making the Deformable BEAS a cost-effective alternative to rigid bullnoses.[1]

A cost savings due to a reduction of injuries or fatalities because of fewer lashing failures during impacts with a Deformable BEAS has not been calculated[2], but this navigation safety structure has been shown to reduce these possibilities. The authors speculate that this would be an area of interest for the towing industry.

[1] Additionally, these "total" industry costs do not include the cost of lost and damaged barges as well as cargo lost, not to mention the potential for loss of life during the initial accident or during salvage operations.

[2] Recall from Ebeling, et al. (2010) that a study was made of accident records at three locks and dams; Smithland, Cannelton, and Markland. At Smithland, a total of 95 accidents were reported between barge tows and the upper approach walls between 1981 and 2007. At Cannelton, a total of 26 allisions involving the upper approach walls occurred between 1983 and 2007. At Markland, a total of 27 reported accidents occurred between 1988 and 2008. From this information, the authors observe that there are typically 1 to 5 accidents per year. Some but not all of these accidents involve head-on or glancing blow impacts with the bullnoses. Impacts with the bullnose are the most severe, increasing the likelihood of injuries due to lashing failures.

References

American Association of State Highway and Transportation Officials (AASHTO). 1991. *Guide Specification and Commentary for Vessel Collision Design of Highway Bridges, Volume I: Final Report*. 444 North Capitol Street, N.W. Suite 225, Washington, D.C.

American Institute of Steel Construction. 1989. *Manual of Steel Construction, Allowable Stress Design, Ninth Edition*, 1East Wacker Drive, Suite 3100, Chicago, Illinois.

Arroyo, J. R., and R. M. Ebeling. 2004. A Numerical Method for Computing Barge Impact Forces Based on Ultimate Strength of the Lashings between Barges, *ERDC/ITL TR-04-2*. Vicksburg, MS: U.S. Army Engineer Research and Development Center.

Arroyo, J. R., and R. M. Ebeling. 2005 (Mar). Barge Train Maximum Impact Forces Using Limit States for the Lashings between Barges, *ERDC/ITL TR-05-1*. Vicksburg, MS: U.S. Army Engineer Research and Development Center.

Celik, O. C., J. W. Berman, and M. Bruneau. 2006. Hysteretic Energy Dissipation in Laterally Restrained Steel Tube and Solid Bar Braces, *First European Conference on Earthquake Engineering and Seismology, Paper 274*, Geneva Switzerland. http://www.eng.buffalo.edu/~bruneau/ECEES%202006%20Geneva%20-%20Celik%20Berman%20Bruneau.pdf

Computers & Structures, Inc. 2000. *SAP2000 Integrated Software For Structural Analysis & Design*, 1995 University Avenue, Suite 540, Berkeley, CA.

Ebeling, R., A. N. Mohamed, J. R. Arroyo, B. C. White, R. W. Strom, and B. C. Barker. 2011. Dynamic Structural Flexible-Beam Response to a Moving Barge Train Impact Force Time-History Using Impact_Beam, *ERDC TR-11-XX* (in publication). Vicksburg, MS: U.S. Army Engineer Research and Development Center.

Ebeling, R. M., J. E. Hite,, R. W. Strom, and B. C. White. 2010 (Aug). Deformable Bullnose Energy Absorbing System, Report 1: Initial Development and Concept Design, *ERDC TR-10-7*. Vicksburg, MS: U.S. Army Engineer Research and Development Center.

Ebeling, R. M., and T. W. Warren. 2009 (Aug). Limiting Impact Force Due to Yielding and Buckling of the Plates and Internal Structural Frame at the Bow of a Barge during Its Head-on Impact with a Bullnose or Cellular Structure, *ERDC/ITL TR-09-3*. Vicksburg, MS: U.S. Army Engineer Research and Development Center.

Ebeling, R. M., and T. W. Warren. 2008 (Nov). Limiting Impact Force Due to Yielding and Buckling of the Plates and Internal Structural Frame at the Impact Corner of the Barge during Its Glancing Blow Impact with a Lock Approach Wall, *ERDC/ITL TR-08-2*. Vicksburg, MS: U.S. Army Engineer Research and Development Center.

Franco, J. J. and L. J. Shows. 1968. Navigation Conditions at Lock and Dam No. 9, Arkansas River, hydraulic model investigation, *Technical Report No. 2-817*. U.S. Army Engineer Waterways Experiment Station, Vicksburg, MS.

Franco, J. J. and C. D. McKellar. 1968. Navigation Conditions at Ozark Lock and Dam, Arkansas River, hydraulic model investigation, *Technical Report H-68-10*. U.S. Army Engineer Waterways Experiment Station, Vicksburg, MS.

Franco, J. J. and L. J. Shows. 1971. Lock and Dam No. 14, Arkansas River Navigation project, hydraulic model investigation, *Technical Report H-71-1*. U.S. Army Engineer Waterways Experiment Station, Vicksburg, MS.

Headquarters, U. S. Army Corps of Engineers. 2004. Barge impact analysis for rigid walls. *Engineer Technical Letter 1110-2-563*. Washington, DC.

Navigation Economics PDT. 2011 (March). *Summary Report on Increased Transportation Costs due to the Main Lock Chamber Closures*, 2010 Update, 11 March 2011, Draft Report submitted by FY10 Navigation Budget EC Annex PDT and submitted to the HQUSACE Navigation Business Line Manager.

Schneider, S. P., 1998. Axial Loaded Concrete-Filled Steel Tubes, *ASCE Journal of Structural Engineering*.

Tai, T. S., and H. H. Huang, and H. T. Hu. 2009. Axial Compression and Energy Absorption Characteristics of High-Strength Thin-Walled Cylinders under Impact Load, *Theoretical and Applied Fracture Mechanics*. http://140.116.36.16/paper/34.pdf

Trelleborg Marine Systems, 2007. High Performance Fenders, Section 1; Super Cone Fenders, online catalogue at www.trelleborg.com/marine.

U.S. Army Engineer Waterways Experiment Station. 1957. Navigation Conditions at Markland Locks and Dam, Ohio River, hydraulic model investigation, *Technical Report No. 2-446*. Vicksburg, MS.

REPORT DOCUMENTATION PAGE

Form Approved
OMB No. 0704-0188

1. REPORT DATE *(DD-MM-YYYY)*	2. REPORT TYPE	3. DATES COVERED *(From - To)*
July 2011	Report 2 in a series	

4. TITLE AND SUBTITLE

Deformable Bullnose Energy Absorbing System (BEAS); Report 2: Head-On Impact with a Deformable BEAS and Introducing a Collapsible Arch

5a. CONTRACT NUMBER

5b. GRANT NUMBER

5c. PROGRAM ELEMENT NUMBER

6. AUTHOR(S)

Robert M. Ebeling, Barry C. White, Ralph W. Strom, John E. Hite, Jr., Bruce C. Barker, and Richard W. Haskins

5d. PROJECT NUMBER

5e. TASK NUMBER

5f. WORK UNIT NUMBER

7. PERFORMING ORGANIZATION NAME(S) AND ADDRESS(ES)

U.S. Army Engineer Research and Development Center
Information Technology Laboratory
3909 Halls Ferry Road
Vicksburg, MS 39180-6199

(see reverse)

8. PERFORMING ORGANIZATION REPORT NUMBER

ERDC TR-11-5

9. SPONSORING / MONITORING AGENCY NAME(S) AND ADDRESS(ES)

Headquarters, U.S. Army Engineer District
441 G. Street, NW
Washington, DC 20314-1000

10. SPONSOR/MONITOR'S ACRONYM(S)

11. SPONSOR/MONITOR'S REPORT NUMBER(S)

12. DISTRIBUTION / AVAILABILITY STATEMENT

Approved for public release; distribution is unlimited.

13. SUPPLEMENTARY NOTES

14. ABSTRACT

An impact between a tow and the bullnose of a lock approach wall can result in the tow breaking up with loose barges moving out of control toward the lock or navigation dam with serious consequences. Project operations can be severely affected or even shut down. The loose barges can cause a high safety risk to personnel involved and if the navigation pool is lost or the lock is damaged, significant economic impacts may result. This Technical Report discusses the second stage of research into the development of a Deformable Bullnose Energy Absorbing System (BEAS) impact structure that would help reduce or prevent lashing failures and loose barges due to an impact between a tow and a lock approach wall bullnose.

In simulations, the first improvement for limiting approach velocity to maintain barge integrity was achieved by the proper selection of lashing layout. The second improvement was achieved by the introduction of the Deformable BEAS. For a head-on collision between a three by five barge train at 3.3 feet per second and a rigid bullnose, barge train integrity is lost. For the same barge train, this report shows that the addition of an impact nosing with double stacked, soft base isolators for a Deformable BEAS extends the maintenance of barge train integrity to 4.5 feet per second. For a head-on collision between a three by four barge train at 3.0 feet per second and a rigid bullnose, barge train integrity is lost. For the same barge train, this report shows that the addition of the collapsible front arch to an impact nosing with double stacked, soft base isolators for a Deformable BEAS extends the maintenance of barge train integrity to 4.7 feet per second. These results imply that the addition of other innovative energy absorbing features could allow for even higher approach velocities.

15. SUBJECT TERMS

Allision
Barge
Base isolator
Bullnose
Collapsible Front Arch
Frangible Section Impact
Guard wall Lock approach wall
Guide wall Tow

16. SECURITY CLASSIFICATION OF:			17. LIMITATION OF ABSTRACT	18. NUMBER OF PAGES	19a. NAME OF RESPONSIBLE PERSON
a. REPORT	b. ABSTRACT	c. THIS PAGE			19b. TELEPHONE NUMBER *(include area code)*
UNCLASSIFIED	UNCLASSIFIED	UNCLASSIFIED		124	

7. PERFORMING ORGANIZATION NAME(S) AND ADDRESS(ES) (concluded)

U.S. Army Engineer Research and Development Center
Coastal and Hydraulics Laboratory
3909 Halls Ferry Road
Vicksburg, MS 39180-6199